Dissertation presented to the Faculty of the Department of Graduate Studies of the Aeronautics Institute of Technology, in partial fulfillment of the requirements for the Degree of Master in Engineering of the Professional Master's Program in Aeronautics Engineering in the Graduate Program in Aeronautics and Mechanics Engineering.

CARLOS AUGUSTO CONSTANTINO

HYDRAULIC ACTUATION SYSTEM MODELING: AN ANALYSIS OF HIGH FREQUENCY MODELING

Dissertation approved in its final version the signatories below

_____

Prof. Dr. Luiz Carlos Sandoval Góes
Advisor

_____

Dr. Fernando José de Oliveira Moreira
Co-advisor

_____

Prof. Dr. Celso Massaki Hirata
Head of the Faculty of the Department of Graduate Studies

Campo Montenegro
São José dos Campos, SP – Brazil
2010

Cataloging-in-Publication Data
Documentation and Information Division

Constantino, Carlos Augusto
Hydraulic Actuation System Modeling: An analysis of high frequency modeling / Carlos Augusto Constantino. São José dos Campos, 2010.
121f.

Master´s Dissertation – Course of Mechanical and Aeronautics Engineering – Aerospace System and Mechatronics – Aeronautical Institute of Technology, 2010. Advisor: Prof. Luiz Carlos Sandoval Góes, Ph.D.

1. Modeling. 2. Fly-By-Wire. 3. Hydraulic Actuator. I. General Command for Aerospace Technology. Aeronautics Institute of Technology. Aeronautics and Mechanics Engineering Division. II. Hydraulic Actuation System Modeling: An analysis of high frequency modeling

BIBLIOGRAPHIC REFERENCE

CONSTANTINO, Carlos Augusto. **Hydraulic Actuation System Modeling: An analysis of high frequency modeling**. 2010. 121. Dissertation of Master of Sciences in Mechanical and Aeronautics Engineering – Aeronautics Institute of Technology, São José dos Campos.

CESSION OF RIGHTS

AUTOR NAME: Carlos Augusto Constantino
PUBLICATION TITLE: Hydraulic Actuation System Modeling: An analysis of high frequency modeling
PUBLICATION KIND/YEAR: Dissertation / 2010

_____
Carlos Augusto Constantino
São José dos Campos - SP

HYDRAULIC ACTUATION SYSTEM MODELING: AN ANALYSIS OF HIGH FREQUENCY MODELING

Carlos Augusto Constantino

Dissertation Committee Composition:

Prof. Dr. Luiz Carlos Sandoval Góes	Chairperson/Advisor - ITA
Dr. Fernando José de Oliveira Moreira	Co-Advisor – EMBRAER
Prof. Dr. Emília Villani	ITA
Marco Antonio de Oliveira Alves Jr	EMBRAER

ITA

To my parents, Walter and Maria, and to my grandparents Antônio (in memoriam), Vilma (in memoriam), Walter (in memoriam) and Gioconda.

Acknowledgement

I would like to thank Prof. Góes and Fernando for the orientation, patience and for the productive discussions.

I would like to thank my parents, which without their support I couldn't be here.

I would like to thank Tatiana for her important support through this work.

I would like to thank my colleagues from EMBRAER for always be willing to help me solve my questions.

I would like to thank all my friends who helped me in any way through this work.

Resumo

O objetivo deste trabalho foi desenvolver um modelo de alta fidelidade representativo até altas freqüências de um Sistema de Comando de Vôo com atuação hidráulica na configuração ativo-ativo. O uso de arquiteturas *Fly-By-Wire* e de sistemas de atuação hidráulica em modo ativo-ativo trouxe novos desafios de engenharia como o *force-fight* entre atuadores e seu consumo de vida em fadiga num cenário normal e de falha, como falhas oscilatórias. Uma vez que estes casos de falha podem existir até altas freqüências, faz-se necessário a criação de um modelo de alta fidelidade do sistema de comando de vôo representativo até altas freqüências. O modelo aqui desenvolvido possui um modelo em alta fidelidade de uma EHSV, de um atuador hidráulico, do loop de posição e de uma superfície de controle, assim como outros modelos complementares de forma a ser possível analisar o sistema como um todo até altas freqüências. Foi analisado o desempenho do modelo a uma resposta degrau e resposta em freqüência, mostrando se tratar de um modelo próximo do esperado de um sistema real. Assim como foi analisado a resposta em freqüência dos seus componentes, mostrando ser um modelo representativo até alta freqüência. Além da análise de desempenho, foi estudado o comportamento no cenário de uma falha oscilatória, mostrando o nível esperado de carga na estrutura, assim como o seu consumo de vida em fadiga, mostrando assim a necessidade de um monitoramento de tais falhas.

Abstract

The objective of this work was to develop a high fidelity model representative up to high frequencies of a Flight Control System with hydraulic actuation on active-active mode. The usage of a Fly-By-Wire architecture and hydraulic actuation system on active-active mode has brought new engineering challenges like the force-fight between actuators and its structure fatigue life consumption on normal and failure scenarios such as oscillatory mal-functions. Once that these failure modes can exist up to high frequencies, it makes necessary the development of a high fidelity model of a flight control system representative up to high frequencies. The model herein developed has a high fidelity model of an EHSV, hydraulic actuator, a position loop and the control surface, as well as other models complementary in order that it can be possible to analyze the whole system up to high frequencies. It was analyzed the performance of the model at step input response and frequency response, showing to be a model close to the expected response of a real system. Also it was analyzed the frequency response of its components showing to be a representative model up to high frequencies. Besides the performance analysis, it was studied the behavior on a oscillatory mal-function scenario, showing the expected level of structure load, as well as its fatigue life consumption, showing the need to monitor these types of failures.

List of Figures

Summary

1. INTRODUCTION

1.1. Brief History of the Flight Control System

The Aeronautic Technology has been highly developed since its beginning and one of the most evolved systems is the Flight Control System (FCS), on this chapter it will be shortly described its development through time showing the most important breakthroughs.

The early aircrafts used mechanical controls, also known as manually operated controls, which is a series of mechanical linkages, such as tension cables, pulleys and rods that connect the pilot to the control surfaces [13].

On mechanical systems the amount of force that can be applied into the surface is directly related to the forces that a pilot can make. However along the years airplanes increased in size and velocity, intensifying the aerodynamics loads that the control surfaces is applied to, therefore the amount of force that the pilot was submitted to control the aircraft increased prohibitively.

This load limitation drove the development of the system, although it is still used today on smaller aircrafts or as a secondary system used in the event of a failure, for instance the A-10 Thunderbolt or the T-46 [2].

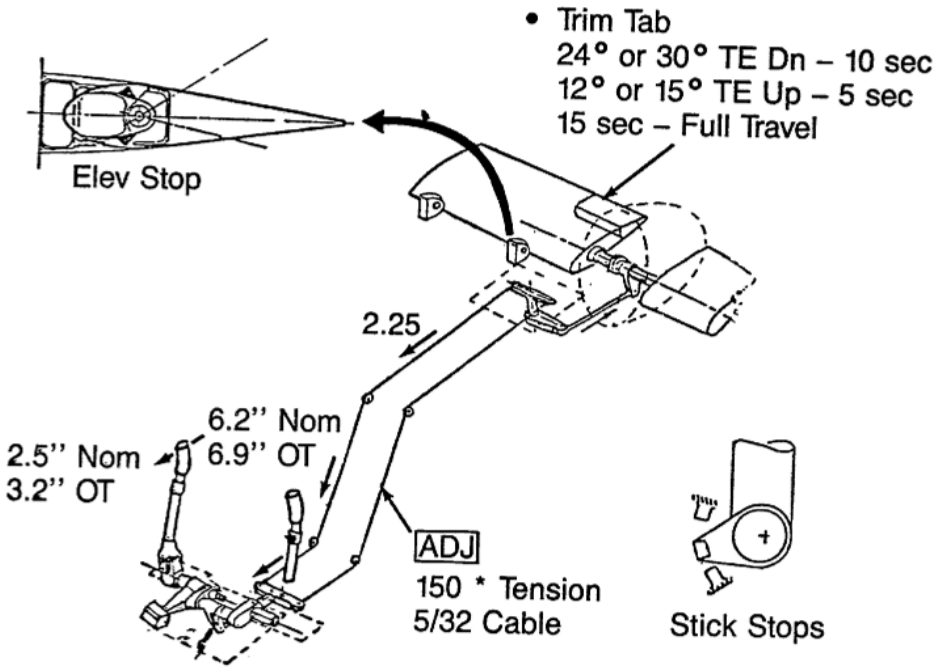

Figure 1-1 – Fairchild Republic T-46, Pitch Control Schematic

Source: SAE International AIR4094 “Aircraft Flight Control Systems Descriptions”

To solve the mechanical control issues it was developed the hydraulic powered system, which consists in a linkage between the pilot command and a servovalve that controls a hydraulic powered actuator [13].

This system is largely used today for military or civil aircrafts, for instance the F-15A Eagle [3] which longitudinal control schema is shown on Figure 1-2.

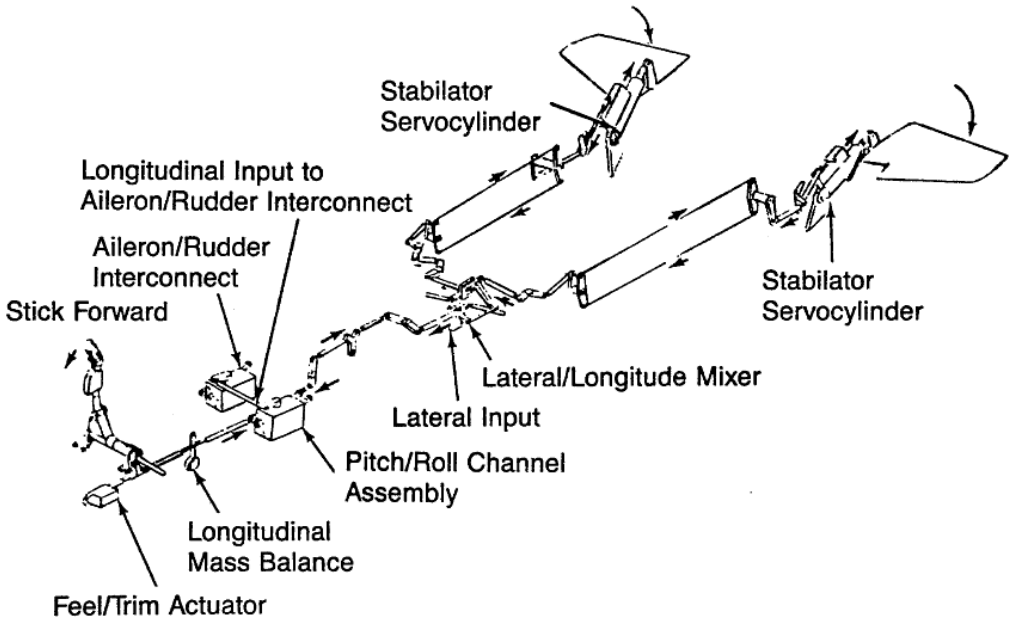

Figure 1-2 – McDonnell-Douglas F-15A Eagle, FCS – Longitudinal Controls

Source: SAE International AIR4094 “Aircraft Flight Control Systems Descriptions”

Usually it is used more than one actuator per surface due to safety requirements, being each one connected to a different hydraulic supply. Although the number of actuators that will be used on each surface can depend on others factors besides safety, for instance performance requirements.

Each actuator has a specific normal operation mode, such as active, bypass, damped or blocked. Whether will be used one or another depends on the safety and performance requirements of the system. Therefore an extensive amount of combination between these different operation modes can be created. Two of the most common designs are the active-bypass and the active-active.

The active-bypass design consists in the surface commanded by one actuator while the other is set to a bypass state and will only be used in case of a failure of the active one. On the

active-active design both actuators work in parallel to move the surface, in case of an actuator failure, the system will go to the active-bypass mode.

Each one of the designs has its advantages and drawbacks. Therefore the usage of one besides the other depends on each FCS design.

The use of hydraulic powered system allowed the industry to develop faster and bigger aircrafts, but eventually the size of the aircrafts were too big and the usage of cables to transmit the pilot command to the actuators started to have a huge impact on weight and performance of the aircraft. This drove another very important breakthrough for the FCS technology, the advent of Fly-by-Wire System.

The Fly-by-Wire system consists on the same actuators connected to the surface, but instead of cables transmitting the pilot command to the servovalve, is used an electronic signal processed by a Flight Control Computer for a given pilot input. Fly-by-Wire systems can be found, for instance, on the Boeing 777 and the Airbus A320 [4].

This system allowed also the implementation of a closed loop control law of the aircraft, allowing the development of higher performance aircrafts.

Others relevant technologies developed were, for example, the Sidestick, substituting the column wheel with the advantage of esthetics and possible weight reduction; or the electro-hydrostatic servo actuators, where is used an electrical supply power to drive a dedicated hydraulic pump joined to the actuator, and since there is no need for a hydraulic supply line, there might be a weight reduction depending on the aircraft size, also it easily provides more redundancy, highly desirable on military aircrafts that has a critical

survivability requirement, this system is used in the Lockheed Martin F-35 and as a backup system on the A380 [13].

1.2. Subject of Work

The work here presented will study a Fly-by-Wire and hydraulic powered flight control system with an active-active configuration and will be analyzed one of its critical drawbacks, the Force-Fight that is generated between the actuators.

When both actuators move the same surface in parallel, it is expected that the displacement of each actuator is not perfect aligned to the other, and this misalignment will generate a torsion force on the surface called Force-Fight and might cause structural damage depending on the amount of load encountered.

There are methods on the industry used to eliminate the Force-Fight by developing an active control of each actuator individually aiming to reduce the difference of the amount of force that each actuator is developing, but these controls do not eliminate completely the Force-Fight especially at dynamic conditions.

Nevertheless the aircraft structure can be designed to tolerate a predicted level of Force-Fight throughout the aircraft life, unless a failure that generates a higher Force-Fight occurs, such as an oscillatory mal-function.

Electrical and mechanical failures can results in an oscillating Force-Fight load, which will consume the structural fatigue life, these failures are called Oscillatory Mal-Function (OMF) and will be described in details later on this work.

If the structure design considers an OMF scenario it would make the size and weight of the structure prohibitive, therefore the system response in the presence of an OMF has to be carefully studied and monitored during the aircraft operational life.

The studies developed on industries up to date were made considering a model of low frequencies dynamics of the hydraulic actuation. The subject of this work intent to study the system response considering that it is possible to have structural fatigue damage even for frequencies up to 100Hz, for that was developed a high fidelity model considering relevant dynamics up to high frequencies.

2. SYSTEM DESCRIPTION

2.1. FCS Description

This chapter will present an overview of the flight control system selected for this work. The hydraulic powered Fly-by-Wire system can be basically divided by these 3 parts:

1. Pilot Input
2. Electronic System
3. Hydraulic Actuation System

The Pilot Input can be made by a column wheel or a sidestick, either one, used with the rudder pedals, must transmit the pilot command in the aircraft 3 axes.

This command is then sent to the Electronic System, which will process the signal and send a correspondent command to the servovalve of the hydraulic actuator, such that the resultant surface displacement meets the pilot input.

2.2. Electronic System Description

The Electronic System might incorporate a computer with the control law of the airplane, on this case the pilot input will be processed in order to make the optimized maneuver; and only the processed command will be sent to the actuator.

For the scope of this work, it won't matter if the command is sent by the pilot or by the flight control computer, therefore it will not be modeled any control law processor. Nevertheless in order to send a command to the servovalve of the actuator, the angular command must be converted to a current command.

To make this conversion it is implemented a position loop, where the signal error between the actuator command and the real position is processed and converted in a current command to the servovalve. This position loop is critical in order to meet performance requirements of the actuation system and will be implemented herein.

2.3. Hydraulic Actuation System Description

The actuation system is composed by a series of control valves, such as the servovalve, mode select valve, check valve, pressure relief valve and solenoid operated valves, all of them are joined together in order to allow a safe and proper function of the actuator.

A schematic diagram of a hydraulic actuator can be seen on the Figure 2-1, where:

1. Servovalve
2. Mode Select Valve
3. Solenoid Operated Valve
4. Anti-Cavitation Valves
5. Check Valves
6. Reservoir
7. Actuator
8. Piston Ram LVDT
9. Surface of control

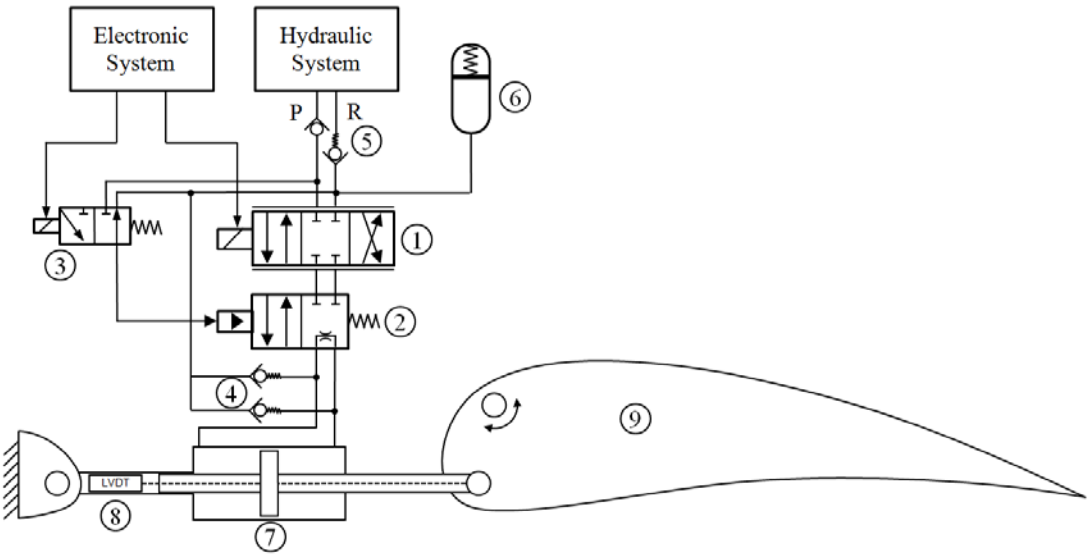

Figure 2-1 – Hydraulic Diagram

Source: Developed by the author

The servovalve is a solenoid commanded valve which connects the pressure and return lines from the hydraulic system to each chamber of the actuator depending on the amount of current that is inserted at the solenoid.

The electromagnetic field created on the solenoid reacts with the permanent magnet inside the servovalve rotating the flapper, which will create a differential pressure on each side of the spool.

The differential pressure will unbalance the spool forces resulting in a displacement on the direction of the resultant force. The displacement will open the orifices on the spool sleeve, therefore connecting the pressure and return lines to each chamber line.

The Figure 2-2 extracted from Merritt [10] shows the schematic electro-hydraulic servovalve.

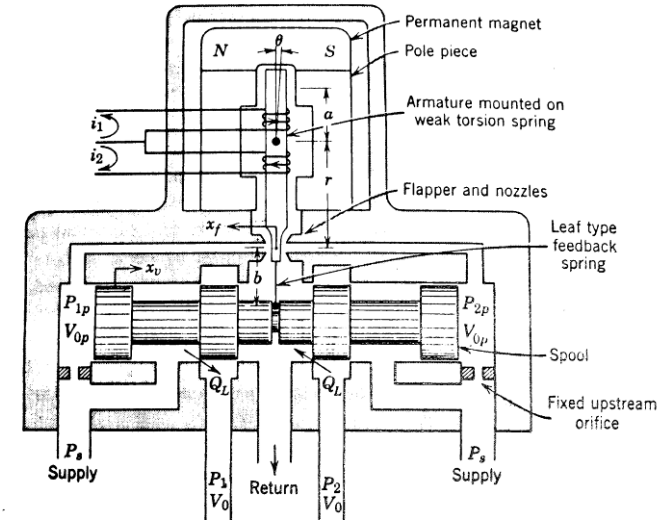

Figure 2-2 – 2 Stage Electro-Hydraulic Servovalve (EHSV) Schematic

Source: Merritt, Herbert E. – “Hydraulic Control Systems”

The mode select valve herein presented is a two-mode valve, active and damped mode, in the industry there is also tri-mode valves, where one of the mode is the active and the others are a combination of damped, bypass and blocked mode.

The active mode is when the actuator is powered to move the surface; the damped mode is when the actuator is set to a damping state in order to guarantee safety requirements such as flutter suppression.

The bypass mode is used in the absence of damping necessity so the actuator is set free to move in order to not degrade the movement of the other active actuator connected to the surface. The blocked mode is when the paths of the chambers lines are disconnected, this mode is normally used in case of a high damping requirement.

The mode select valve is piloted by a solenoid operated valve, which is a valve that connects the hydraulic or the return pressure to the pilot line according to an input command from the Electronic System.

In case of the loss of the Electronic System, the actuator will automatic be set to damped state. The same will happen in case of a hydraulic loss since it is piloted by the hydraulic pressure line. Therefore the system is protected in the event of a hydraulic or electrical failure.

The Anti-Cavitation Valve are used to prevent the pressure inside each chamber to be less than the return pressure, which will possibly cause cavitation on the actuator. This valve is very similar to the Check Valves, where its function is to allow the flow to move only to one side.

All the check valves have a spring in order to keep the flow blocked in one direction. The inlet check valve, connected to the pressure line, has a very low cracking pressure to not degrade the actuator performance, although the return check valve has a high cracking pressure in order to guarantee a minimum pressure inside the actuator in case of a rupture of the hydraulic line.

The Reservoir is used to guarantee a minimum fluid volume and pressure inside the actuator in case of a hydraulic loss considering all the external leakages of the actuator. The pressure and fluid volume must be guaranteed since the damping characteristics of the actuator changes drastically with a reduction of the pressures inside the chambers.

The Actuator is composed by a piston and a sleeve, the piston normally is balanced, which means that the area of both sides are the same, thus the force is the same on both sides. There are some specific applications where the piston is unbalanced, used on asymmetrical loads application and when there is a restriction of installation envelope.

The Piston Ram LVDT is a Linear Variable Differential Transformer (LVDT) which is used to measure the surface position and close the position loop in order to obtain the commanded surface position.

For last there is the Control Surface, which its displacement is the intent of the whole hydraulic actuation system. The work herein developed will consider that the hydraulic actuation system is connected to the Elevator control surface. Although the model developed can be applied for any control surface connected to two actuators in active-active mode.

All the components described on this chapter will be later on modeled in order to develop the whole hydraulic actuation system. Only the Reservoir was not modeled, that is

due to the assumption that it will not impact on the actuator dynamics. Nevertheless the modeling of the Reservoir and the analysis of its impacts on the dynamics of the actuator can be suggested for future works.

3. FCS MODEL

On this chapter it will be detailed the Hydraulic Actuation System as it was implemented on the model of study. The model was developed with the MATLAB® and Simulink® software, one of the best development tools for this kind of application.

As described before, the FCS architecture chosen for this work can be basically divided by the Pilot Input, the Electronic System and by the Hydraulic Actuation System. Nevertheless in order to emulate the whole system it must be modeled the Hydraulic System, which will provide the hydraulic pressures for the Actuation System.

The Aerodynamic loads on the control surface should also be modeled in order to have a better representation of a real flight condition. Although it was decided to not model the aerodynamics loads, this is because it was considered that it would add an unnecessary complexity to the model. Nonetheless it was left an input to the aerodynamic load, which can be suggested to be modeled on future works.

Each one of the system components will be modeled accordingly to its influence on the final results. Therefore some components will be represented at a low fidelity basis, although the critical components will be designed at a high fidelity level of confidence even at high frequencies.

The overview of the whole system can be seen on the Figure 3-1.

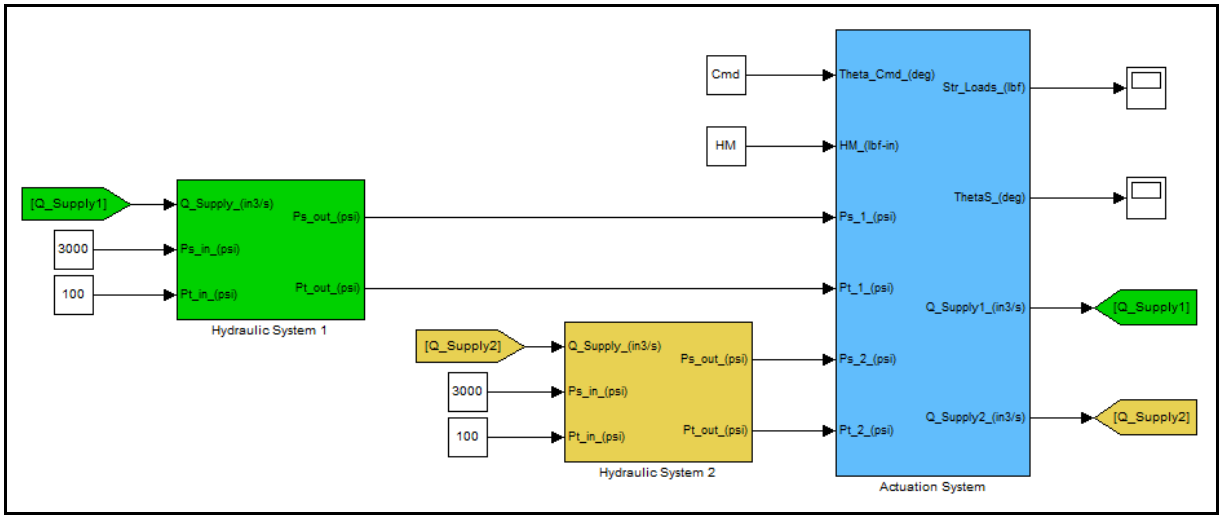

Figure 3-1 - Overview of the Hydraulic Actuation System

Source: Developed by the author

It can be seen on the Figure 3-1 only the Hydraulic System and the Actuation System, this is due to the decision to group all the Flight Control Systems (FCS) in one block.

Being the inputs and outputs of the Actuation System:

- Theta_Cmd_(deg): The Theta Command in degrees is the input signal from the Pilot or the Flight Control Computer to the Actuation System;
- Load_(lbf-in): The Hinge Moment of the aerodynamic load, herein used as a fixed value due to the absence of an aerodynamics model;
- Ps_1_(psi), Ps_2_(psi), Pt_1_(psi) and Pt_2_(psi): The hydraulic pressures, being Ps the supply pressure and the Pt, the return pressure. These pressures are provided by the Hydraulic System, which modeling will be described later on;

- Str_Loads_(N): The resultant loads applied on the Surface Structure by the actuation system;

- ThetaS_(deg): The resultant Control Surface Position in degrees.

- Q_Suppy1_(in3/s) and Q_Suppy2_(in3/s): The consumed flow from the Hydraulic System due to the actuator displacement.

It must be clear that it was adopted the English Units System, this was due to the fact that many units used on hydraulic actuation system are usually stated on the English system, such as psi for the hydraulic pressures, in for the actuator stroke, square in for the actuator piston area and in for the actuation kinematics.

It can be noticed that for the Actuation System block it is written on the inputs and outputs the signal unit, however this was not made for the sub-blocks, therefore it has to be clear that all the units used are on the English Units System.

3.1. Hydraulic System

The Hydraulic System modeled is based on a fixed pressure pump usually found on airplanes, this pump does not regulate the flow however it controls the stagnation pressure of the pump line.

Through the Bernoulli equation it can be found the relation between the stagnation, dynamic and static pressure, as described by Fox and McDonald [8], considering:

- Permanent flow;
- Incompressible fluid;
- Without friction;
- Through a pipe line;
- Without big variations of elevations.

Thus the Bernoulli equation is:

$$p_0 = p + \frac{1}{2}\rho V^2 \tag{3.1}$$

Being:

p_0 : Stagnation Pressure, psi

p : Static Pressure, psi

$\frac{1}{2}\rho V^2$: Dynamic Pressure, psi

Once we have a constant stagnation pressure, as we increase the hydraulic flow through the line, the dynamic pressure increases and the available static pressure decreases.

Since the actuation system force is generated by the static pressure, the effects of a pressure loss due to the actuator displacement must be designed in order to have a minimum degree of fidelity from the hydraulic supply.

However there is also the pressure loss of the hydraulic system, due to the line flow and the tubing losses which must be considered.

The pressure loss due to a line flow described by Fox and McDonald [8] is given by:

$$p_1 - p_2 = \rho \cdot h_l \tag{3.2}$$

$$h_l = f \frac{L}{D} \frac{V^2}{2} \tag{3.3}$$

$$f = \varphi\left(Re, \frac{e}{D} \right) \tag{3.4}$$

$$Re = \frac{\rho \bar{V} D}{\mu} \tag{3.5}$$

Being:

h_l : The pressure loss, psi.in³/lbs

ρ : The fluid density, lbs/in³

f : The friction factor, function of Reynolds and the tubing properties, dimensionless

L : The length of the hydraulic line, in

D : The hydraulic line diameter, in

V : The fluid velocity, in/s

e : The tubing roughness, in

$\bar{V}$: The average fluid velocity, in/s

μ : The fluid viscosity, lbs/(in.s)

For laminar flow the value for the friction factor f [8] is:

$$f = \frac{64}{Re} \tag{3.6}$$

Once Reynolds is a function of velocity, the resultant pressure loss is proportional to V instead of V square, although in a turbulent flow or in a line singularity such as line curves and junctions, the pressure loss is proportional to V square.

Since the Hydraulic system usually is designed to operate on a laminar regime in order to have the minimum hydraulic loss, it will be considered herein that the hydraulic loss can be stated as on the equation (3.7), where the hydraulic loss is a function of the hydraulic flow multiplied by a constant value.

$$p_1 - p_2 = C_1 \cdot V \tag{3.7}$$

Therefore the resultant modeling of the Hydraulic System developed can be seen on the Figure 3.1.

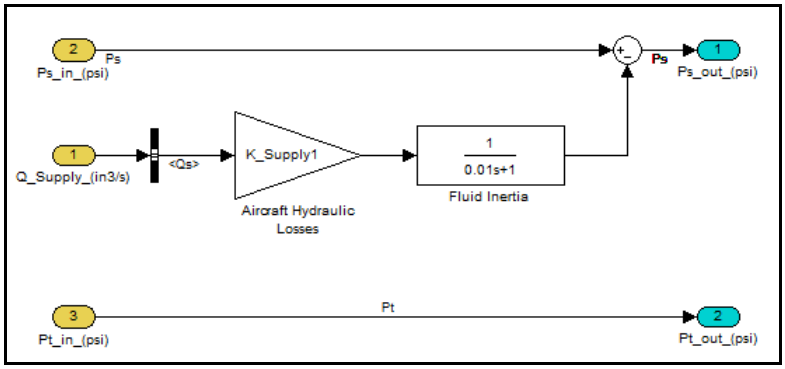

Figure 3.1 – Hydraulic System Block

Source: Developed by the author

As can be seen on the Hydraulic System block, the pressure of supply Ps is subtracted by the pressure loss as a function of the hydraulic system properties (K_Supply) and the hydraulic flow Qs.

Also it was implemented a Fluid Inertia that can be understood as a Low Pass Filter, where the high frequency variations of flow does not impact the pressure due to the inertia of the hydraulic line.

Pt_in and Pt_out are the representation of the return pressure line, since it is directly connected to the hydraulic system reservoir, it can be considered that the variations of flow will not change due to the displacement of the hydraulic actuator.

3.2. Actuation System

The hydraulic actuation system was divided in 3 parts: Electronic System, Actuator and Surface, as can be seen on the Figure 3-2 below.

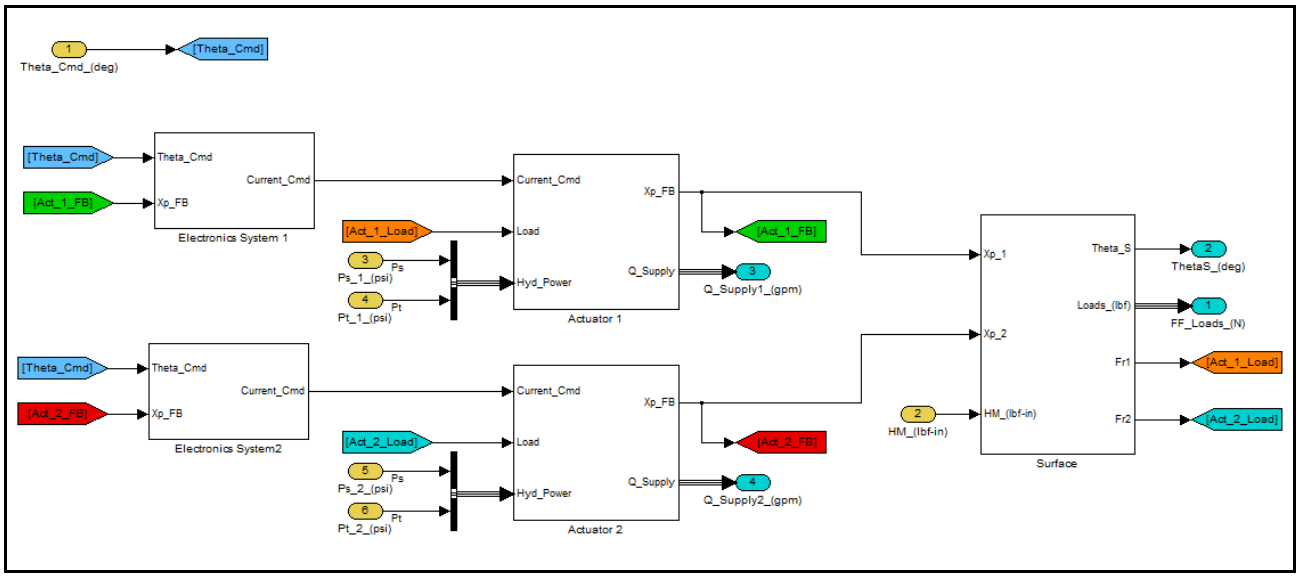

Figure 3-2 – Actuation System Block

Source: Developed by the author

The Electronic System represents the signal processing and the position loop. Since it was idealized as being a digital processor, and since the pilot input signal was considered to be analog, as well as the position feedback from the piston ram lvdt, it makes necessary to model a digital-to-analog converter inside the Electronic System.

The position loop is where it is evaluated the equivalent current command to the servovalve, according to the error between the commanded position and the feedback position.

The Actuator block represents the valves and the piston dynamics. The inputs are the Hydraulic pressure given by the Hydraulic System 1 and 2 as well as the current command. The results of the actuator block are the piston ram position and the flow required from the Hydraulic System.

The Surface block represents the modeling of the control surface, where for a given increment of each actuator piston ram position, the surface reacts according to a mass-spring-damper system. As explained before, since one actuator dynamics always differ from the other, it is expected that a certain level of Force-Fight will be generated for any actuator displacement, which will be evaluated inside the Surface block.

3.2.1. Electronic System

The electronic block is divided by two Hardware parts and the position loop, as can be seen on the Figure 3-3.

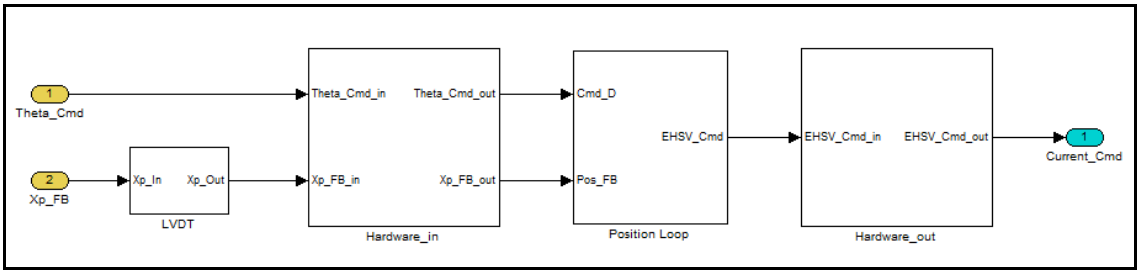

Figure 3-3 – Electronic Block

Source: Developed by the author

For this project it was considered the concept of a command signal transmitted analogically to the computer where the position loop is processed digitally, therefore it was designed the Hardware_in block and Hardware_out block where it was modeled a simple analog-to-digital converter.

Also it was modeled the LVDT block, which represents the dynamics and the proprieties of the LVDT sensor, as will be explained on the next item.

3.2.1.1. LVDT

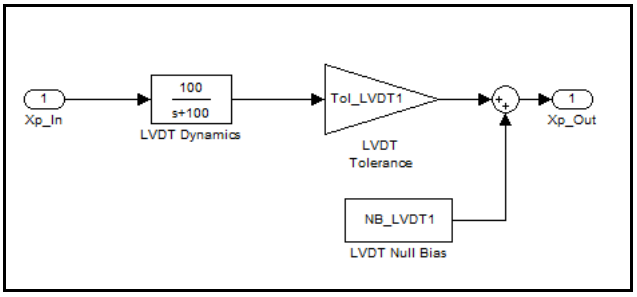

Figure 3-4 – LVDT Block

Source: Developed by the author

The LVDT block has a low-pass filter of 100Hz to emulate the dynamics of the LVDT. Also it has a tolerance gain, Tol_LVDT1, and a null bias error, NB_LVDT1.

3.2.1.2. Hardware_in

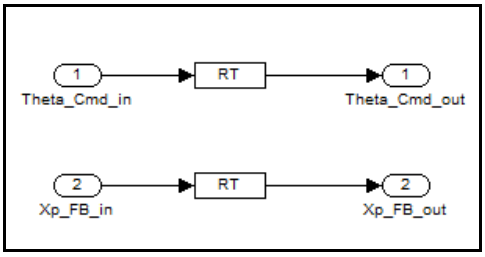

Figure 3-5 – Harware_in Block

Source: Developed by the author

The Hardware_in block has a Rate Transition in order to emulate the analog-to-digital converter, in such a way that the signal downstream of the Rate Transition is at 500Hz, which is the time step of the computer that has the position loop.

3.2.1.3. Position Loop

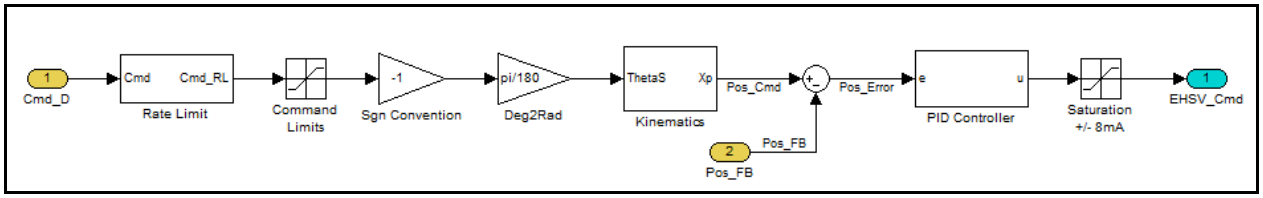

Figure 3-6 – Position Loop Block

Source: Developed by the author

The Position Loop Block converts the given Theta command into EHSV current. To do so, it has a digital PID Controller of the position error between the commanded and feedback position.

The theta commanded signal is treated in order to be transformed in a linear command to the actuator. First the rate of the command is limited in order to not demand too much velocity of the actuator, therefore depleting the hydraulic system due to a high flow demand.

After limiting the command rate, the command is limited to the surface design stops, for instance, in this case of study it was considered an elevator with a deflection limit of +15º and -25º.

Then the command signal is multiplied by -1, this is due to the aircraft signs convention, once that for the actuation system a positive increment of position means a positive increment of angular displacement, but, due to the installation assumed (see Figure 3-7), this positive increment means a trailing edge up of the surface, and for the aircraft convention this is at the negative direction.

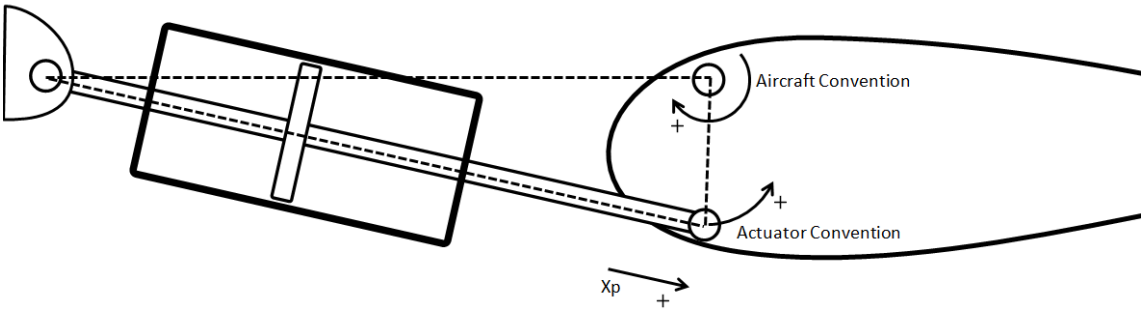

Figure 3-7 – Signal Convention

Source: Developed by the author

Afterward the signal in theta command is converted in linear command by the kinematics block, which is subtracted by the feedback position from the ram lvdt, resulting in the position error.

The position error is then inserted on the discrete PID controller resulting on the current command to the servovalve limited at ±8mA, which is the considered maximum allowable current of the servovalve modeled.

3.2.1.3.1. Rate Limit Block

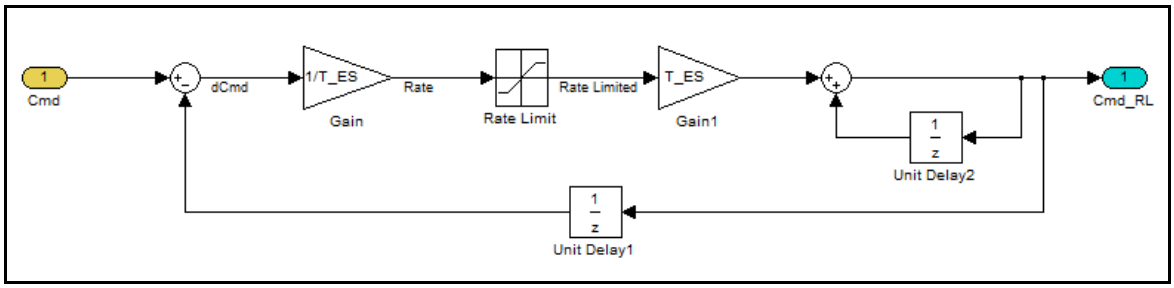

Figure 3-8 – Rate Limit Block

Source: Developed by the author

The commanded theta inserted on the Rate Limit block is then subtracted by the last value of theta after the rate limiting process, resulting in a ΔCmd, which means the delta command required to reach the actual command position. After that it is divided by the time step of the Electronic System, T_ES, resulting on the required commanded rate which is then limited by the Rate Limit.

The limited rate is then multiplied by the time step resulting on the delta commanded position already limited, which is added to the previous value of command resulting on the final commanded position.

3.2.1.3.2. Kinematics Block

The Kinematics Block evaluates the equivalent linear displacement of the actuator for the commanded surface angular position.

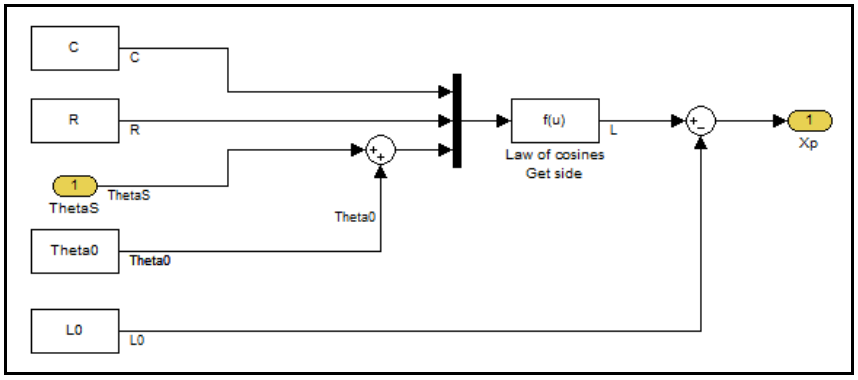

Figure 3-9 – Kinematics Block

Source: Developed by the author

Taking as reference the triangle RLC as shown on Figure 3-10, for a given command of surface angular position, it is added the neutral value of theta. By the Law of Cosines it can be found the equivalent value of L. Once the output must be an increment of linear displacement, it is subtracted the value of L at neutral, resulting in the linear command Xp.

The equation implemented on the Kinematics block “Law of Cosines – Get Side” is given by:

$$L = \sqrt{C^2 + R^2 - 2CR\cos\theta} \tag{3.8}$$

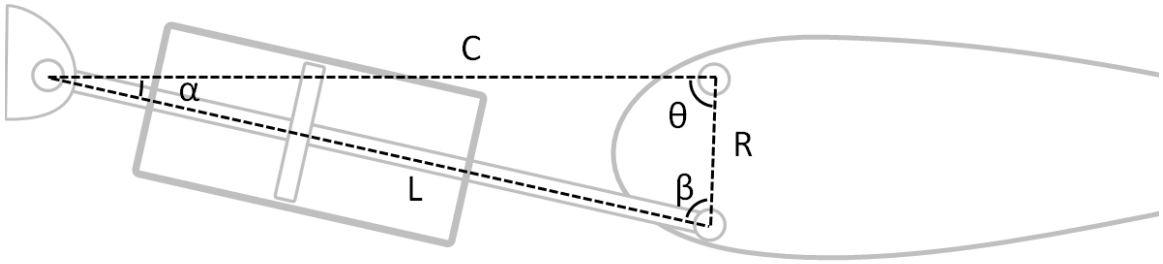

Figure 3-10 – Kinematics

Source: Developed by the author

3.2.1.3.3. PID Controller

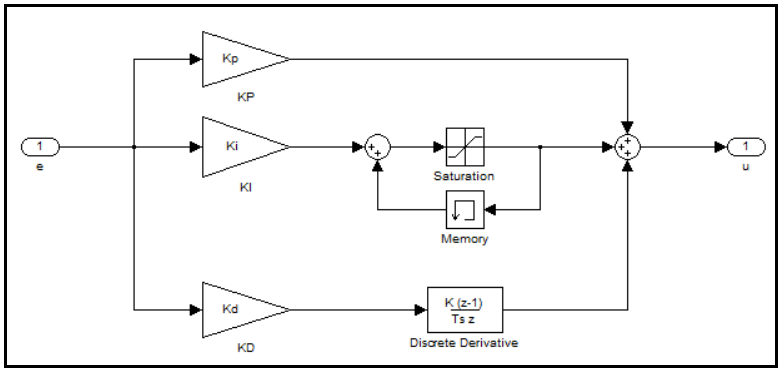

Figure 3-11 – PID Controller Block

Source: Developed by the author

The PID Controller Block is a classic discrete PID, with Kp, Ki and Kd as proportional, integral and derivative gains respectively. The integral path has an integral saturation, in order to not windup the integral path.

3.2.1.4. Harware_out Block

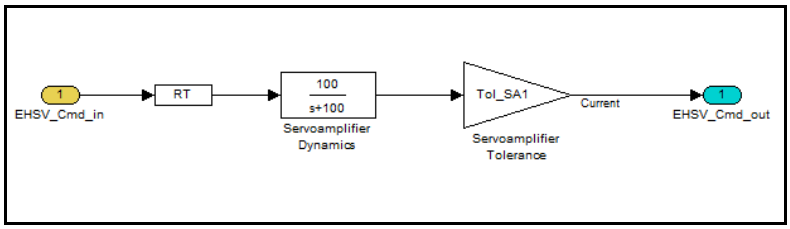

Figure 3-12 – Hardware_out Block

Source: Developed by the author

The Harware_out block has the Rate Transition emulating a digital-to-analog converter. Also it has a Servoamplifier Dynamics which modeled as a low pass filter at 100Hz and an error gain, Tol_SA1.

3.2.2. Actuator Block

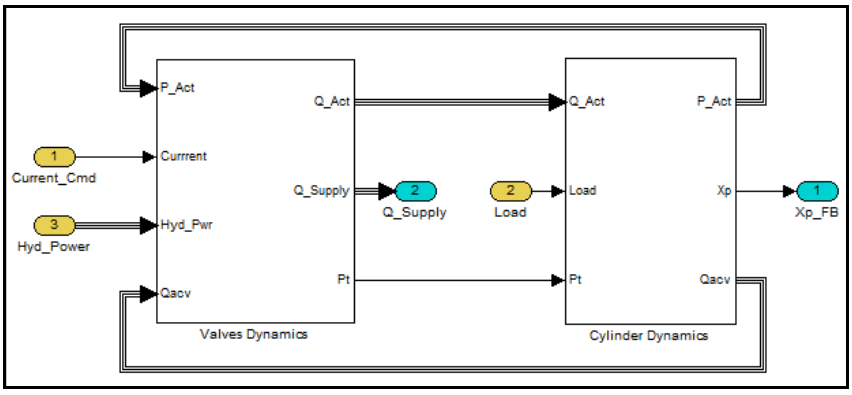

Figure 3-13 – Actuator Block

Source: Developed by the author

The actuator Block is composed by the Valve and the Cylinder Dynamics. The Valve Dynamics Block evaluates the dynamics of the EHSV and the inlet and return check valves, defining the hydraulic pressures inside the inlet and return lines, which, used with the pressure of each chamber, will result in the flow through each chamber, as well as the hydraulic supply demand. The signal of Qacv is the flow going through the Anti-Cavitation valve, herein designed inside the Cylinder Dynamics and will be furthermore explained.

The Cylinder Dynamics evaluates the amount of hydraulic pressure resultant inside each actuator chamber for a given hydraulic flow in and out the cylinder, which, integrated in a 2nd order piston dynamics, will result in the piston position, Xp.

3.2.2.1. Valves Dynamics

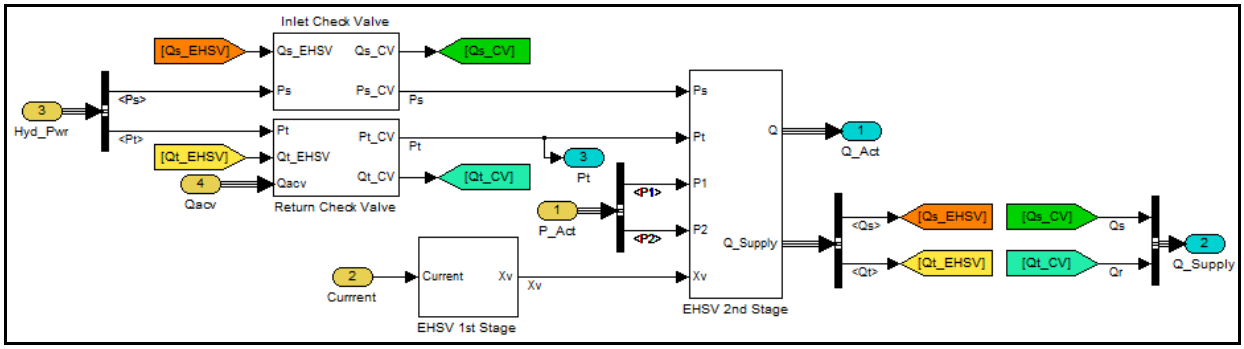

Figure 3-14 – Valves Dynamics

Source: Developed by the author

The Valve Dynamics Block, as mentioned before, evaluates the EHSV and the check valves dynamics. Therefore it was divided in 3 parts, the Inlet Check Valve Block, the Return

Check Valve Block and the EHSV herein represented by two blocks, the EHSV 1st Stage Block and the EHSV 2nd Stage Block.

The hydraulic pressure provided by the hydraulic system is inserted on the Inlet and Return Check Valves, which, in possession of the other flows going inside and outside the respective line volume, will evaluate the remaining pressure downstream the check valve, and also the resultant flow through the hydraulic system.

The pressures downstream the check valves will be used as input to the EHSV, which, with the current command, will evaluate the resultant spool position inside the 1st Stage block, and, with the spool position, will evaluate the resultant hydraulic flow through each path of the EHSV inside the 2nd Stage block.

3.2.2.1.1. Inlet Check Valve

The Inlet Check Valve is used to prevent a returning flow to the hydraulic system. The Figure 3-15 illustrates a schematic check valve.

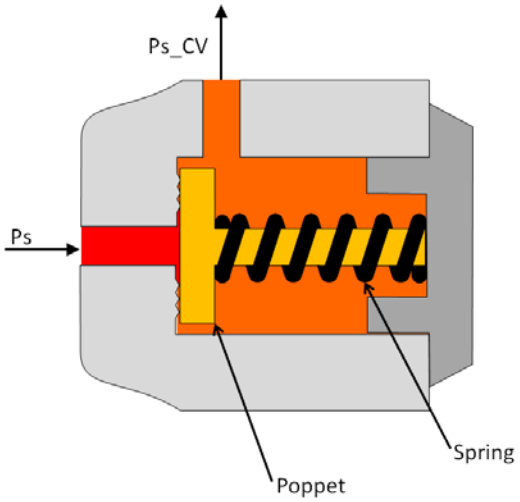

Figure 3-15 – Inlet Check Valve Schema

Source: Developed by the author

There are innumerous types of check valves available in industry [14]. However the one implemented on the model is based on the Figure 3-15. The supply pressure Ps is inserted through a hole which is closed by the poppet preloaded by the spring on the back.

Therefore only after the inlet pressure reaches a value higher than the loaded spring plus the force applied by the remaining pressure inside the check valve, Ps_CV, is that the poppet will open and release the flow through the valve.

The equation of the flow through an orifice can be applied to evaluate the flow of the valve, although the value of the discharge coefficient is considered variable according to the differential pressure of the valve.

The discharge coefficient will be zero when the pressure Ps_CV plus the cracking pressure Pcv is higher than the Ps. Thus the discharge coefficient will rise up to its maximum value equivalent to a fixed orifice value, herein considered 0.67.

The amount of pressure required to reach the maximum discharge coefficient depends on each check valve characteristics, therefore it was assumed herein that this will occur when the differential pressure reaches two times the cracking pressure.

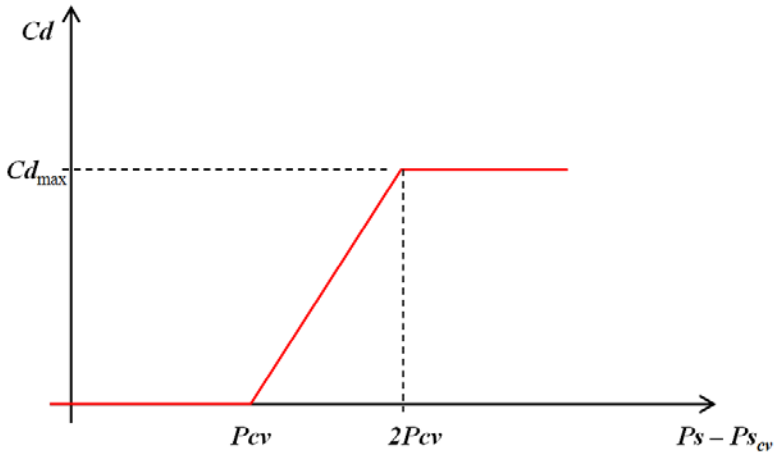

Figure 3-16 – Discharge Coefficient for a Check Valve

Source: Developed by the author

Therefore the flow though the valve can be evaluated by the Bernoulli Equation for incompressible fluids as can be found on Fox [8] and is given by:

$$Q_{CV} = C_d A_{CV} \sqrt{\frac{2\Delta P}{\rho}} \tag{3.9}$$

Where:

Q_{CV} = Flow though the valve, in³/s

C_d = Coefficient of Discharge, dimensionless

A_{CV} = Check Valve Orifice Area, in²

ΔP = Delta Pressure on the valve sides, psi

ρ = Fluid density, lbs/in³

To evaluate the pressure Ps_CV it can be used the continuity equation given by:

$$Q_{net} = \frac{dV}{dt} + \frac{V}{\beta_e}\frac{dP}{dt} \tag{3.10}$$

Where:

Q_{net} = Net Flow through the volume, in³/s

$\frac{dV}{dt}$ = Volume variation during time, in³/s

β_e = Bulk Modulus, psi

$\frac{V}{\beta_e}\frac{dP}{dt}$ = Fluid compressibility, in³/s

The volume of control is the line between the check valve and the EHSV, as represented on the Figure 3-17.

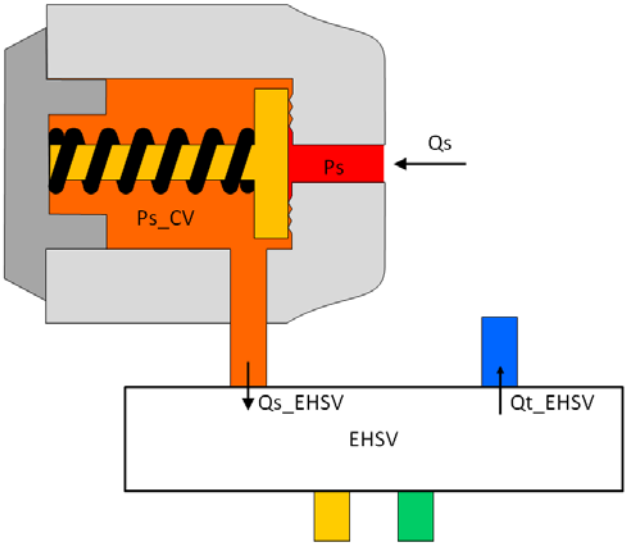

Figure 3-17 – Inlet Check Valve Volume

Source: Developed by the author

The net flow through the volume is Qs minus Qs_EHSV. And, as the volume does not change in time, the component of the volume variation is equal to zero. Therefore the equation (3.10) can be written as:

$$Ps_{CV} = \frac{\beta_e}{V}\int (Q_s - Q_{sEHSV})dt \tag{3.11}$$

The Figure 3-18 and Figure 3-19 shows the Inlet Check Valve as designed on the model based on equations (3.9) and (3.11).

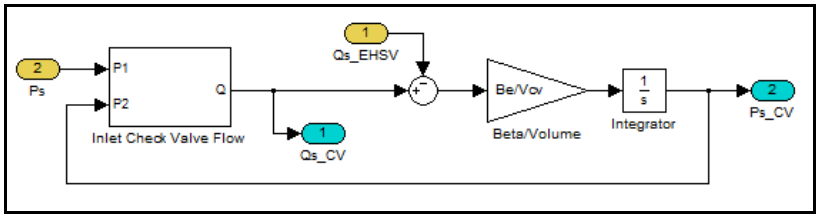

Figure 3-18 – Inlet Check Valve Block

Source: Developed by the author

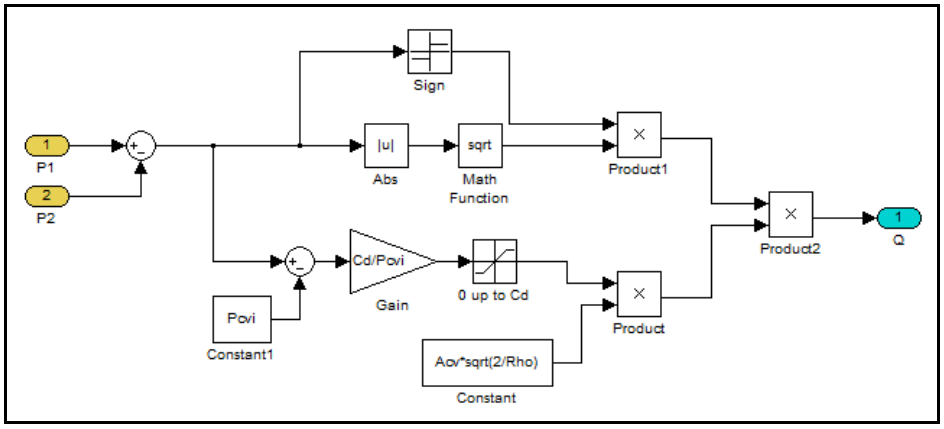

Figure 3-19 – Inlet Check Valve Flow Block

Source: Developed by the author

3.2.2.1.2. Return Check Valve

The Return Check Valve is essentially the same valve as the Inlet Check Valve, but in this case its intent is to prevent pressure lost inside the actuator in case of a failure in the hydraulic system.

The minimum pressure required inside the actuator in a failure scenario usually is around 100psi. Therefore the cracking pressure of the return check valve must be sized for this particular case.

The volume of the return line is not as simple as it is on the inlet line, as shown on the Figure 2-1. It can be seen that on the return line is connected the Return Check valve, the EHSV, the Anti-Cavitation valves and the Reservoir.

As mentioned before, the Reservoir will be not implemented on this design once that it should not have an impact on the dynamics of the actuator.

The Anti-Cavitation Valves will be implemented furthermore, although for the evaluation of the net flow inside the volume, the value of the anti-cavitation valves flow will have to be considered. Therefore the net flow for the return line is given by:

$$Q_{net} = Q_{tEHSV} - Q_t - Q_{AC} \tag{3.12}$$

The Figure 3-20 and Figure 3-21 show the return valve block implementation as described above.

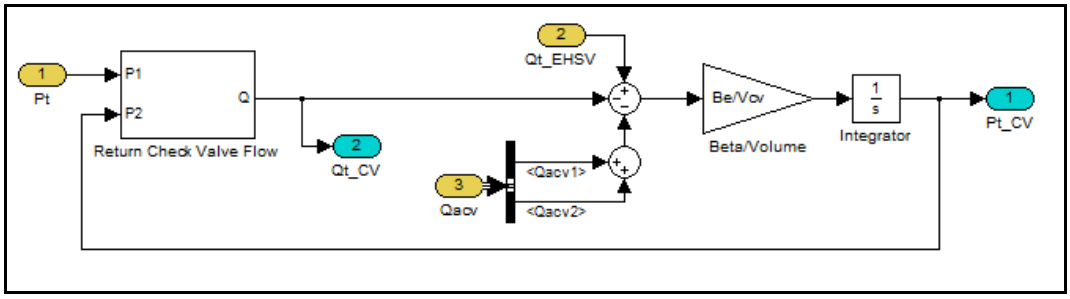

Figure 3-20 – Return Check Valve Block

Source: Developed by the author

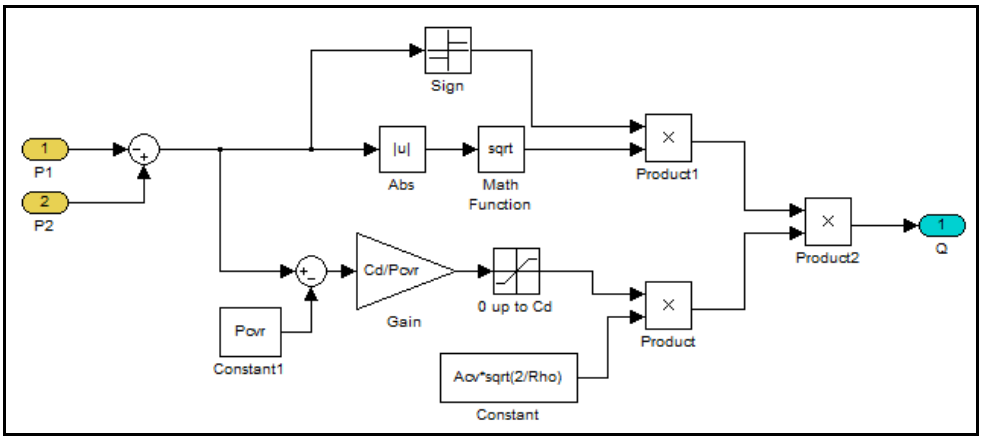

Figure 3-21 – Return Check Valve Flow Block

Source: Developed by the author

3.2.2.1.3. EHSV 1st Stage Block

The modeling of a “Two-Stage Electrohydraulic Servovalve with Force Feedback” can be found on Merritt [10]. The schematic of the servovalve is shown on the Figure 2-2.

In order to achieve a hydraulic actuation system modeling representative up to high frequencies, is crucial to model a high detailed servovalve, therefore some clarifications of how the ESVH works will be described herein.

An electromagnetic field is generated though the solenoid when a current is inserted on the EHSV. This field reacts with the permanent magnet inside the servovalve creating a torque force on the flapper.

Thus the flapper directs the hydraulic flow to one side of the spool, increasing the pressure in one side of the spool making it moves to the opposite direction of the flapper displacement, until the feedback spring force balances the flapper torque.

The EHSV can be controlled by a flapper or a jet pipe, although, from the point of view of modeling, the both servovalves types are the same.

The flapper, represented on the Figure 2-2, has a flapper that obstructs the flow between the pressure and return, therefore creating a differential pressure on the spool sides.

The jet pipe, represented on the Figure 3-22, has a hydraulic flow going inside the jet pipe. At neutral position the flow is distributed equally between the spool sides, and when the jet pipe moves it creates a differential pressure on the spool sides.

A schematic of the EHSV operation can be seen on the Figure 3-22.

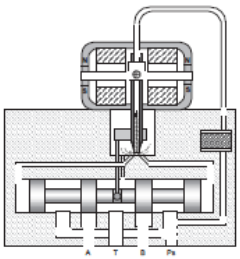

Figure 1a - At Neutral

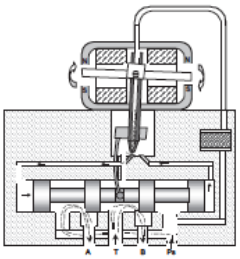

Figure 1b - With Input Current

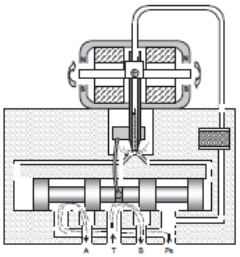

Figure 1c - Stabilized with Current

Figure 3-22 – EHSV Operation

Source: http://www.moog.com/literature/ICD/jet_pipe_servovalves_overview.pdf accessed at 15/01/10

The armature torque equation can be written as by Merritt [10]:

$$K_t \Delta i = J_a s^2 \theta + K_{an} \theta + r P_{Lp} A_N + (r+b) K_f \left[(r+b)\theta + x_v \right] \tag{3.13}$$

Where:

K_t = torque constant of the torque motor, in.lb/mA

Δi = delta current as input to the servovalve, mA

J_a = inertia of armature and any attached load, in.lb.s²

θ = rotation angle of the flapper, rad

K_{an} = net spring rate, in.lb/rad

r = distance between center of armature and flapper, in

$P_{Lp} = P_{1p} - P_{2p}$ = flapper valve load pressure, psi

A_N = nozzle area, in²

b = distance between flapper and spool, in

K_f = spring constant of the cantilevered feedback spring at the free end, lb/in

x_v = spool position, in

The value of the coefficient $rP_{Lp}A_N$ was considered very small and should not interfere on the spool dynamics. Therefore it was neglected from the equation. Also it is a standard practice on the servovalves design that the value of K_{an} is equal to zero in order to maximize the spool velocity constant [10], therefore the transfer function between the current and the flapper angle is:

$$\frac{\Delta\theta}{K_t\Delta i - (r+b)K_f\Delta x_v} = \frac{1}{J_a s^2 + K_f (r+b)^2} \tag{3.14}$$

The transfer function of the flapper to the spool position is given by Merritt [9]:

$$\frac{\Delta x_v}{\Delta x_f} = \frac{\frac{K_{qp}}{A_v}}{s\left(\frac{s^2}{\omega_{hp}{}^2} + \frac{2\delta_{hp}}{\omega_{hp}} + 1\right)} \tag{3.15}$$

Where the variables not yet defined are:

$\Delta x_f = r\Delta\theta$ = linear displacement of the flapper, in

$\omega_{hp} = \sqrt{\frac{2\beta_e A_v^{\,2}}{V_{0p} M_v}}$ = hydraulic natural frequency of pilot stage, rad/s

$\delta_{hp} = \frac{\omega_{hp} K_{cp} M_v}{2A_v^{\,2}}$ = damping ratio of pilot stage, dimensionless

K_{qp} = flow gain of flapper valve, in³/s/psi

A_v = area of spool, in²

β_e = Bulk Modulus, psi

V_{0p} = contained volume at each end spool, in³

K_{cp} = flow pressure coefficient of pilot valve, in³/s/in

In possession of these equations it is possible to create the block diagram of the servovalve as can be seen on Figure 3-23.

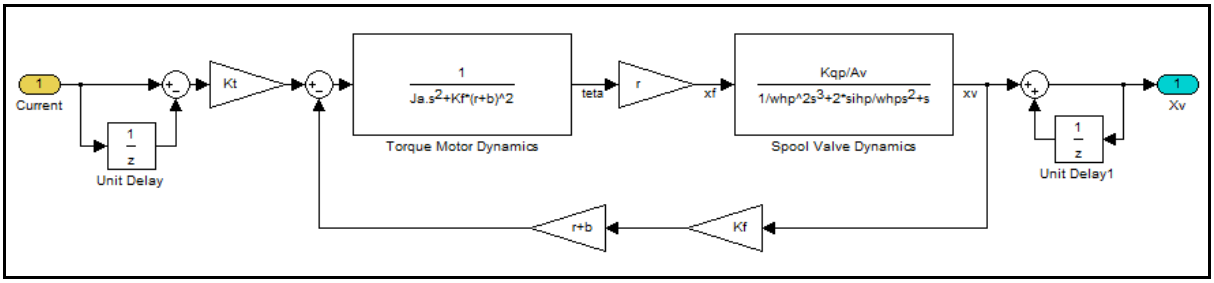

Figure 3-23 – EHSV 1st Stage Block

Source: Developed by the author

It must be clear that input and output of the EHSV is a non-linear value and as the equation defined by Merritt are linear, it has to be evaluated the delta current at the block entrance and the sum value at the output.

3.2.2.1.4. EHSV 2nd Stage Block

The 2nd Stage Block evaluates the flow through each path on the EHSV for a given spool position.

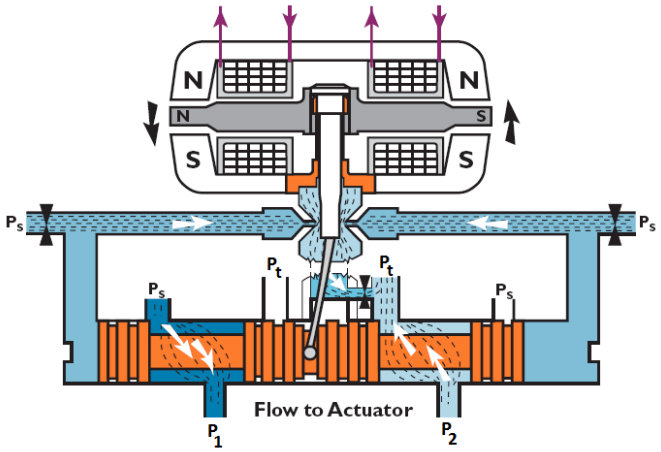

Figure 3-24 – EHSV Flow Paths

Source: Adopted from http://www.moog.com/literature/ICD/Valves-Introduction.pdf accessed at 15/01/10

As can be seen on the Figure 3-24, when the spool moves to the left, the flow through the land between P_s and P_1 is released, the same occurs between P_2 and P_t, where P_1 and P_2 means the pressure on extension and retraction chamber of the actuator respectively, and P_s and P_t means the supply and return pressure respectively.

If the spool moves to the other direction, the released flow will be between P_s and P_2, and P_1 and P_t.

Although the main flow is the ones described above, it has to be considered a leakage value through each land, once that some amount of leakage is inherent of the construction of the valve. Therefore, for instance, when the spool moves to the left, is expected a leakage flow between P_1 and P_t, also between P_s and P_2.

Also there is a 5^{th} path between P_s and P_t that will always have some amount of flow. This is due to the concept of the valve of using the supply pressure to direct the flow to the sides of the spool in order to generate the differential pressure on the spool sides.

Therefore it was created a block with all the flows paths designed, as can be seen on the Figure 3-25.

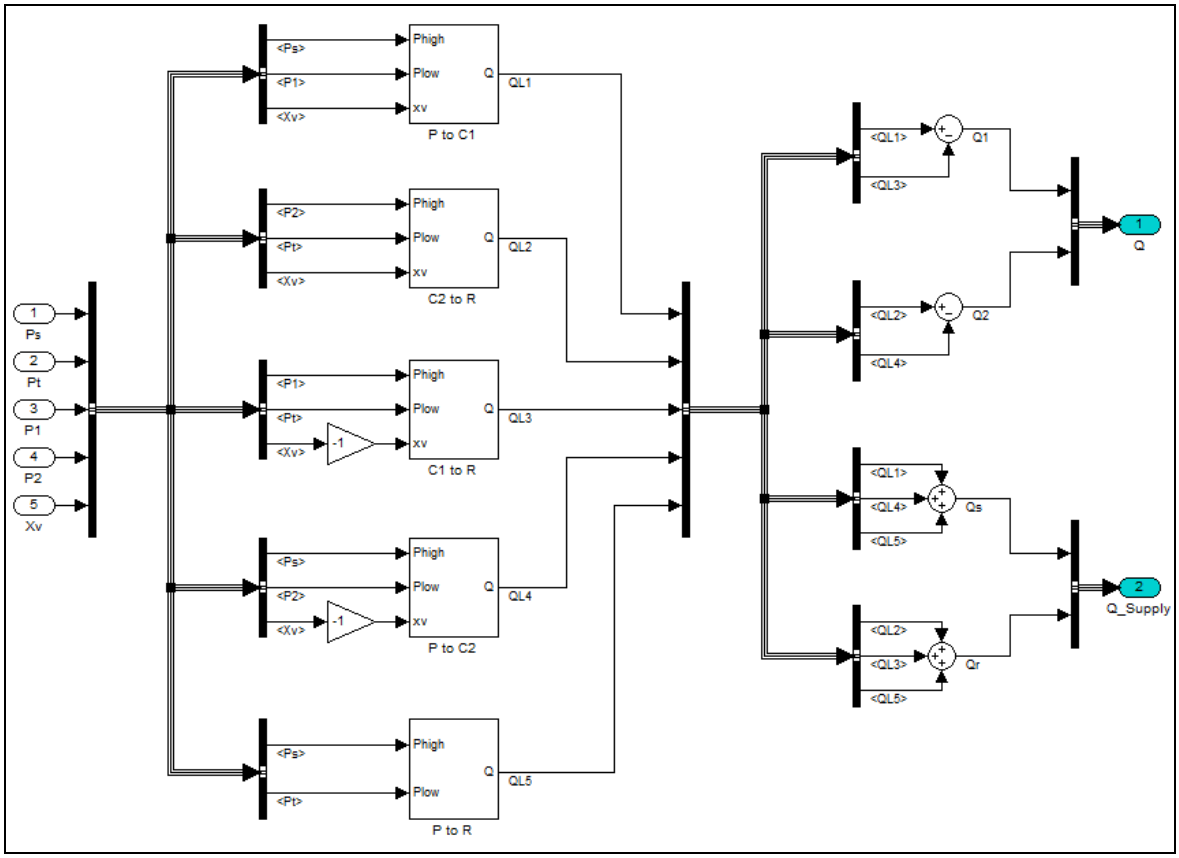

Figure 3-25 – EHSV 2nd Stage Block

Source: Developed by the author

The first part is to evaluate the flow through each path using the equation (3.9). Herein, it was assumed that the P_s is higher than P_1 and P_2, and P_t is lower than P_1 and P_2.

The Figure 3-26 represents the flow evaluation of Q_{L1}, Q_{L2}, Q_{L3} and Q_{L4}. The Figure 3-27 represents the flow evaluation of Q_{L5}.

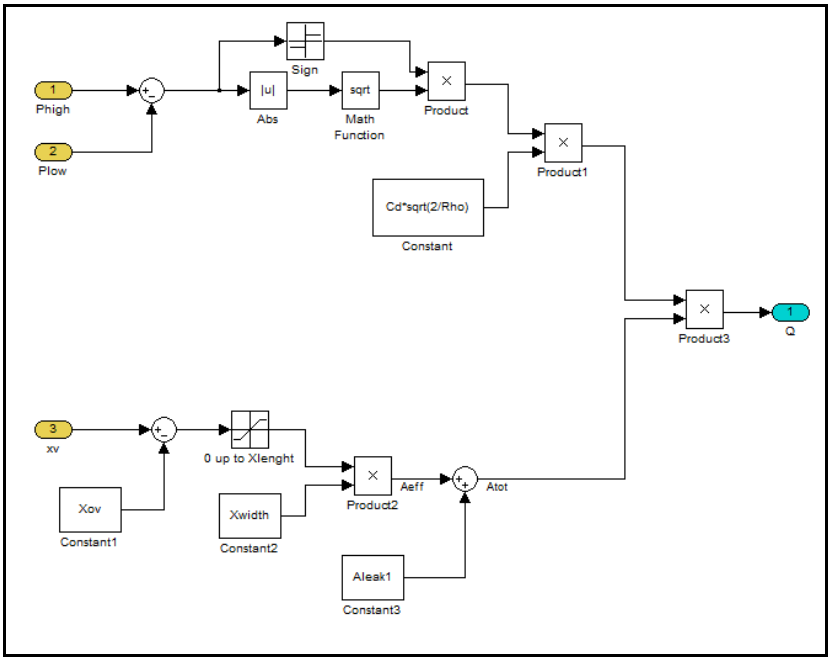

Figure 3-26 – Flow Evaluation through the EHSV paths

Source: Developed by the author

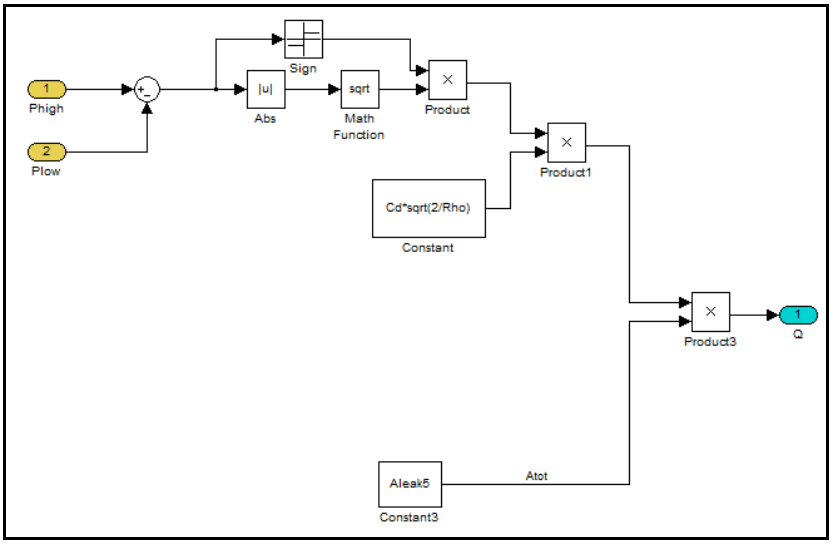

Figure 3-27 – Flow Evaluation between Ps and Pt inside the EHSV

Source: Developed by the author

In order to evaluate the orifice area for the EHSV paths, it was considered a rectangular orifice with a fixed width of Xwidth and a variable length with a maximum value of Xlength, as can be seen on the Figure 3-28.

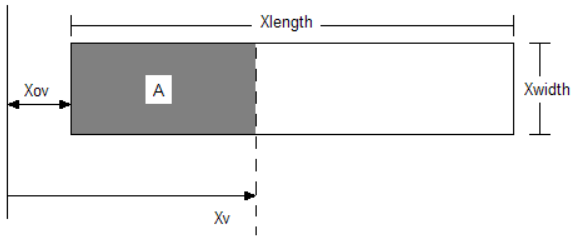

Figure 3-28 – Spool Orifice

Source: Developed by the author

The Xov is the overlap value of the spool, therefore only after Xv is greater than Xov that some amount of flow will pass through the orifice. The valve can be designed to have an overlap or an underlap, depending on design drivers of each system. Herein it was considered an overlap design, although a negative value of Xov represents an underlap configuration.

The way that the spool position was assumed, being the zero the value at neutral, it has to be noted that the path through P_s to P_2 and P_1 to P_t is open for negative values of Xp, therefore the value of Xp is multiplied by -1 prior to be inserted on the block.

After evaluating the flow through each path, the flows are joined in order to evaluate the resultant flow through each chamber, as well as through the hydraulic lines. Therefore the resulting flows can be evaluated by:

$$Q_1 = Q_{L1} - Q_{L3} \tag{3.16}$$

$$Q_2 = Q_{L2} - Q_{L4} \tag{3.17}$$

$$Q_s = Q_{L1} + Q_{L2} + Q_{L5} \tag{3.18}$$

$$Q_t = Q_{L3} + Q_{L4} + Q_{L5} \tag{3.19}$$

Being:

Q_1: Flow between the servovalve and the actuator extension chamber

Q_2: Flow between the actuator retraction chamber and the servovalve

Q_s: Flow between the hydraulic supply line and the servovalve

Q_t: Flow between the servovalve and the hydraulic return line

Q_{L1}: Flow through the path between P_s and P_1

Q_{L2}: Flow through the path between P_2 and P_t

Q_{L3}: Flow through the path between P_1 and P_t

Q_{L4}: Flow through the path between P_s and P_2

Q_{L5}: Flow through the path between P_s and P_t

3.2.2.2. Cylinder Dynamics Block

After evaluating the amount of flow that is going into or out of each chamber, it can be evaluated the pressures inside the chambers and, with these values, calculate the piston dynamics resulting on the piston ram position.

The Figure 3-29 shows the Cylinder Dynamics block modeled, which was divided in two parts, the Fluid Dynamics block, which evaluates the pressures on each actuator chamber; and the Piston Dynamics block.

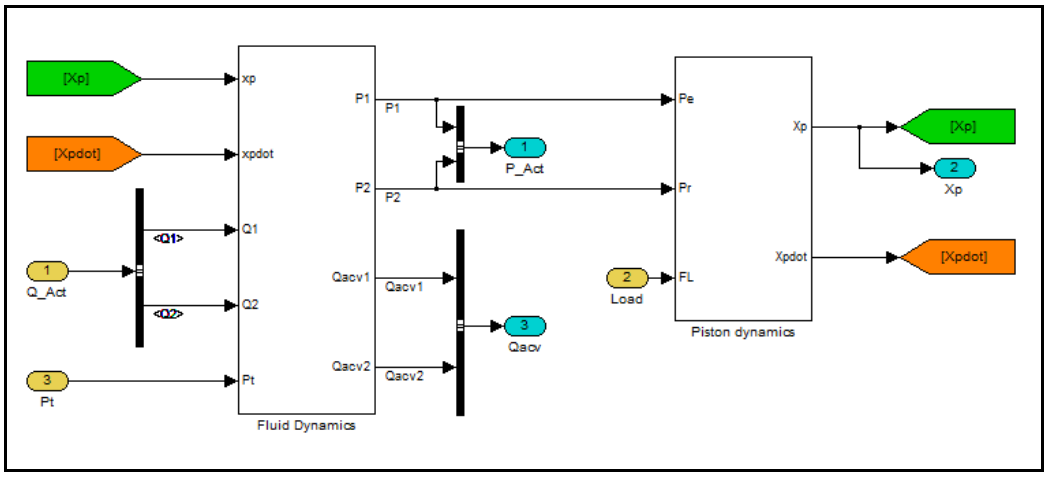

Figure 3-29 – Cylinder Dynamics Block

Source: Developed by the author

3.2.2.2.1. Fluid Dynamics Block

Taking as reference the Figure 3-30 adopted from Merritt [10] and considering that it should be added the anti-cavitation valves on the lines that connects the EHSV to the piston chambers, the continuity equation of the system can be evaluated and given by:

$$Q_1 - Q_{ip} - Q_{ep1} + Q_{AC1} = \frac{dV_1}{dt} + \frac{V_1}{\beta_e}\frac{dP_1}{dt} \tag{3.20}$$

$$Q_{ip} - Q_{ep2} - Q_2 + Q_{AC2} = \frac{dV_2}{dt} + \frac{V_2}{\beta_e}\frac{dP_2}{dt} \tag{3.21}$$

Where:

$Q_{ip} = C_d A_{ip}\sqrt{\frac{2(P_1 - P_2)}{\rho}}$ = internal leakage flow between chambers, in³/s

$Q_{ep1} = C_d A_{ip}\sqrt{\frac{2P_1}{\rho}}$ = external leakage flow on extension chamber, in³/s

$Q_{ep2} = C_d A_{ip}\sqrt{\frac{2P_2}{\rho}}$ = external leakage flow on retraction chamber, in³/s

$Q_{AC1} = C_d A_{CV}\sqrt{\frac{2(P_t - P_1)}{\rho}}$ = flow through the anti-cavitation valve on extension line, in³/s

$Q_{AC2} = C_d A_{CV} \sqrt{\frac{2(P_t - P_2)}{\rho}}$ = flow through the anti-cavitation valve on retraction line, in³/s

$\frac{V}{\beta_e}\frac{dP}{dt}$ = volume variation due to the fluid compressibility, in³/s

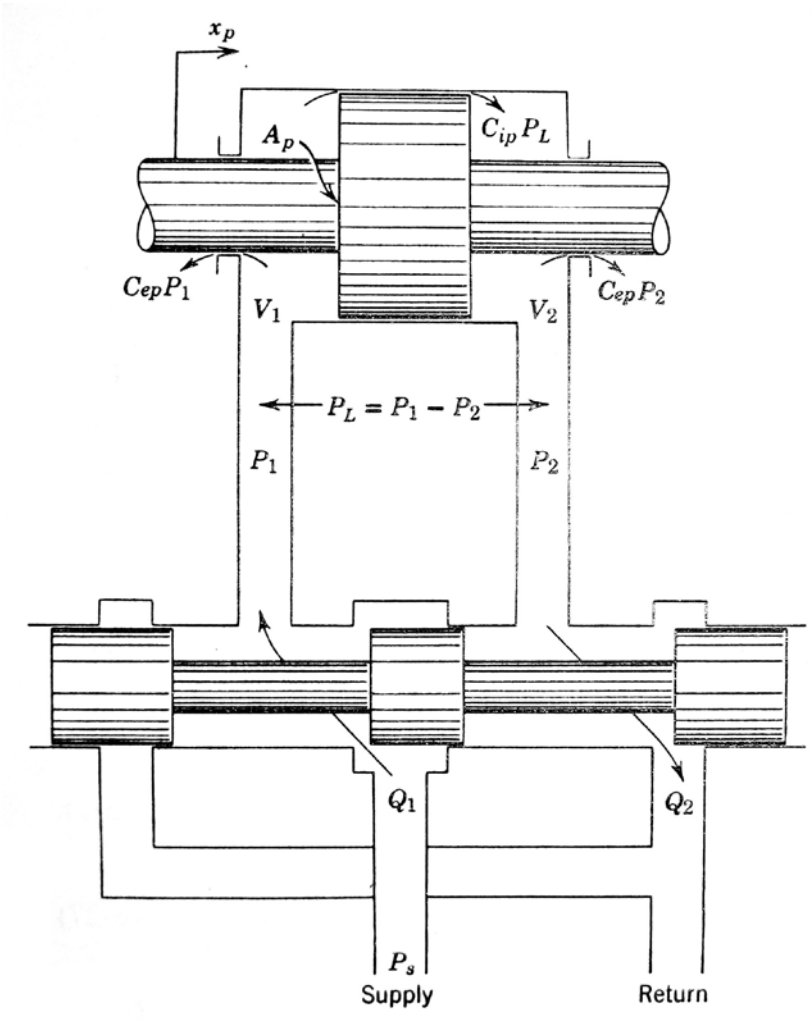

Figure 3-30 – Valve-piston Combination

Source: Adopted from Merritt, Herbert E. – "Hydraulic Control Systems"

The piston volumes can be evaluated as:

$$V_1 = V_{01} + A_p x_p \tag{3.22}$$

$$V_2 = V_{02} - A_p x_p \tag{3.23}$$

Where;

V_{01}, V_{02} = Chamber volume with piston at neutral position, in³

Therefore the pressure on each chamber can be found by the following equations:

$$P_1 = \frac{1}{s}\frac{\beta_e}{V_1}\left(Q_1 - A_p \dot{x}_p - Q_{ep} - Q_{ip}\right) \tag{3.24}$$

$$P_2 = \frac{1}{s}\frac{\beta_e}{V_2}\left(A_p \dot{x}_p - Q_{ep} + Q_{ip} - Q_2\right) \tag{3.25}$$

The Figure 3-31 represents the modeled Fluid Dynamics based on the resultant equations as described above. Note that for the evaluation of the internal and external leakages it was used the same rationale used for the flow through a fixed orifice as described before, therefore the block Int Leak and Ext Leak have the same construction of the block shown on Figure 3-27.

For the Anti-Cavitation valve modeling it was used the same principles of the check valve modeling, therefore the block Anti-Cavitation Valve has the same construction of the block shown on the Figure 3-19 or Figure 3-21.

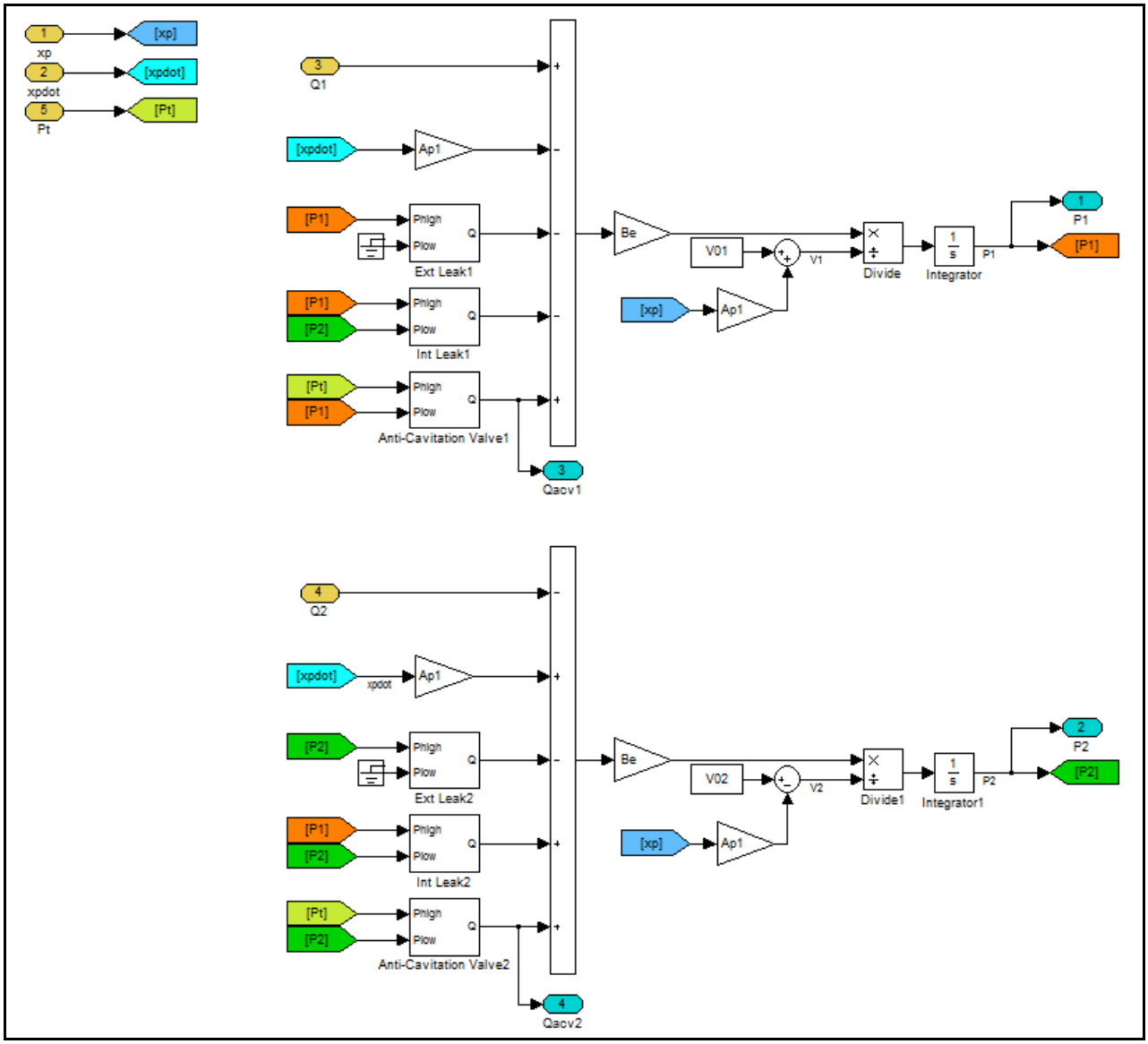

Figure 3-31 – Fluid Dynamics Block

Source: Developed by the author

3.2.2.2.2. Piston Dynamics Block

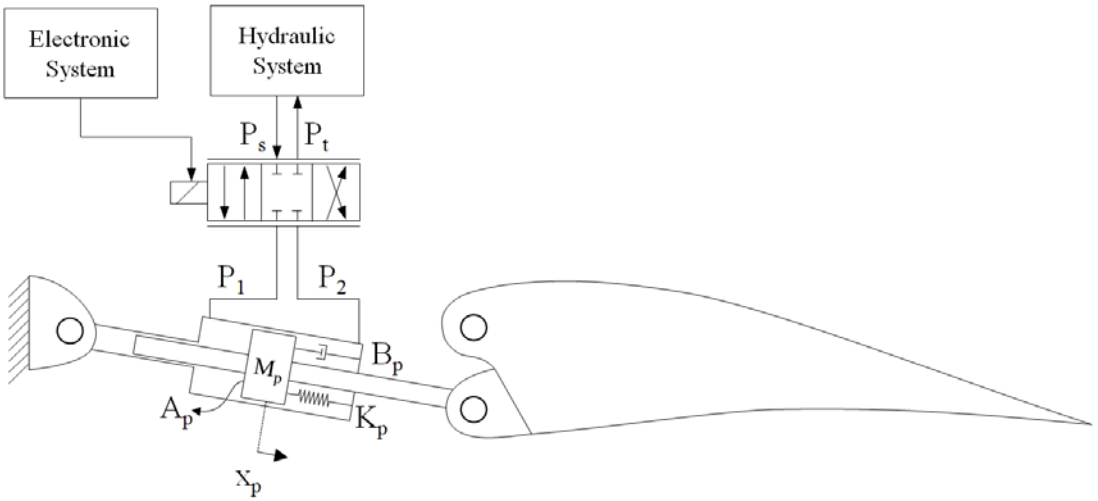

Figure 3-32 – Hydraulic Actuation System Schematic – Piston Dynamics

Source: Developed by the author

The Figure 3-32 represents a schema of the interface of the actuator with the servovalve and the control surface.

As explained before, the dynamics of the servovalve will determine the pressures inside each chamber of the actuator. The difference between the pressures times the piston area results on the amount of hydraulic force imposed on the piston.

This force will impose a piston displacement that will create a reaction due to the piston inertia and the fluid viscosity and stiffness. Also the piston displacement will generate a surface rotation that will react due to its inertia, which will be furthermore explained.

Applying Newton's second law to the forces on the piston, the force equation can be evaluated as shown by Merritt [10].

$$A_p\left(P_1 - P_2\right) = M_p s^2 x_p + B_p s x_p + K_p x_p + F_L \tag{3.26}$$

Where:

A_p = Piston Area, in²

M_p = Piston mass, lbs

B_p = Viscous damping coefficient of piston, in.lbf/s

K_p = Piston stiffness, lbf/in

F_L = External load on piston, lbf

Therefore the equation implemented on the Piston Dynamics Block shown on Figure 3-33 that evaluates the piston position is given by;

$$x_p = \frac{1}{s^2}\frac{1}{M_p}\left(A_p\left(P_1 - P_2\right) - B_p\dot{x}_p - K_p x_p - F_L\right) \tag{3.27}$$

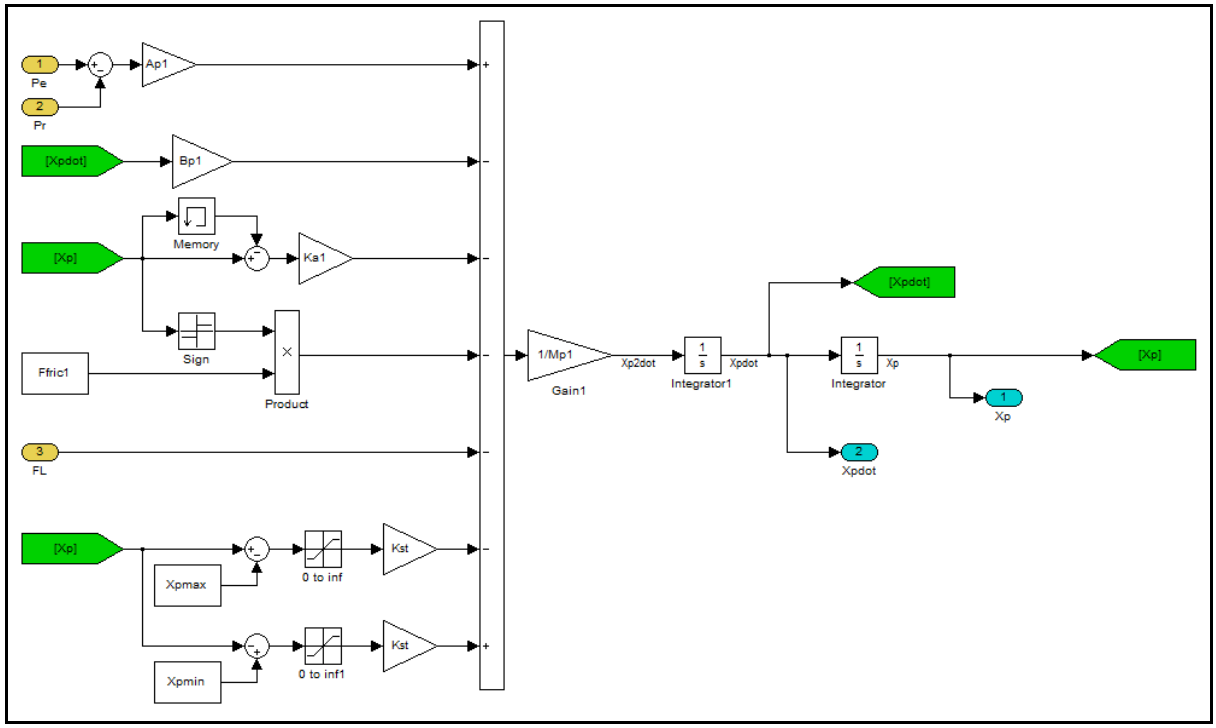

Figure 3-33 – Piston Dynamics Block

Source: Developed by the author

As can be noticed, it was also implemented two additional components on the equation. These components evaluate the forces reacting on the piston in case of the actuator hitting the piston structural stop.

It is a design driver of the actuator stroke to be high enough in order to never have the piston hitting the actuator structure stop. This is driven by the fact that the loads generated on this condition can easily consume excessive fatigue life of the actuator, unless when it was already designed to withstand this amount of load.

The output of the block is the piston head position. Thus, in possession of this value, the forces to move the surface will be evaluated by the Surface Block that will be described on the next chapter.

3.2.3. Surface

The Surface block will evaluate the angular position of the control surface, as well as the reaction forces generated due to the actuator displacement. In order to better understand the surface dynamics, consider the Figure 3-34 where it is shown the interface between the surface and the actuators.

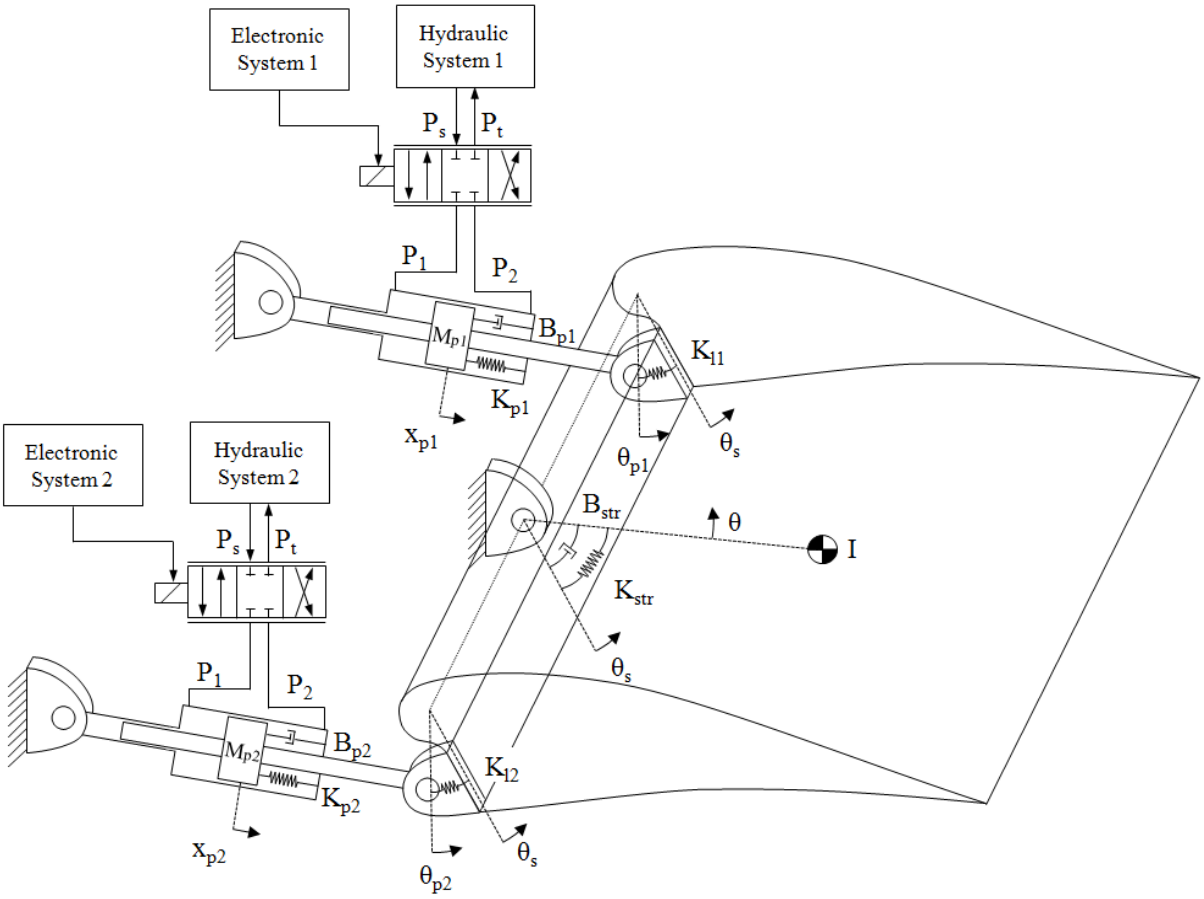

Figure 3-34 – Hydraulic Actuation System Schematic – Surface Dynamics

Source: Developed by the author

As described on the previous chapter, the Piston Dynamics block will evaluate the piston dynamics, Xp1 and Xp2, which will impose a rotation of the surface. The correspondent rotation due to the piston displacement is defined by the kinematics of each actuator, resulting in θp1 and θp2.

Thus this rotation will compress or extend an equivalent torsion spring of the piston ram fixture, Kl1 and Kl2, which will impose a rotation of the surface spar, herein considered to have very high torsion stiffness, resulting on a constant value of θs for the whole spar.

Thus the spar dynamics will impose a rotation of the surface, which was herein simplified to have only one articulation point and was reduced to an equivalent stiffness Kstr and a structural damping of Bstr linked to the center of gravity of the surface. Therefore, by evaluating the dynamics of the surface, it can be found the resultant surface angular position given by θ.

In order to solve the dynamic equation of the surface, it was previous evaluated the equivalent stiffness from the piston ram to the surface center of gravity. Applying the Hooke's Law in parts, it can be determined the stiffness force between θp, θs and θ, which is given by:

$$T_1 = K_{l1}\left(\theta_{p1} - \theta_s\right) \tag{3.28}$$

$$T_2 = K_{l2}\left(\theta_{p2} - \theta_s\right) \tag{3.29}$$

$$T = K_{str}\left(\theta_s - \theta\right) \tag{3.30}$$

Being:

T_1: Torque generated from the compression or extension of the actuator 1 fixture, lbf.in

T_2: Torque generated from the compression or extension of the actuator 2 fixture, lbf.in

T : Torque generated from the compression or extension of the control surface, lbf.in

For the equilibrium equation it can be defined the relation between the angular positions in order to find the value of θs function of θp and θ. Thus:

$$T = T_{r1} + T_{r2} \tag{3.31}$$

$$K_{str}\left(\theta_s - \theta\right) = K_{l1}\left(\theta_{p1} - \theta_s\right) + K_{l2}\left(\theta_{p2} - \theta_s\right)$$

$$K_{str}\theta_s + K_{l1}\theta_s + K_{l2}\theta_s = K_{str}\theta + K_{l1}\theta_{p1} + K_{l2}\theta_{p2}$$

$$\theta_s = \frac{K_{str}\theta + K_{l1}\theta_{p1} + K_{l2}\theta_{p2}}{K_{str} + K_{l1} + K_{l2}} \tag{3.32}$$

Thus the torque equation can be rewritten as:

$$T_1 = K_{l1}\left(\theta_{p1} - \frac{K_{str}\theta + K_{l1}\theta_{p1} + K_{l2}\theta_{p2}}{K_{str} + K_{l1} + K_{l2}}\right)$$

$$T_1 = K_{l1}\frac{K_{str}\theta_{p1} + K_{l1}\theta_{p1} + K_{l2}\theta_{p1} - K_{str}\theta - K_{l1}\theta_{p1} - K_{l2}\theta_{p2}}{K_{str} + K_{l1} + K_{l2}}$$

$$T_1 = \frac{K_{l1}K_{str}\left(\theta_{p1} - \theta\right) + K_{l1}K_{l2}\left(\theta_{p1} - \theta_{p2}\right)}{K_{str} + K_{l1} + K_{l2}} \tag{3.33}$$

The same can be applied to the other torque equations, resulting in:

$$T_2 = \frac{K_{l2}K_{str}\left(\theta_{p2} - \theta\right) + K_{l1}K_{l2}\left(\theta_{p2} - \theta_{p1}\right)}{K_{str} + K_{l1} + K_{l2}} \tag{3.34}$$

$$T = \frac{K_{l1}K_{str}\left(\theta_{p1} - \theta\right) + K_{l2}K_{str}\left(\theta_{p2} - \theta\right)}{K_{str} + K_{l1} + K_{l2}} \tag{3.35}$$

Therefore the dynamics of the surface can be given by:

$$I\ddot{\theta} + B_{str}\dot{\theta} - T = -HM \tag{3.36}$$

Being:

I : Surface inertia, lbf.in/(rad/s²)

B_{str} : Structural damping of the surface, lbf.in/(rad/s)

HM : Aerodynamic hinge moment, lbf.in

Note that the aerodynamic hinge moment was inserted with a minus signal due to the aircraft signal convention already explained on the Figure 3-7.

After evaluating the torque forces and determining the surface angular position, it is used the effective horn arm given by the actuator kinematics in order to determine the linear load that is being applied back to the piston, therefore closing the loop.

The Surface block was designed considering the equations herein explained and the resultant model is shown on the Figure 3-35.

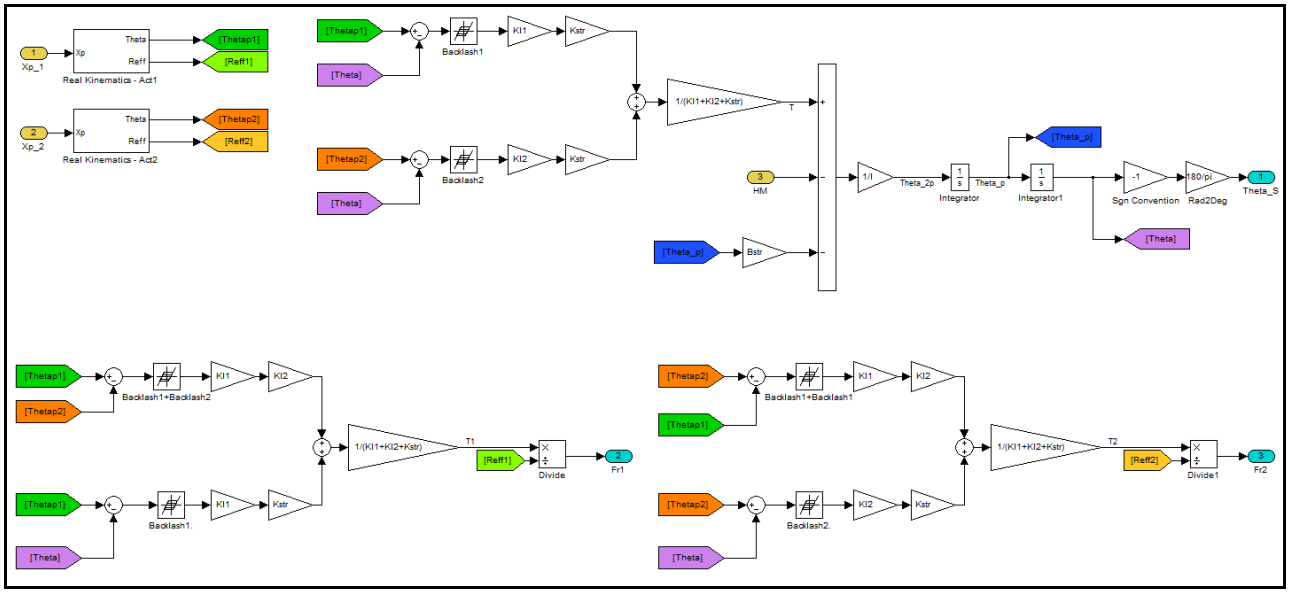

Figure 3-35 – Surface Block

Source: Developed by the author

It can be noticed that it was added a backlash block in order to represent the backlash non-linearity that can be found between θp1, θp2 and θ. This might have a major impact when evaluating the force-fight on failure conditions at high frequencies as will be explained furthermore.

The kinematics was evaluated by a block named Real Kinematics, which will evaluate the angular position θp1 and θp2 as well as the horn arm for the actuator 1 and 2. This block will consider the possible variations between the kinematics of the actuator 1 and 2 due to

installation and manufacturing tolerances of the actuator and its fixtures on the wing and on the control surface.

The Real Kinematics block is shown in details on the Figure 3-36.

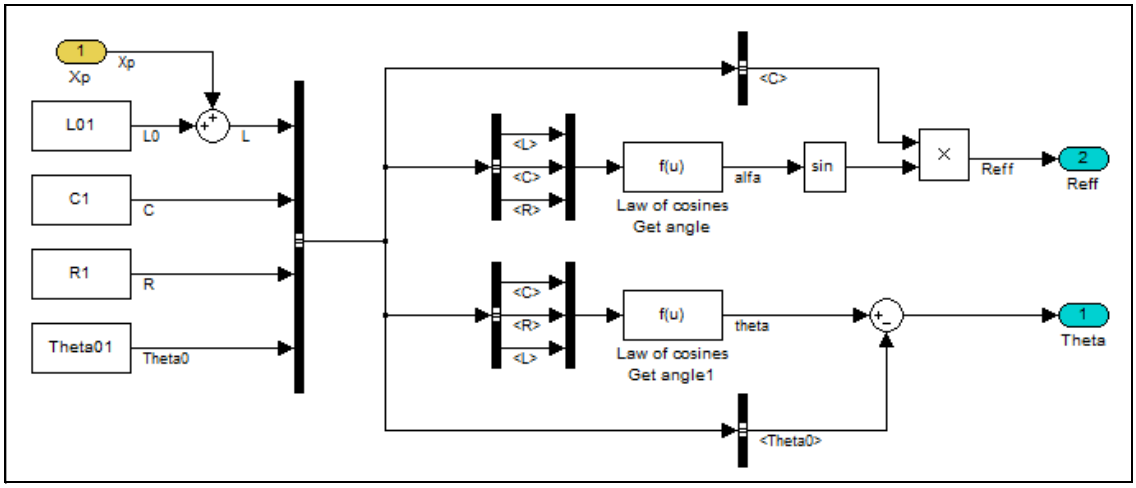

Figure 3-36 – Real Kinematics Block

Source: Developed by the author

The equation implemented on the Real Kinematics block named of “Law of cosines – Get angle” is given by:

$$\alpha = \arccos\frac{L^2 + C^2 - R^2}{2LC} \tag{3.37}$$

$$\theta = \arccos\frac{C^2 + R^2 - L^2}{2CR} \tag{3.38}$$

The angles and sides description can be found on the Figure 3-10.

Therefore the Surface dynamics was completely modeled. Nevertheless some important details of the modeling implemented must be highlighted. The way that the surface

was modeled it will successfully represent the first mode of vibration of the surface, the pure rotation, which might have a major influence when the model is being analyzed at high frequencies.

However it is highly recommended for future works the development of a more detailed surface to be joined to the model designed herein, this is because the other modes of vibration of the surface might alter the results of an analysis up to 100Hz. Nevertheless it is considered that the surface model herein developed will give a high degree of confidence on the results at high frequencies.

The last value that must be evaluated is the resultant Force-Fight that the structure is subjected to. Since the Force-Fight is the difference between the two actuators forces, its value can be easily found by the difference of the feedback forces Fr1 and Fr2:

$$FF = Fr1 - Fr2 \tag{3.39}$$

Therefore the hydraulic actuation system was entirely modeled for the point of view of the scope of this work. Although some improvements can be recommended in order to increase even more the fidelity of the model, it is considered that the model will have a high level of confidence of a real actuation system, even for an analysis at high frequencies as will be shown on the next chapter.

4. SIMULATION OF THE ACTIVE-ACTIVE SYSTEM

This chapter intent to show that the hydraulic actuation system, modeled herein and fully explained on the previous chapter, represents in fact an expected dynamics found on a real actuation system. After that, it will be analyzed some failure modes that generate an oscillatory mal-function, as well as the structure loads developed on each scenario.

4.1. Model Results

The first analysis that must be done with the model intents to show that the dynamic of a hydraulic actuation system is proper represented. Therefore the model will be submitted to two types of analysis, the step input and the frequency response.

4.1.1. Step Input

The Step Input analysis is used to measure some indicators of the system performance [1] [12], such as:

- Delay Time (Td): time required to reach for the first time 50% of the final value;
- Rate Time (Tr): time required to go from 10% to 90% of the final value;

- Peak Time (Tp): time required to reach the first peak value;
- Settle Time (Ts): time required to reach under 2% around the final value
- Overshoot (Mp): maximum percentage of the peak compared to the final value

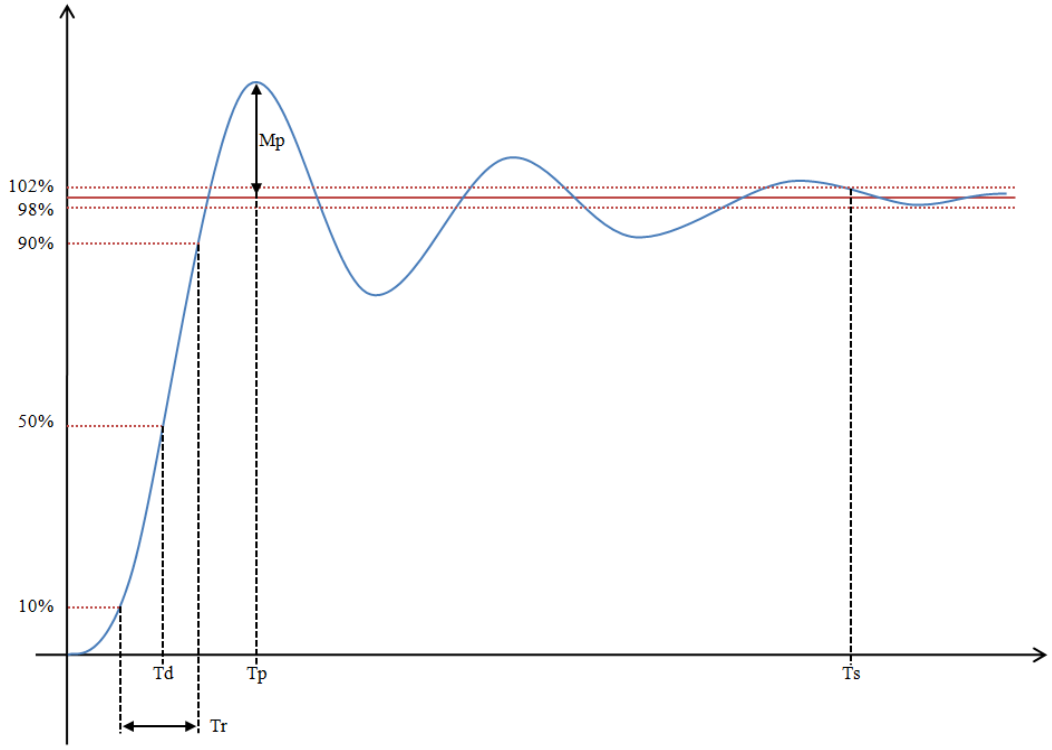

Figure 4-1 – Performance Criteria for a Step Input

Source: Developed by the author

To run the step response on the FCS Model, it was run the script Run_StepInput.m and the Load_Parameters.m that can be found on the appendix. The results are shown on the Figure 4-2 and Figure 4-3, where the first represents the response to a positive step input of +15º; and the second a negative step input of -25º.

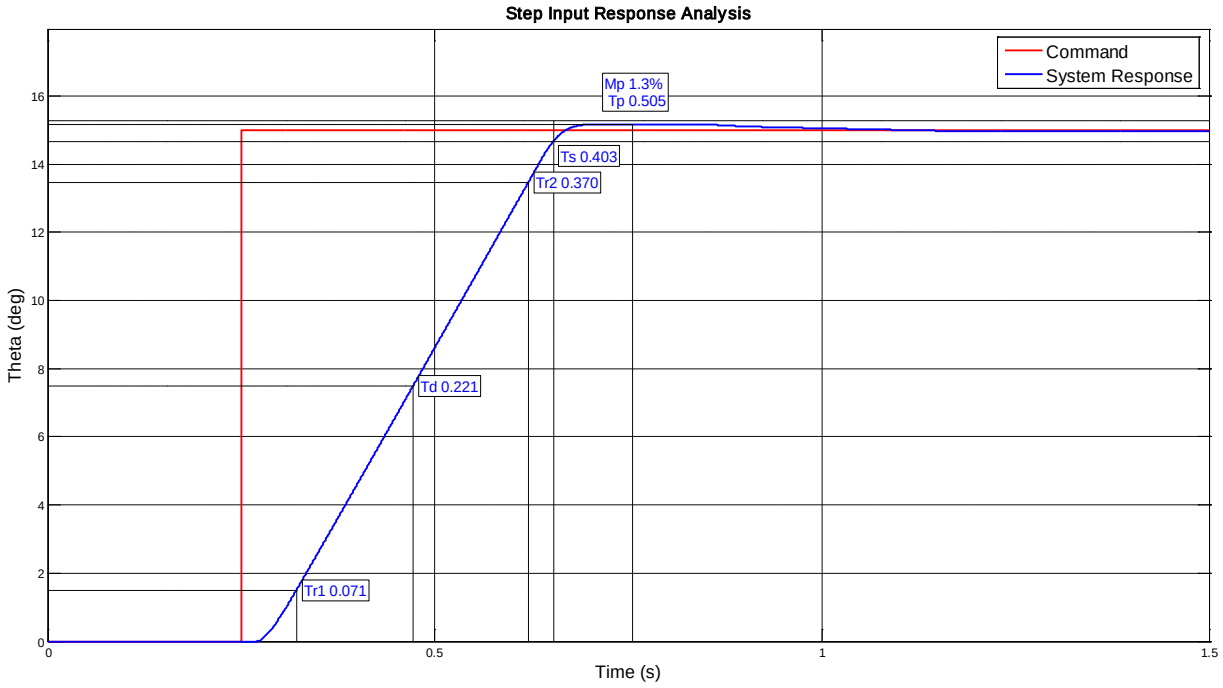

Figure 4-2 – Step Input Response 0º to 15º

Source: Developed by the author

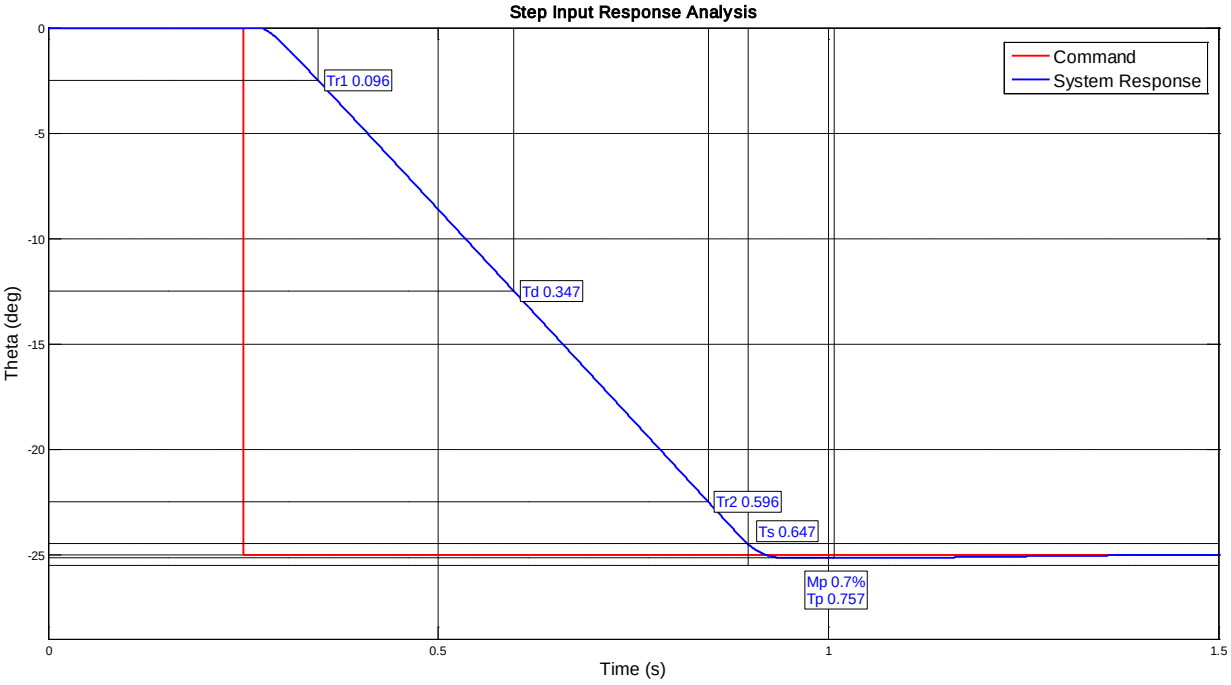

Figure 4-3 – Step Input Response 0º to -25º

Source: Developed by the author

The rate of the actuator was limited on the Position Loop of 40º/s, this can be observed using the values of Tr, which for the first case was 0.299s and the second 0.500s. Considering that the travel between 10% and 90% for the first and the second was 12º and 20º respectively, thus the average rate was 40.1/s and 40/s.

It is expected a difference of the average rate from the limit is due to the fact that the system response is not controlled, as explained before on the position loop description, the command input to the actuator is limited to a correspondent rate of 40º/s.

Once that the average rate of the response was determined, it can be possible to evaluate the amount of time that theoretically the response would take to reach 50%, which corresponds to a travel of 7.5º and 12.5º and divided by the average rate measured will result in 0.187s and 0.313s, which subtracted to the values of Td measured results on a response delay of 0.034s and 0.035s.

Considering that the model has many nonlinearities modeled that impact on the delay time, for instance the backlash, the response delay measured is considered close to a real actuation system.

On both cases the value of settle time was below to the peak time, which means that this system has a high damping factor although it was seen not to impact the rate time, therefore it can be considered a good response.

Also the value of overshoot was very low, which is another good indication, once that a high overshoot may cause excessive load on the surface that could result in a safety issue.

Both of these cases was run without aerodynamic load, which can alter the response significantly, therefore it was run two more cases with 50% of the maximum load that the

actuation was designed to withstand, one case applied as an opposing load and the other as an aiding load.

The area of the actuator modeled is 2in², which subjected to 2900psid will develop 5800lbf, the kinematics implemented results in an effective arm shown on Figure 4-4, where it can be seen that the highest horn arm is 4in around 5º, therefore the maximum Hinge Moment that the actuator can develop is 23 200 lbf.in at 5º.

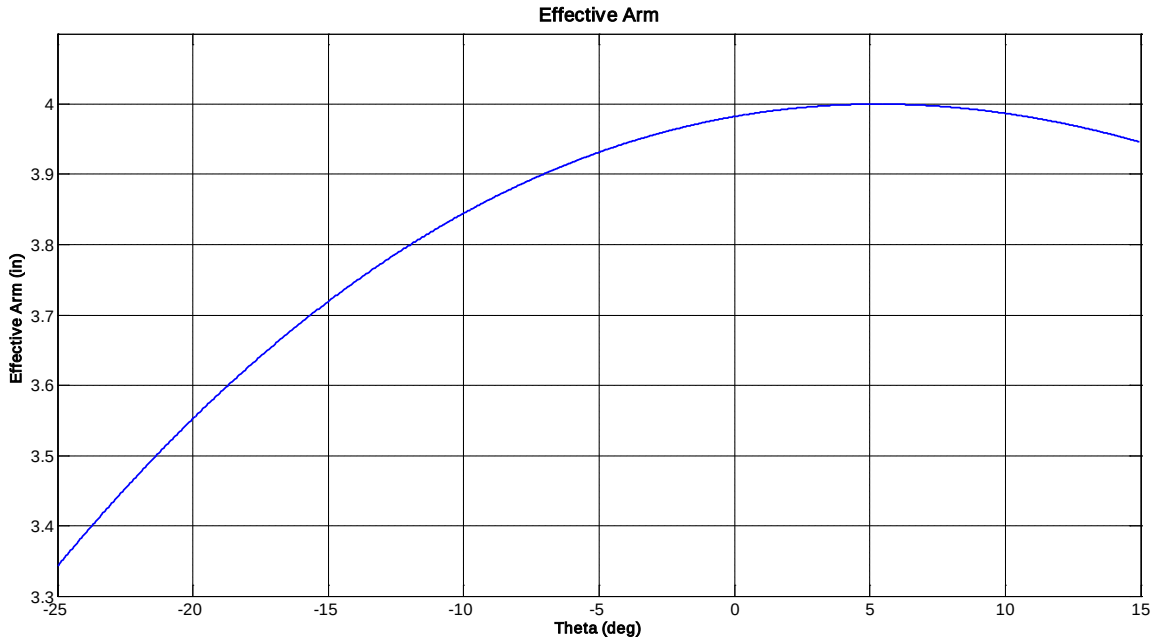

Figure 4-4 – Effective Arm

Source: Developed by the author

The results of these analyses are shown on the Figure 4-5 and Figure 4-8.

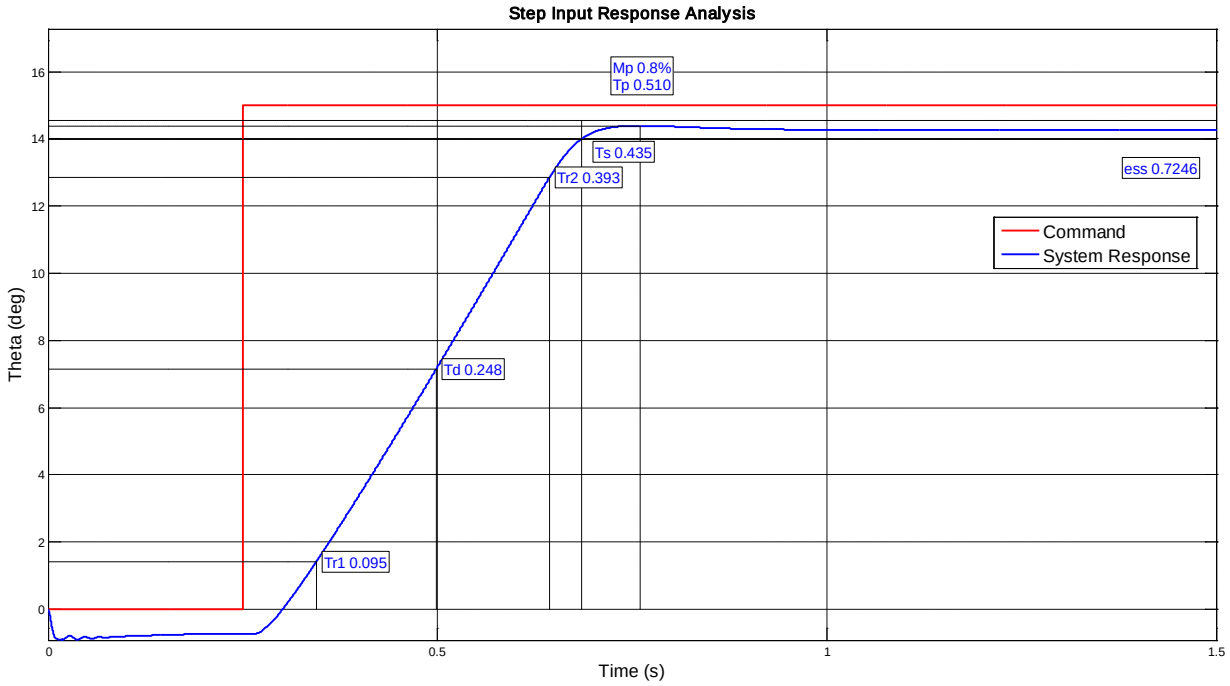

Figure 4-5 – Step Input Response with an opposing load of 50% of maximum load

Source: Developed by the author

For the opposing load case, it can be noticed that the response was not degraded enough to compromise the performance of the actuator, for instance, the rate measured was 40.3º/s, the delay time was increased to 0.061s and there was no overshoot. On this case it was also observed a steady state error of 0.72º due to the mechanical compliance.

Since the angular position is being measured on the center of gravity of the control surface, it is expected the measured steady state error. This is due to the very low surface stiffness, and the fact that the position loop is closed with the piston ram position value, therefore if observed the piston ram position compared to the piston command inside the position loop, as shown on the Figure 4-6, it is observed that the error of the position loop is set to zero, therefore the actuator stops moving, as can be seen on the.

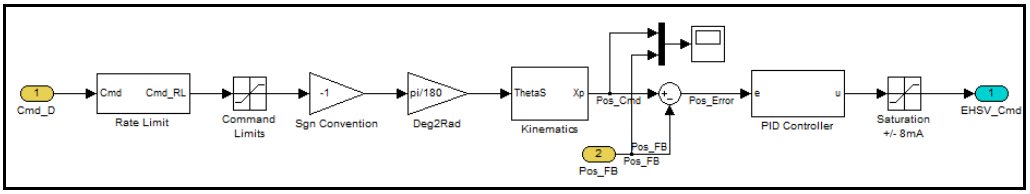

Figure 4-6 – Position Loop with commanded and the feedback position comparison

Source: Developed by the author

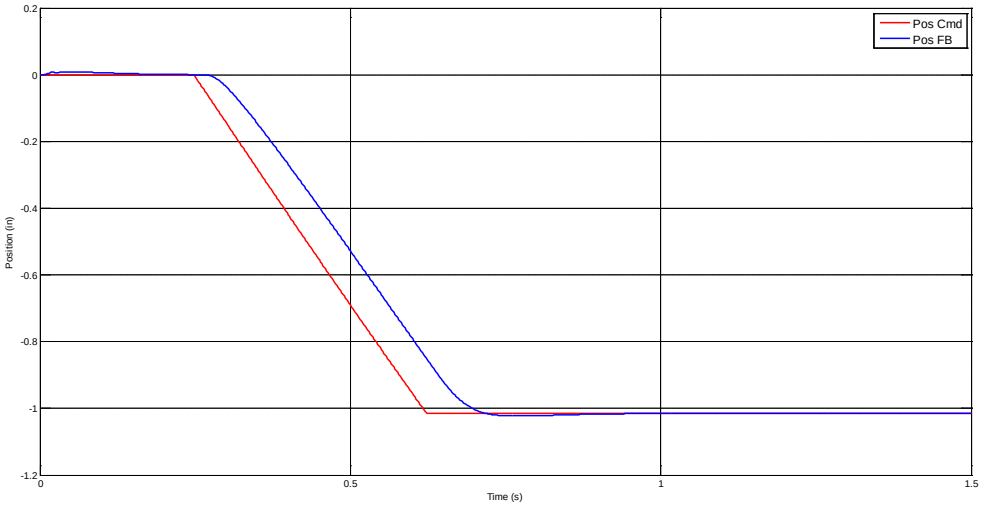

Figure 4-7 – Position command and feedback comparison

Source: Developed by the author

The Figure 4-8 shows the system response to an aiding load of 50% of maximum load.

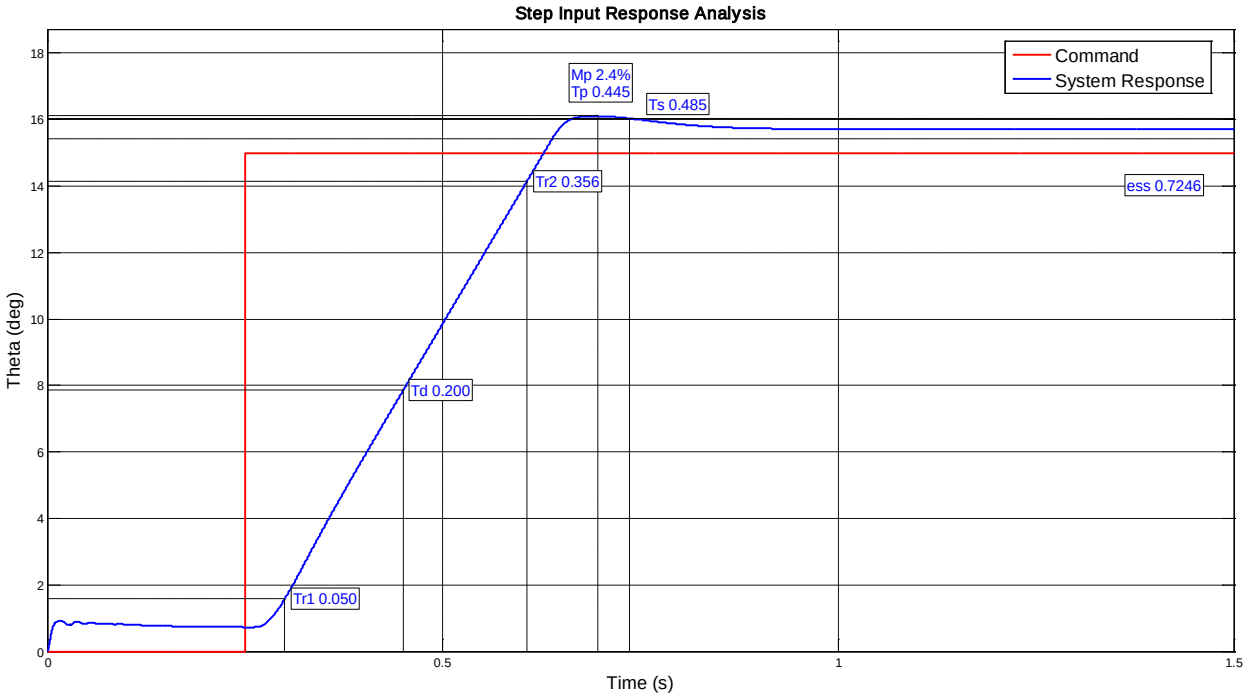

Figure 4-8 – Step Input Response with an aiding load of 50% of maximum load

Source: Developed by the author

The aiding load case is important to evaluate the worst case condition for the overshoot, as can be seen on the results the overshoot was 2.4%, which is still a low level. For this case the steady state error was 0.72º, the same found for the opposing load case, but on the opposite direction.

The last step input response that must be analyzed is the one where each actuator has its own dynamics, thus leading to a force-fight scenario. This might cause some differences on the dynamic response of the surface, therefore it will be analyzed the step input response to a no load condition for a 15 degrees of command, which results can be found on the Figure 4-9. For this analysis it was generated the scrip ff_gen.m where the dynamics of each actuator are differentiated.

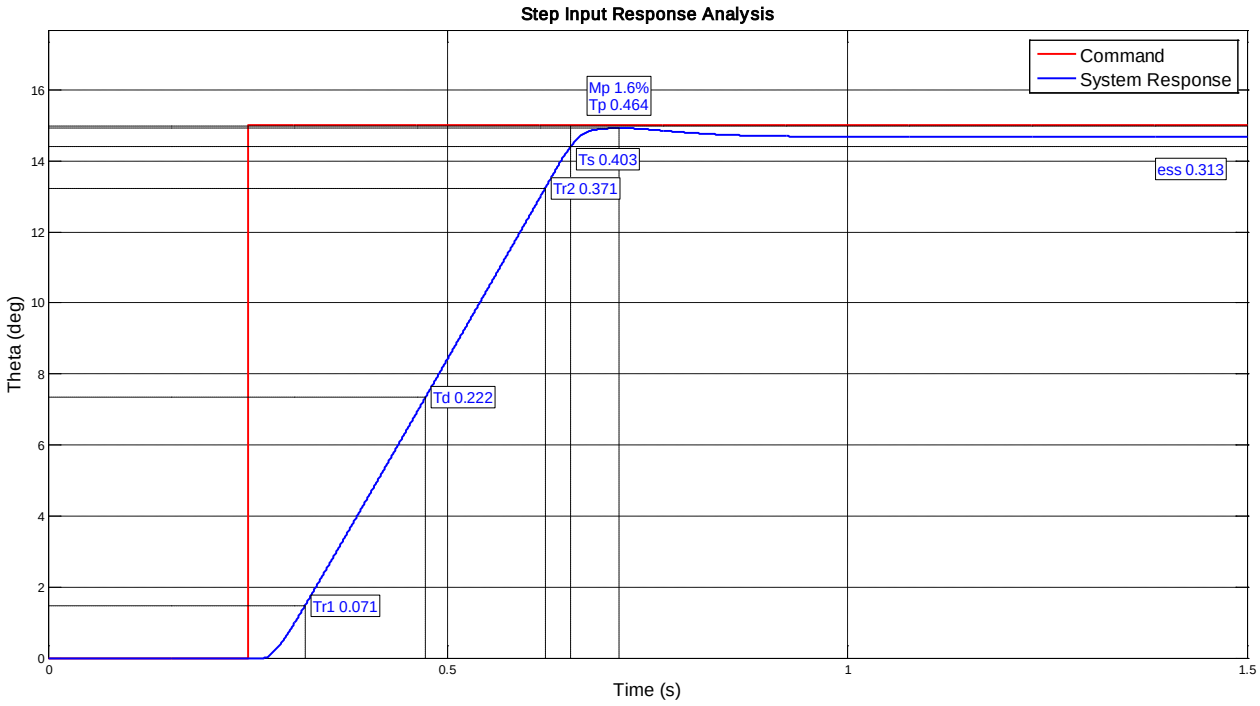

Figure 4-9 – Step Input Response 0º to 15º with Force-Fight

Source: Developed by the author

As can be seen on the Figure 4-9, the average rate measured was 40º/s, the delay time was 0.035s and the settle time was 0.403s, which is lower than the peak time of 0.464s with an overshoot of 1.6%. Also it can be noticed a steady state error of 0.31º, due to the different dynamics that was applied to each one of the actuators. Therefore the position loop error resulted was zeroed, although the surface did not reached its expected final value.

The amount of load that the surface structure was subjected to is represented on the Figure 4-10, which can be noticed that, for the final position, it was developed a Force-Fight level of 2728lbf, which is equivalent to the 23.5% of the full Force-Fight that can be encountered on the structure.

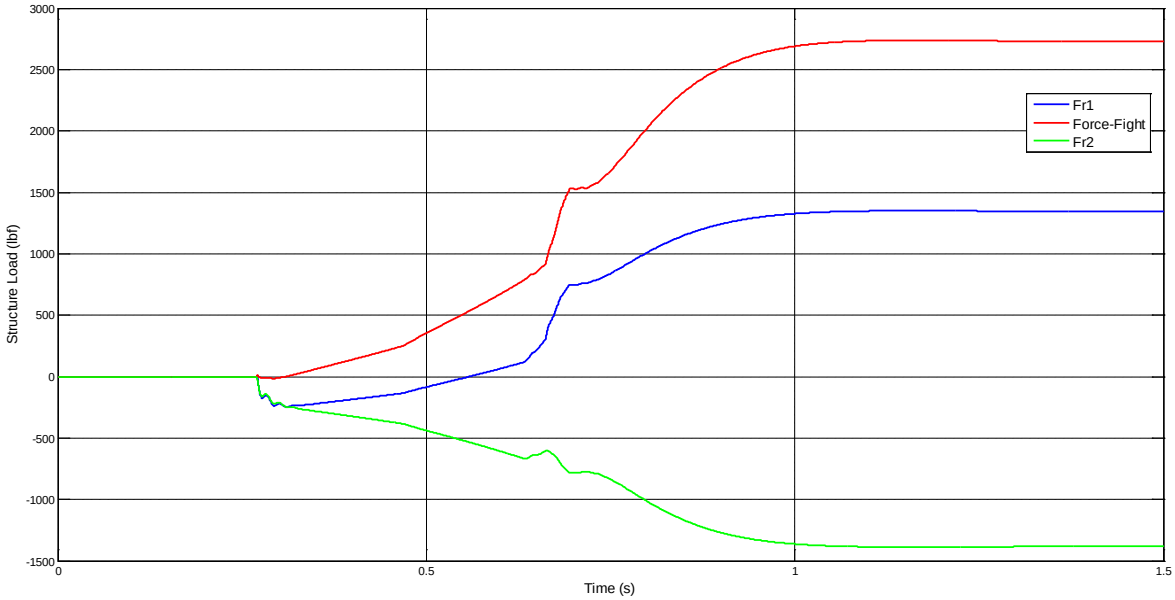

Figure 4-10 – Structure Loads for the step response analysis with force-fight

Source: Developed by the author

Taking into consideration all the cases for the step input herein presented, it can be concluded that, from the step input response perspective, the hydraulic actuation system modeled was designed properly and can represent in a high level of confidence the dynamics of the actuators as well as the structure forces that is being generated.

4.1.2. Frequency Response

The frequency response analysis is used to verify the response of the actuator system under a sine wave input of command going from 0.1Hz up to 100Hz. This analysis is made without the presence of aerodynamic load and without inserting a different dynamics for each actuator.

At low frequencies the actuator is expected to response exactly to the input signal, but as the frequency increases the nonlinearities of the system starts to make more effect on the response of the actuator decreasing the Gain, which is the ratio of the output over the input sign measured in decibels; as well as is expected to increase the Phase, which is the delay between the measured sine wave and the response.

There are two criteria that will be used here to analyze the frequency response of the actuation system modeled, the first is the gain and phase margins; and the second is the frequency at which the system gain is at -3dB, which means that the response amplitude is close to 70% of the input command.

The gain and phase margins are explained on Ogata [12] and herein summarized:

Gain Margin: the gain margin is the gain at which the phase will be at -180º. A positive gain margin means that the system is stable, whether a negative, instable. Also the value of the gain margin means how much the gain of the system can be increased without changing the system stability.

Phase Margin: the phase margin is the amount of phase necessary to change the system stability. A positive phase margin means a stable system and a negative, instable.

The frequency at -3dB is considered to be the highest frequency in which the actuator will respond with a representative level, values higher than 5Hz is expected in a good active-active hydraulic actuation system [6].

On this analysis it is used a first order Fourier transform in order to evaluate the Gain and Phase values. The results are shown on the Figure 4-11, Figure 4-12 and Figure 4-13.

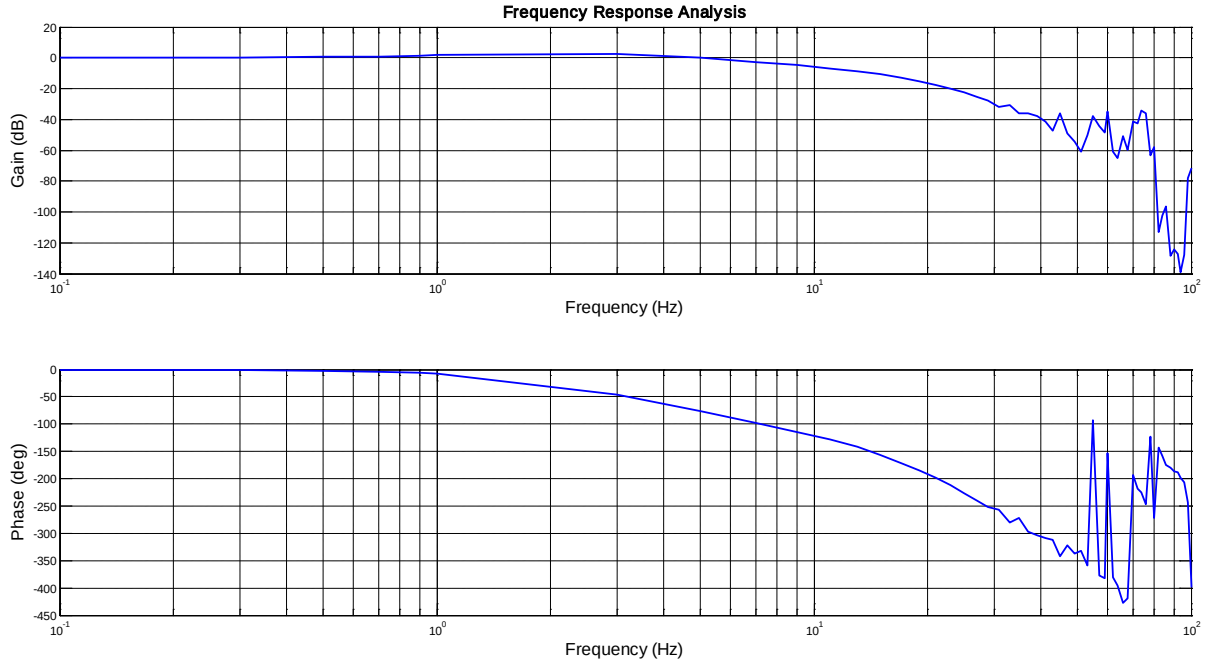

Figure 4-11 – Frequency Response Analysis

Source: Developed by the author

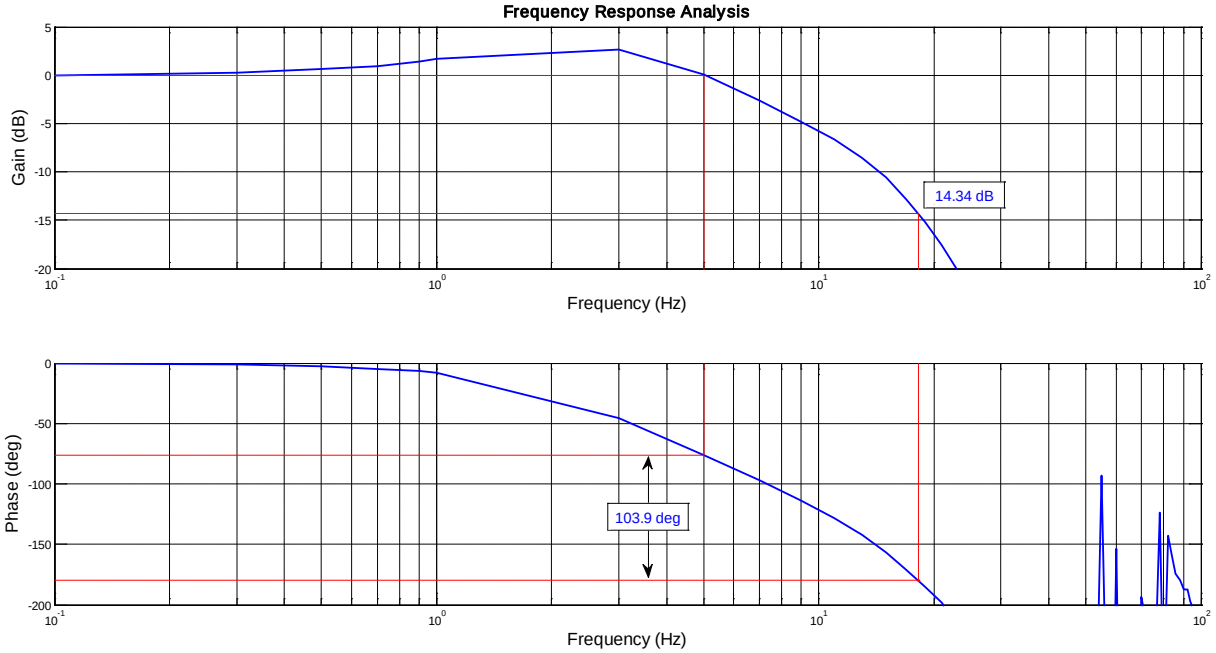

Figure 4-12 – Gain and Phase Margins

Source: Developed by the author

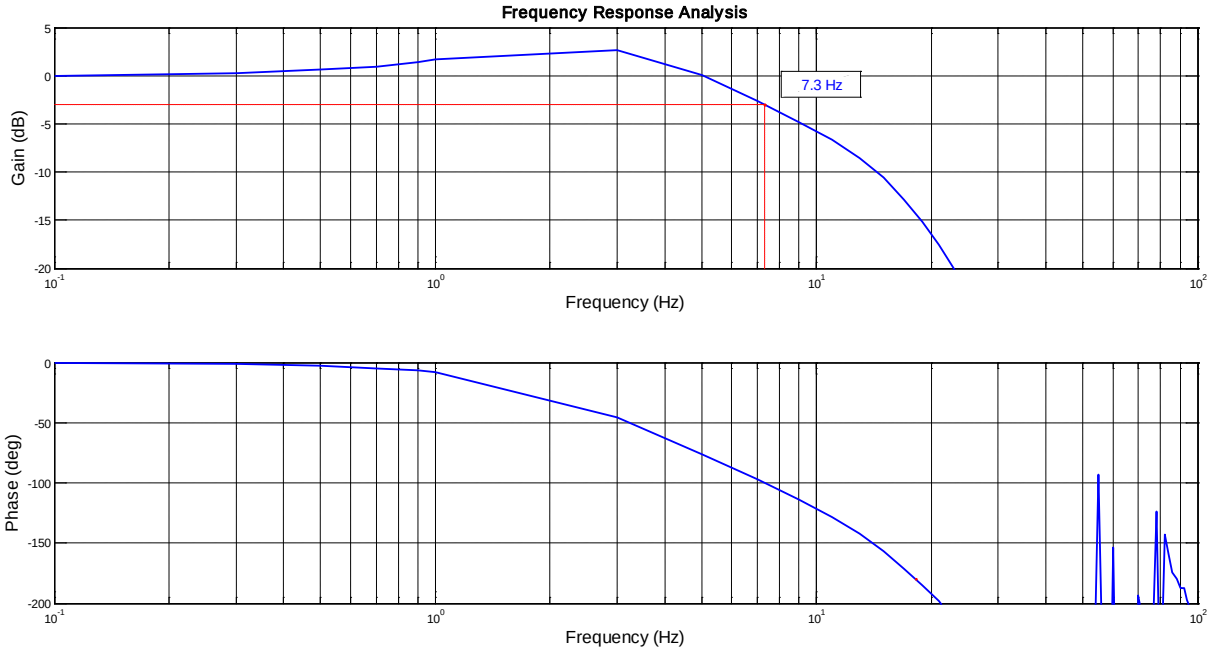

Figure 4-13 – Frequency at -3dB

Source: Developed by the author

As shown on Figure 4-12 the Gain margin is 14.34dB and the Phase margin is 103.9º, therefore the system is stable. Also, a Gain margin higher than 10dB is considered enough margin for real actuation systems [6].

The Figure 4-13 shows that the frequency at -3dB is 7.3Hz, therefore the system will have a good response for frequencies up to 7.3Hz, which is considered high enough [6].

Therefore considering the conclusions made by the Step Input analyses and with the results of the Frequency Response analyses, it is possible to conclude that the system herein developed is stable, fast and representative of a real hydraulic actuation system.

4.2. High Frequencies Analysis

One of the most important improvements made on this model was the high detailed model of the EHSV, which has relevant dynamics close to the hydraulic natural frequency of valve, which can be evaluated as shown on Merritt [10] and also presented on the chapter 3.2.2.1.3 as:

$$\omega_{hp} = \sqrt{\frac{2\beta_e A_v^{\,2}}{V_{0p} M_v}} \tag{4.1}$$

Substituting by the values used on the model as shown on the appendix:

$\beta_e = 1\times10^5\ psi$
$A_v = \pi D_v^{\,2}/4$
$D_v = 0.2in$
$V_{0p} = A_v L_v$
$L_v = 0.1in$
$M_v = 0.25lbs$

Hence the resultant hydraulic frequency of the valve is:

$\omega_{hp} = 501.3\,rad/s$

Or:

$f_{hp} = 79.8Hz$

Therefore if the EHSV is excited at the frequency f_{hp} the valve will resonate, just as shown on the Figure 4-14 that represents the frequency response of the servovalve.

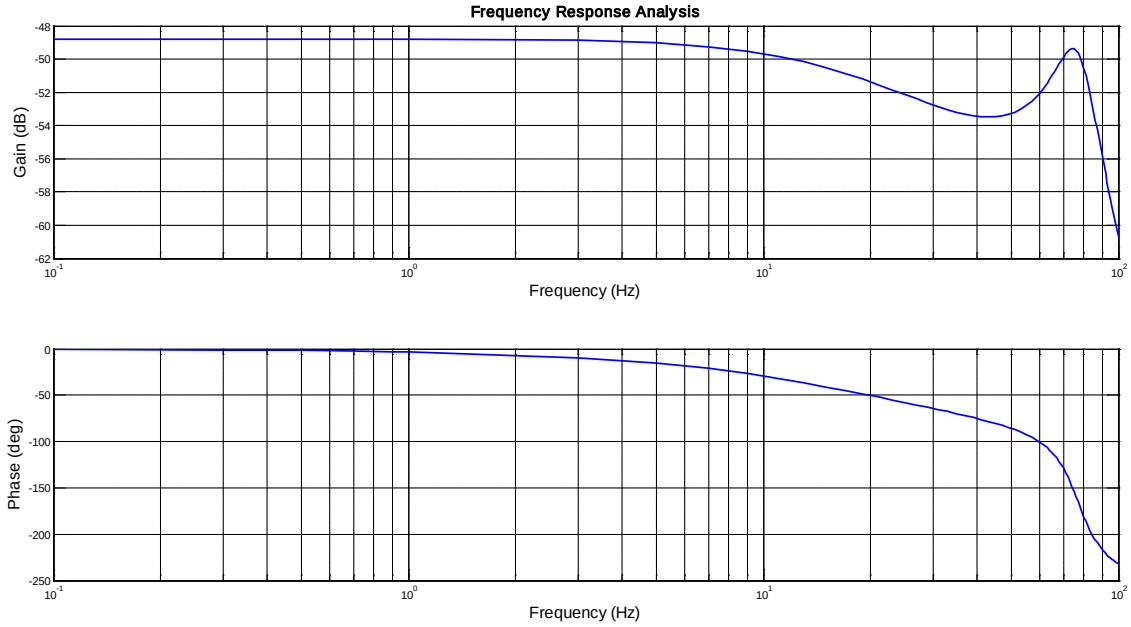

Figure 4-14 – Frequency Response of the EHSV

Source: Developed by the author

The frequency response shown on Figure 4-14 was run with a sine wave input of ±1mA, and as an output resulted at a spool position in inches.

It can be observed that between 70Hz and 80Hz a resonance frequency was excited, the difference between the resonance frequency observed and the predicted is due to some model simplifications and due to the damping ratio of the valve dynamics.

The result of this analysis has shown that the model of the EHSV is representative at high frequency, which is a major improvement of this model compared to a simplified implementation.

Another important dynamic to be evaluated its representativeness up to high frequency, is the control surface dynamics. The natural frequency of the surface can be evaluated by the following equation:

$$\omega_n = \sqrt{\frac{K_{eq}}{I}} \tag{4.2}$$

Where, Keq means the equivalent stiffness of the surface, considering Kl1, Kl2 and Kstr. Using as reference the Figure 3-34, the Keq can be evaluated by:

$$K_{eq} = \left(K_{str}{}^{-1} + \left(K_{l1} + K_{l2} \right)^{-1} \right)^{-1} \tag{4.3}$$

The values used for Kstr, Kl1, Kl2 and I are:

$K_{str} = 1,5 \cdot 10^6 \, lbf/in$
$K_{l1} = 1,5 \cdot 10^6 \, lbf/in$
$K_{l2} = 1,5 \cdot 10^6 \, lbf/in$
$I = 8 in \cdot lbf/rad/s^2$

Therefore the natural frequency of the surface is:

$$\omega_n = 353,55 \, rad/s \tag{4.4}$$

Or:

$$f_n = 56,27 Hz \tag{4.5}$$

Therefore when evaluated the frequency response of the surface it will be seen a resonance around 56Hz. The Figure 4-15 shows the frequency response of the control surface for a sine wave input of ±0.1in of amplitude applied simultaneously to Xp1 and Xp2, resulting

in the surface angular position. It must be highlighted that the structural damping was reduced in order to show the resonance of the surface, otherwise the exact resonance frequency wouldn't be shown on the frequency response.

As can be seen on the Figure 4-15, the resonance frequency is around 55Hz according to the model, which is very close to the calculated natural frequency.

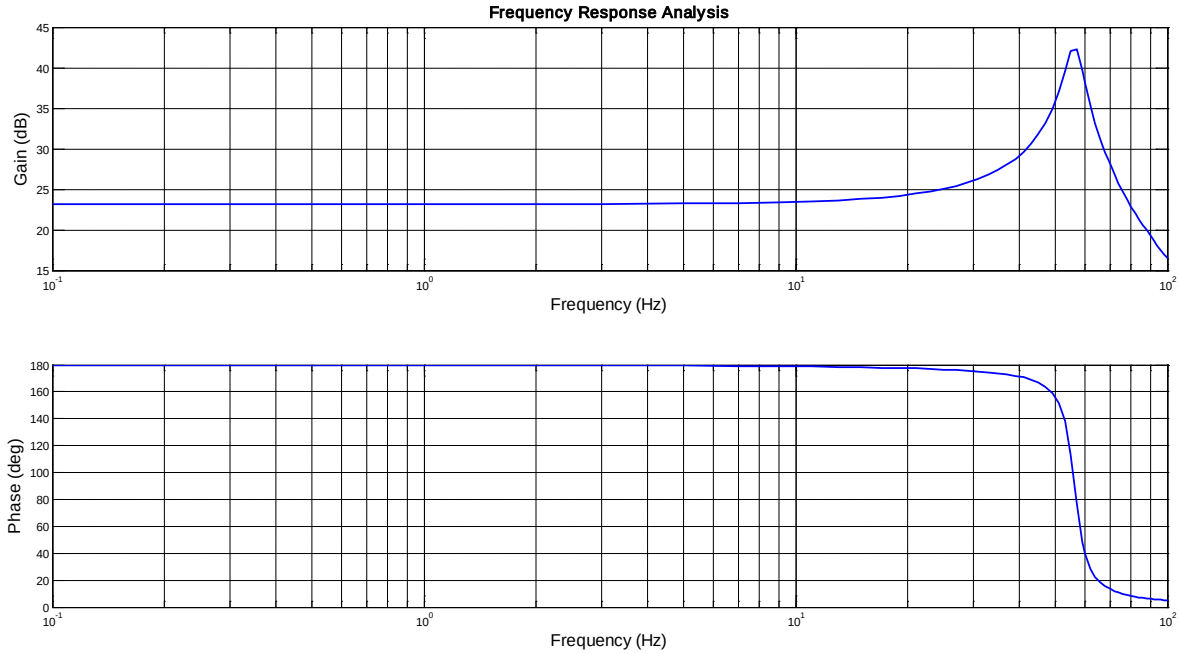

Figure 4-15 – Frequency Response of the Control Surface

Source: Developed by the author

Therefore, as shown on the frequency responses of the servovalve and the control surface, it is considered that the model developed herein has a high level of fidelity even for a high frequency analysis.

Further analyses could be done in order to show that other components modeled herein also have a high level of confidence at high frequency. Nevertheless it was considered that

this would require experimental data. Therefore it is highly recommended for further works the comparison of this model and a real system in order to confirm that the most important behaviors of the hydraulic actuation system is being captured even at a high frequency simulation.

4.3. Oscillatory Mal-Function Analysis

This chapter will present the analysis made for the Oscillatory Mal-Function (OMF) scenario, as well as its impact on the structure fatigue consumption. An OMF might occur typically from three failures: the electrical failure at the exit of the electronic system, the mechanical rupture of the feedback spring inside the servovalve and a failure of the piston ram lvdt.

It was considered that the electrical failure will have the worst scenario, generating the highest level of load with the highest range of frequencies. Nevertheless it is highly recommended for future works the details of each possible failure that may generate an oscillatory mal-function.

4.3.1. Electrical Failure

The electrical failure at the exit of the electronic system can be caused by some electronic hardware component, which may induce an oscillatory spurious signal as a

command to the servovalve, which will then generate an oscillatory delta pressure inside the chamber of the failed actuator.

When a delta pressure between the chambers of the actuator is generated, it will force the piston to move, which will generate a rotation of the surface. Since the command of the surface will remain constant, for instance at zero, the other actuator will oppose this force, trying to bring the surface back to the commanded position. That is when is generated a force-fight between the actuators.

At low frequencies, the force-fight is expected to be maximum, which means that one actuator will develop a maximum force in one direction and the other will oppose this force at the same magnitude, this is called full force-fight.

As the frequency increases, it is expected that the good actuator will not be fast enough to build up the full force-fight, thus the level of force-fight will be reduced. This is due to the fact that, at high frequencies, the frequency response of the actuation system will reduce in gain and phase.

Also is expected that at some frequency the induced movement of the piston will be so low that it will be inside the backlash between the piston ram and the surface, therefore it will not generate any force-fight between the actuators. It is clear than the importance of the non-linearity of a real system for this type of analysis.

Thus, in order to simulate the electrical failure on the electronic system, it was modified the Hardware_out block, descript on the chapter 3.2.1.4, for the actuator 1, resulting on the block shown on the Figure 4-16.

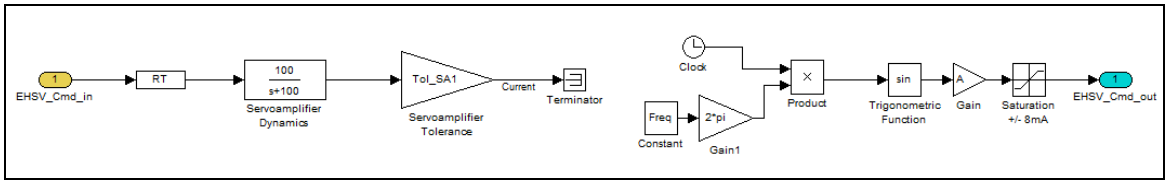

Figure 4-16 – Hardware_out Block Modified for the electrical failure scenario

The modifications intent to eliminate the resultant signal of the electronic system and insert an oscillatory signal limited in ±8mA, therefore, for values of the gain A much higher than 8mA, it is inserted an square wave of frequency of value Freq.

When simulated a square wave of frequency of 1Hz the resultant structure forces on the actuators, Fr1 and Fr2, are shown on the Figure 4-17, and the resultant surface deflection is shown on the Figure 4-18.

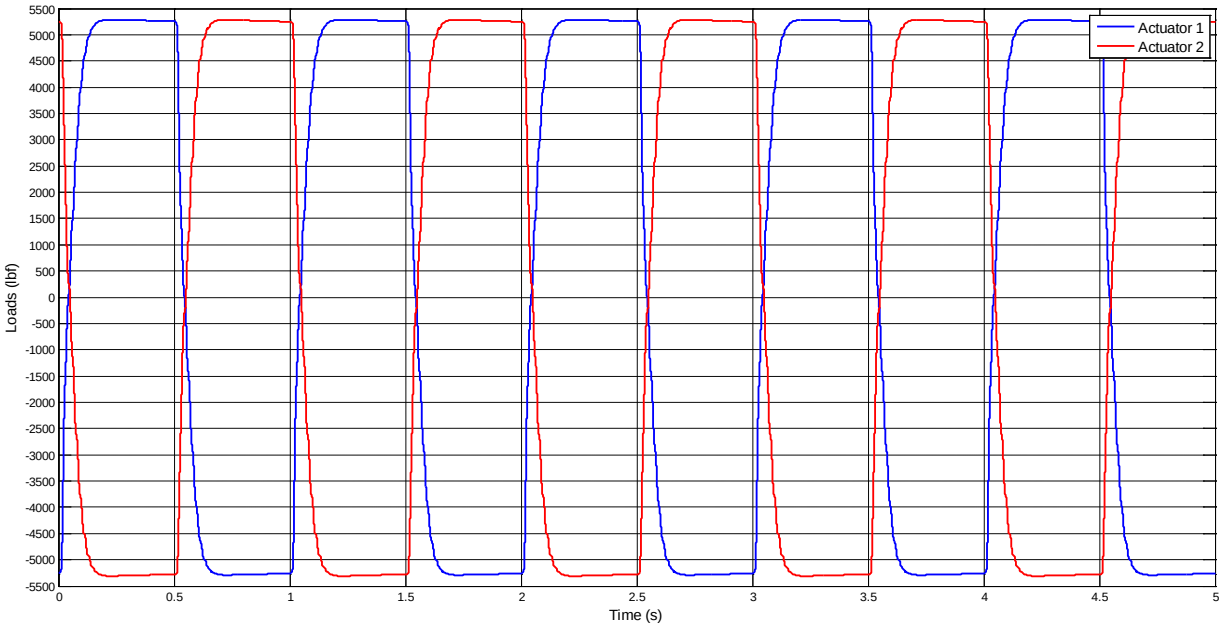

Figure 4-17 – Structure loads on actuators for an electrical failure of 1Hz

Source: Developed by the author

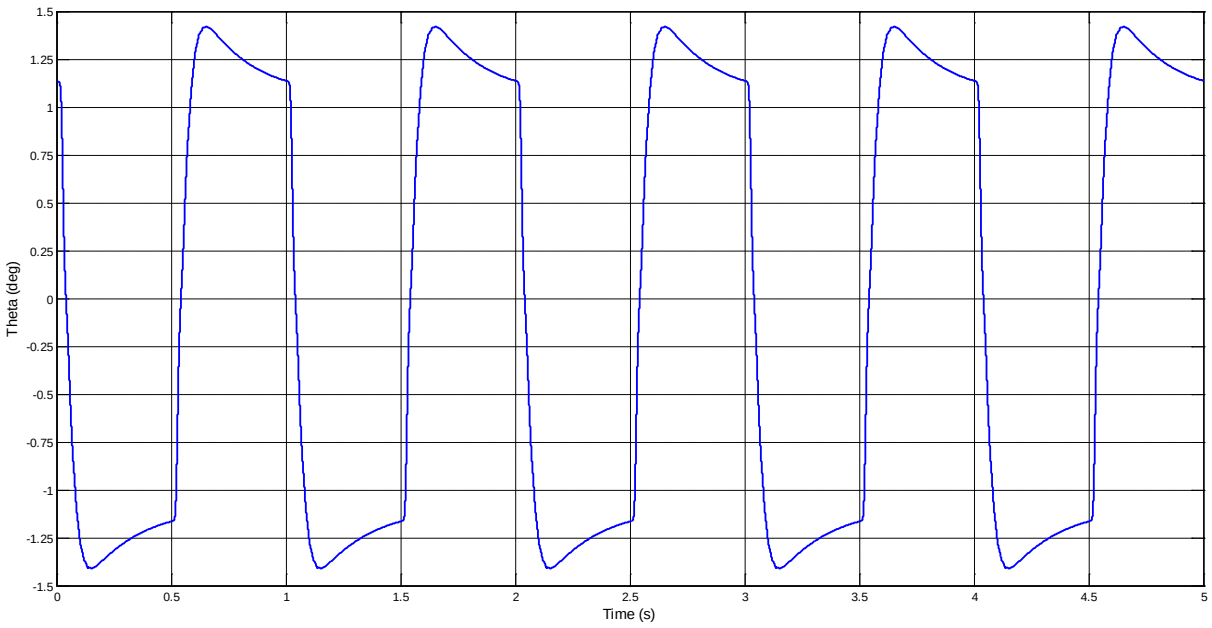

Figure 4-18 – Surface travel for an electrical failure of 1Hz

Source: Developed by the author

Therefore, as shown on the figure above, the amount of load developed on both actuators was approximately 5300lbf, which is less than the maximum force of the actuator of 5800lbf, this is due to the fact that some amount of force is being used to overcome the friction and the piston damping, since that, for this frequency, the piston did not stopped moving when the square wave changed its signal. Also this amount of piston rate demands some hydraulic flow, which reduces the amount of available pressure from the hydraulic system. The amount of surface deflection seen for this failure scenario had a peak of approximately 1.4deg.

When simulated a failure scenario of a square wave at a frequency of 50Hz, the resultant structure loads and deflections are shown on the Figure 4-19 and Figure 4-20.

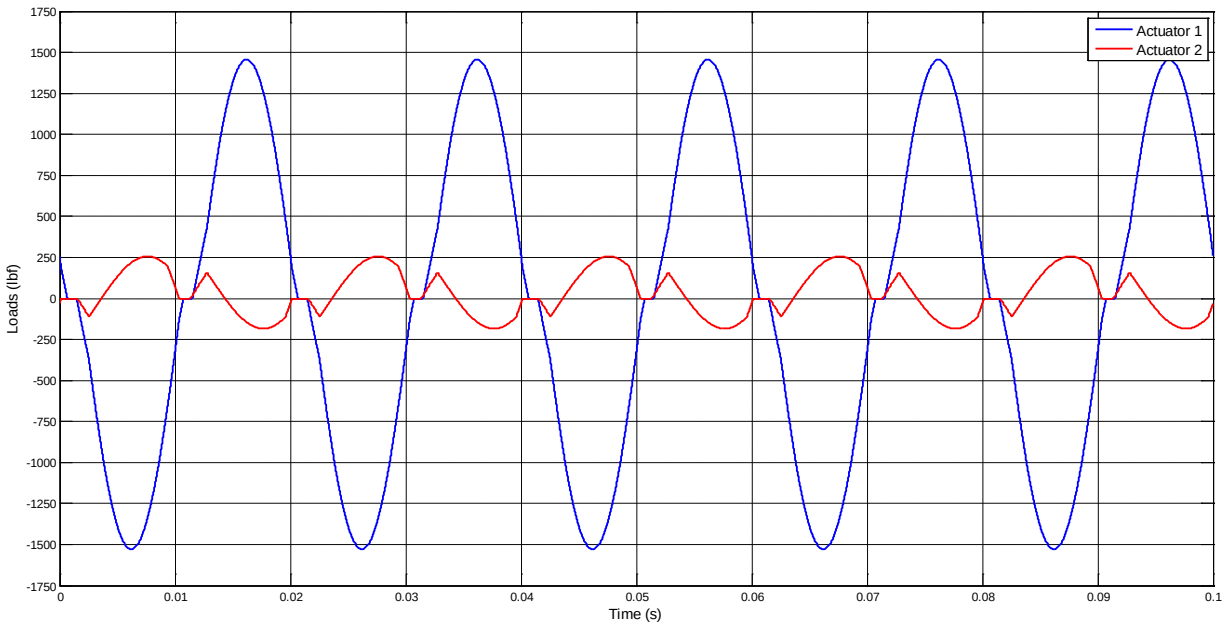

Figure 4-19 – Structure loads on actuators for an electrical failure of 50Hz

Source: Developed by the author

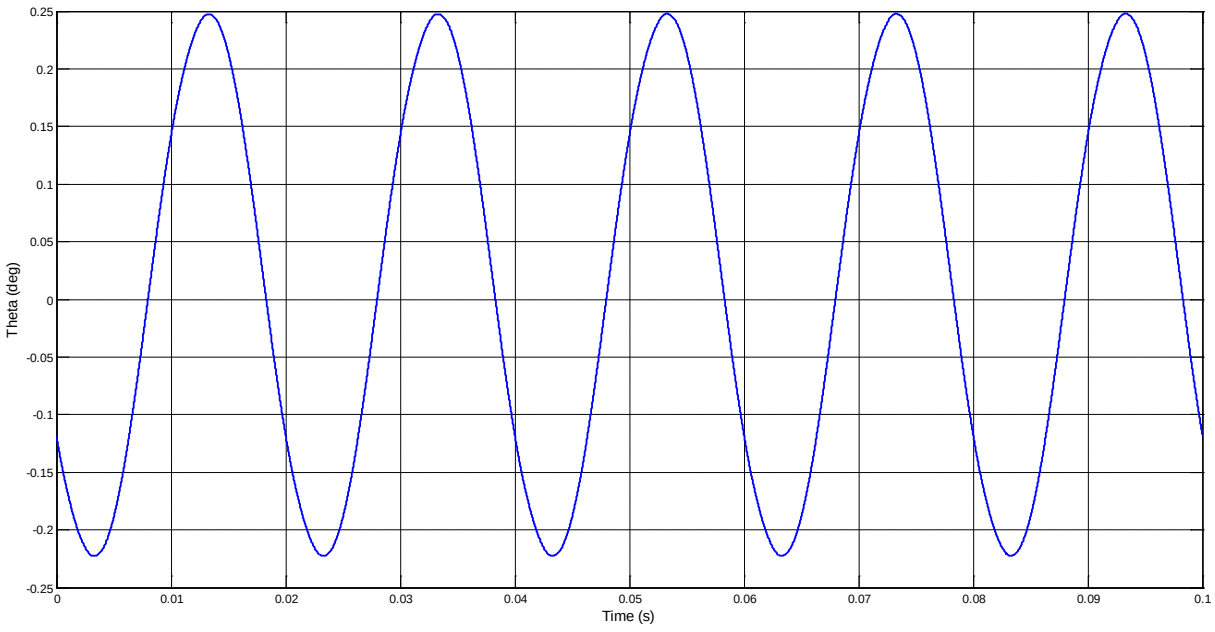

Figure 4-20 – Surface travel for an electrical failure of 50Hz

Source: Developed by the author

For the electrical failure at 50Hz, for the actuator 1 it was developed a load of approximately 1500lbf, although for the good actuator only 250lbf, this is due to the fact that the response of the good actuator is not fast enough to build up the same amount of force developed by the failed actuator.

For this case the surface deflection was equivalent to a sine wave of approximately 0.23deg. It can be noticed that the surface oscillated around a value different than zero, this is due to the dynamics of the actuator, also that the first failed input induced a positive surface deflection.

Also it can be noticed on the resultant loads figure that the non-linearities, such as the backlash, are starting to have a big impact on the results, this influence will get higher as the frequency increases.

The resultant structure loads and deflection when simulated a failure scenario of a square wave of 100Hz can be seen on the Figure 4-21 and Figure 4-22.

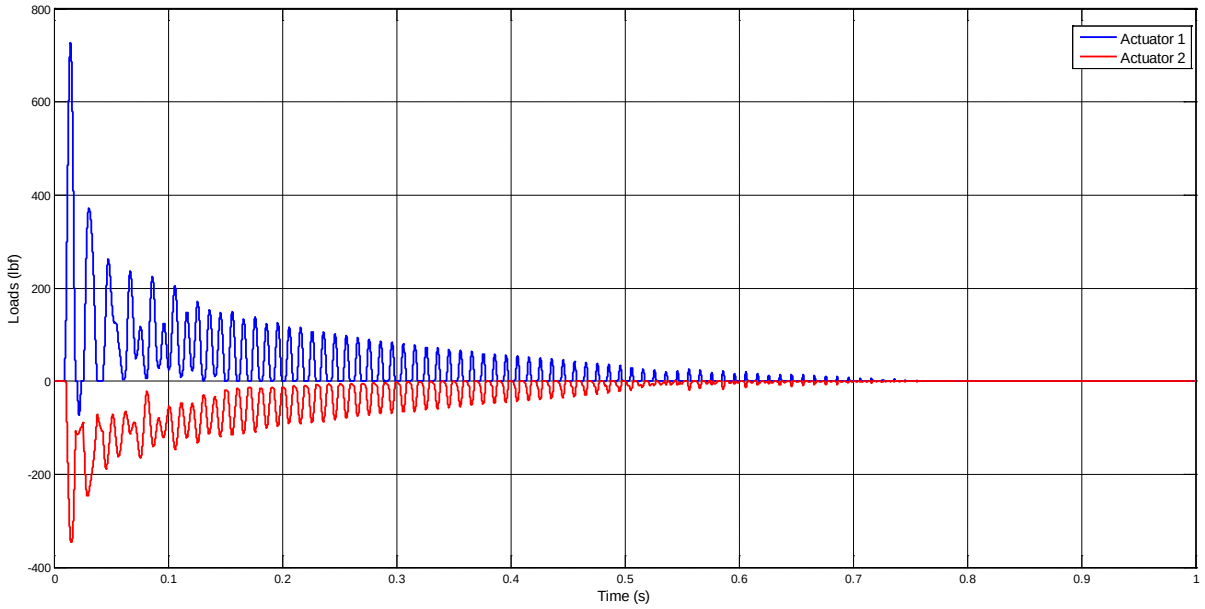

Figure 4-21 – Structure loads on actuators for an electrical failure of 100Hz

Source: Developed by the author

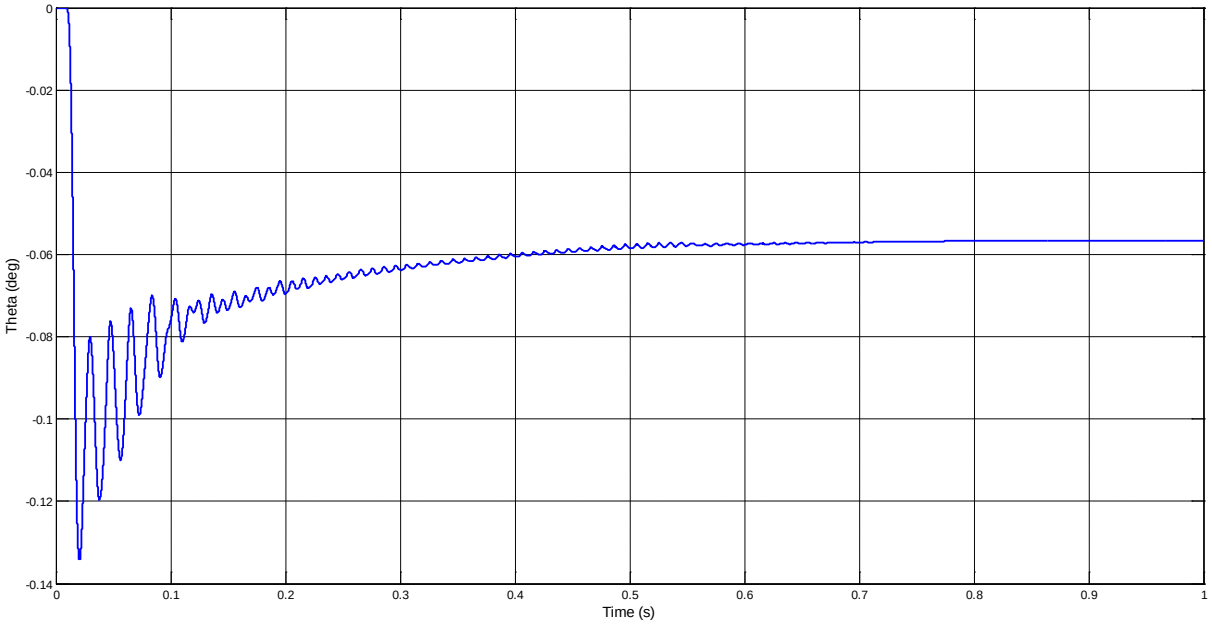

Figure 4-22 – Surface travel for an electrical failure of 100Hz

Source: Developed by the author

As shown on the figures above, for a failure scenario of 100Hz, the non-linearity of the system eliminates the dynamics that was seen at lower frequencies. Therefore, although the failed actuator is oscillating at a high frequency, its dynamics is not transferred to the surface, neither to the other actuator, but stays under the backlash between the actuator and the surface.

As can be seen on the Figure 4-23, the piston ram position oscillates with an amplitude of ±0.001in. Considering that the backlash value implemented is ±0.06deg, which in terms of linear displacement is equivalent to ±0.0043in, thus the failed actuator remains inside the backlash level. Since the amplitude seen of the piston ram position was approximately 23% of the backlash, it is expected that this behavior will be seen at frequencies lower than 100Hz.

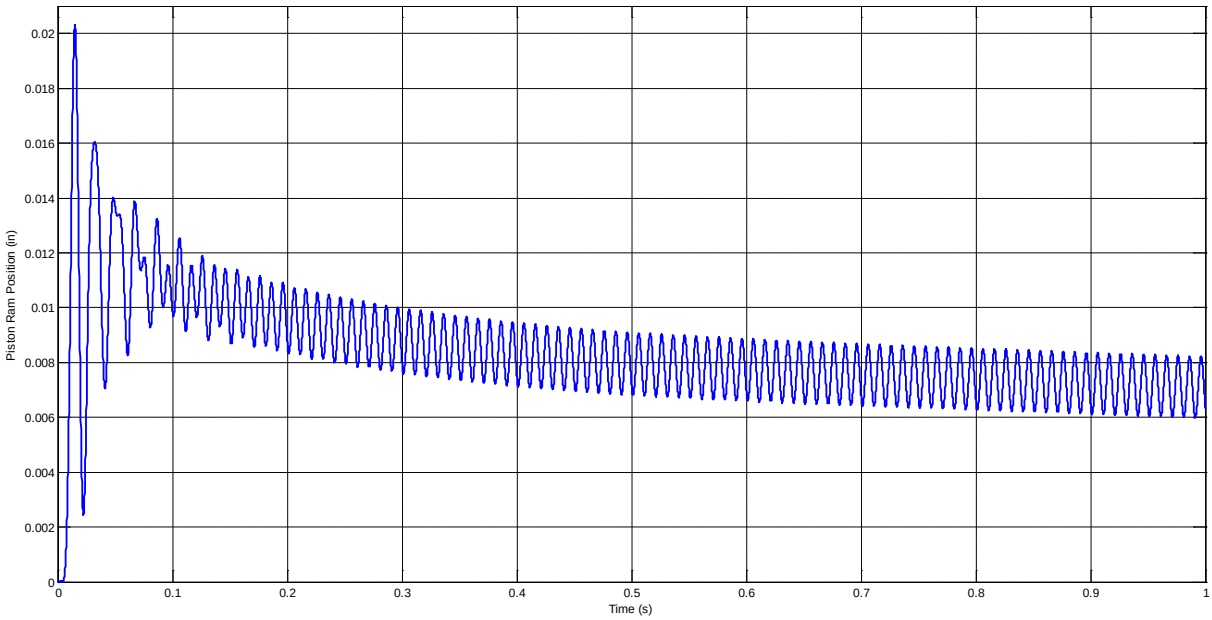

Figure 4-23 – Piston ram position of failed actuator at a 100Hz electrical failure

Source: Developed by the author

Therefore the last analysis than must be made is to vary the frequency from 0.1Hz to 100Hz in order to see the amount of forces developed by the actuators at each correspondent frequency, as well as the surface deflection. The results for this simulation can be seen on the Figure 4-24, Figure 4-25 and Figure 4-26.

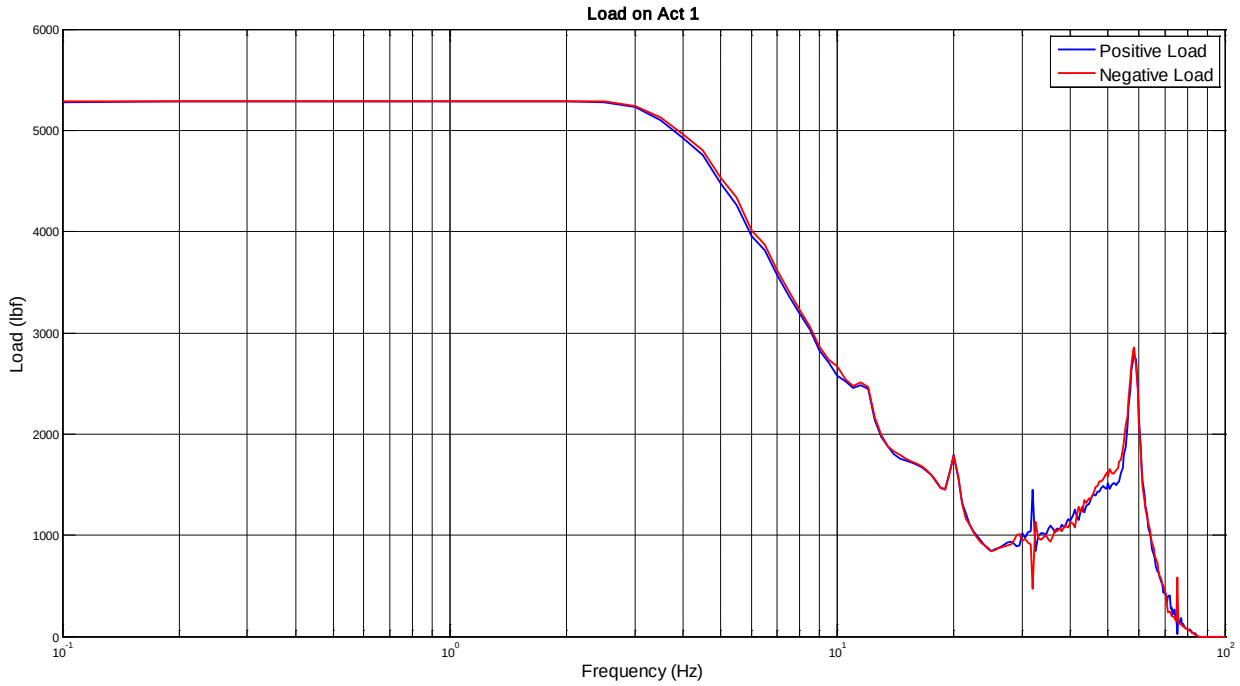

Figure 4-24 – Resultant load on actuator 1 for the square wave electrical failure

Source: Developed by the author

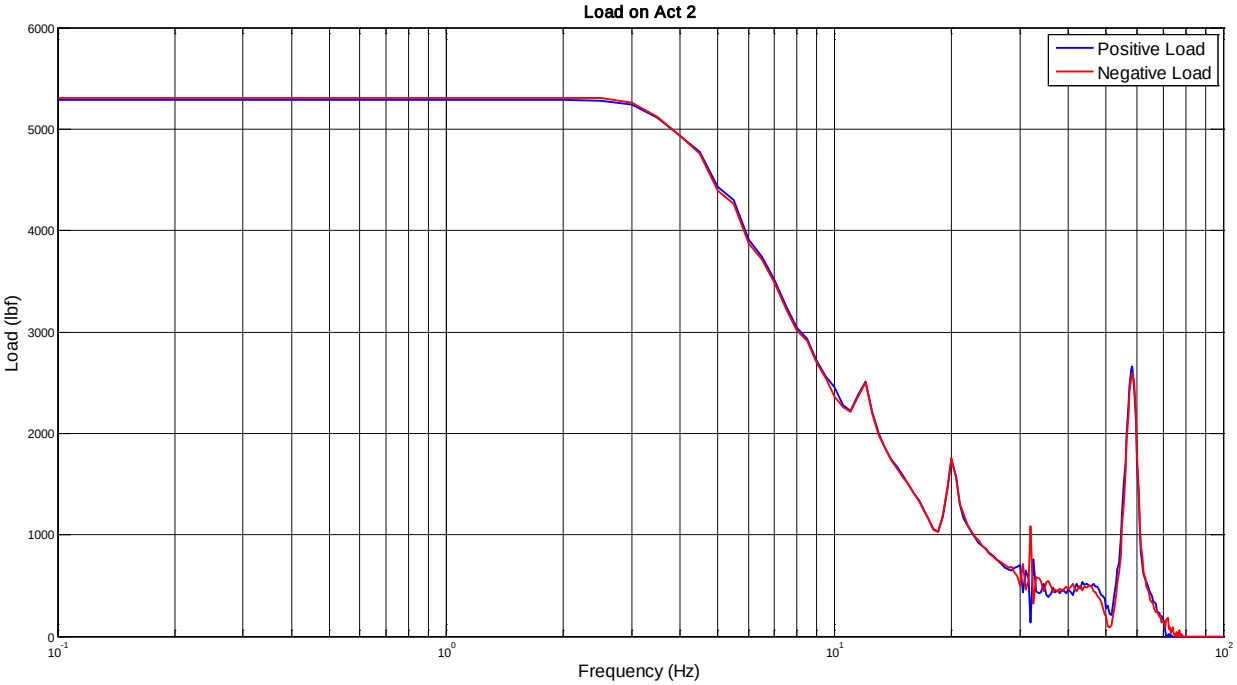

Figure 4-25 – Resultant load on actuator 2 for the square wave electrical failure

Source: Developed by the author

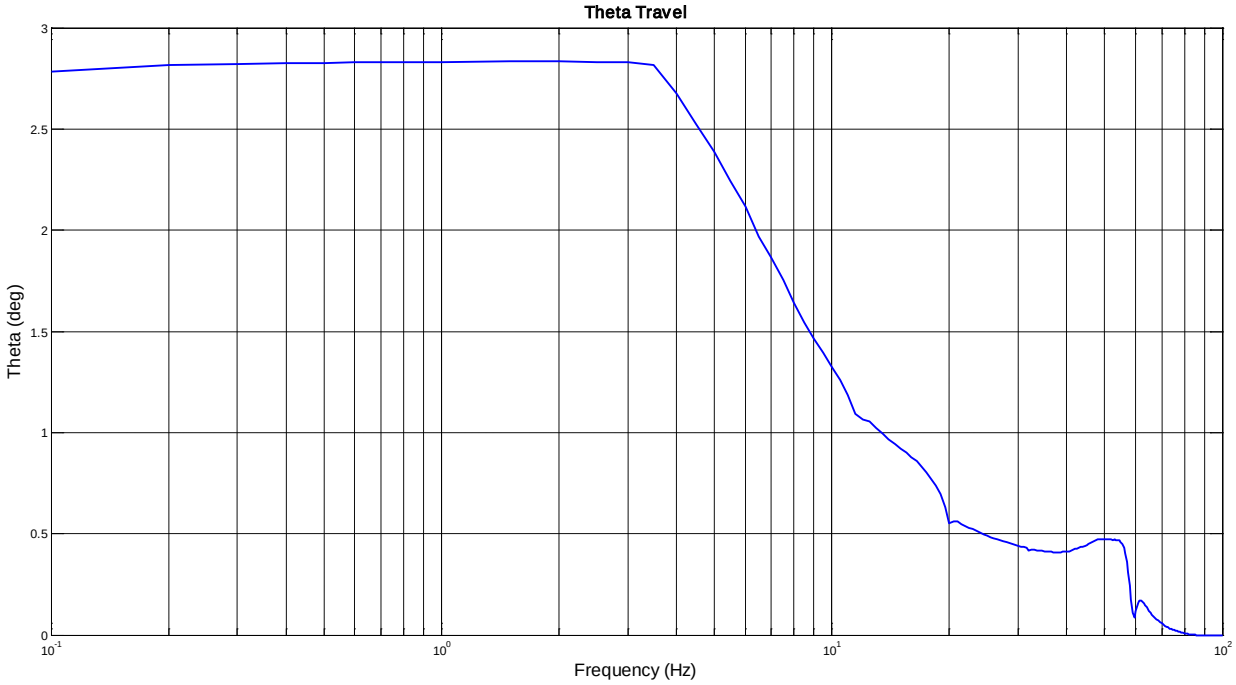

Figure 4-26 – Resultant surface travel for the square wave electrical failure

Source: Developed by the author

The loads on the Figure 4-24 and Figure 4-25 represent the tension and compression loads magnitudes for the frequency range. It can be noticed that the control surface natural frequency has a major impact on the loads frequency response. The Figure 4-26 shows the surface travel regardless to its neutral value, for instance, at 1Hz the surface travel will be approximately 2.8deg, or ±1.4deg, the same value as shown on the Figure 4-18. Also it can be noticed that for frequencies higher than approximately 80Hz, the induced oscillation of the actuator 1 remains inside the backlash, thus not generating any loads on the surface structure.

In order to identify if the amount of force generated on this failure scenario is acceptable from the fatigue life consumption point of view, it must be evaluated the amount of fatigue life that a failure scenario can consume without compromising the structure of the control surface.

Considering that the failure scenario can consume 10% of the fatigue life without compromising the structural integrity of the control surface, thus it must be generated the S-N curve equivalent to 10% of fatigue life consumption for the structural components that is being subjected to the oscillatory load.

On this work it will be analyzed two possible rupture points, the actuator piston rod and the control surface fixture where is assembled the actuator. Consider that the material used for the actuator piston rod is the stainless steel 15-5PH (H1025), which S-N curve for an unnotched plate is given by MIL-HDBK-5J [11] shown on the Figure 4-27.

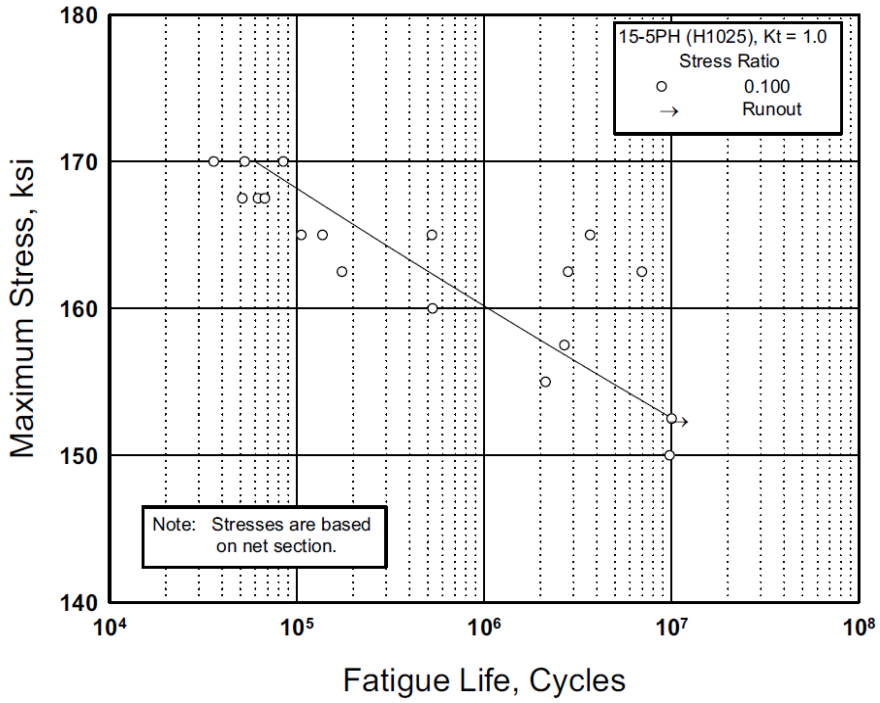

Figure 4-27 – S-N curve for unnotched 15-5PH (H1025) stainless steel plate

Source: MIL-HDBK-5J "Metallic Materials and Elements for Aerospace Vehicle Structures"

The stress ratio is the relation between the stresses in the two loading directions, thus a stress ratio of 1 means that the same stress applied on both directions, whether a stress ratio of 0 indicates an uniaxial stress condition [11].

The stress ratio of the piston rod is around 1, since the load that is being applied in one direction is most of the time close to the same load applied on the oppose direction. Once the data provided by the MIL-HDBK-5J is for a stress ratio of 0.2, which is less than the expected for a stress ratio of 1, it will be assumed half of the maximum stress shown on the Figure 4-27.

In order to evaluate the stress on the piston rod wall, it has to be evaluated its area. The piston rod diameter is equal to 1.5in and its thickness is equal to 0.1in, therefore the area of the piston rod thickness is equal to 0.44in².

Another point that must be studied is how to transform the number of cycles of the S-N curve into frequency, for that it was considered that the failure might occur on the beginning of a flight cycle of 1 hour, since the failure might consume 10% of the fatigue life and still guarantee a safe flight and landing, the number of cycles will be divided by 3600 seconds, resulting on a equivalent frequency. Also it was considered a scatter factor of 4 in order to guarantee a margin of safety due to the scatter behavior of the S-N curve, therefore dividing by 4 the number of cycles.

Thus, considering all the assumptions herein presented, the amount of fatigue life allowable for the failure condition can be compared with the amount of stress which the piston rod is being subjected to. This comparison is shown on the Figure 4-28.

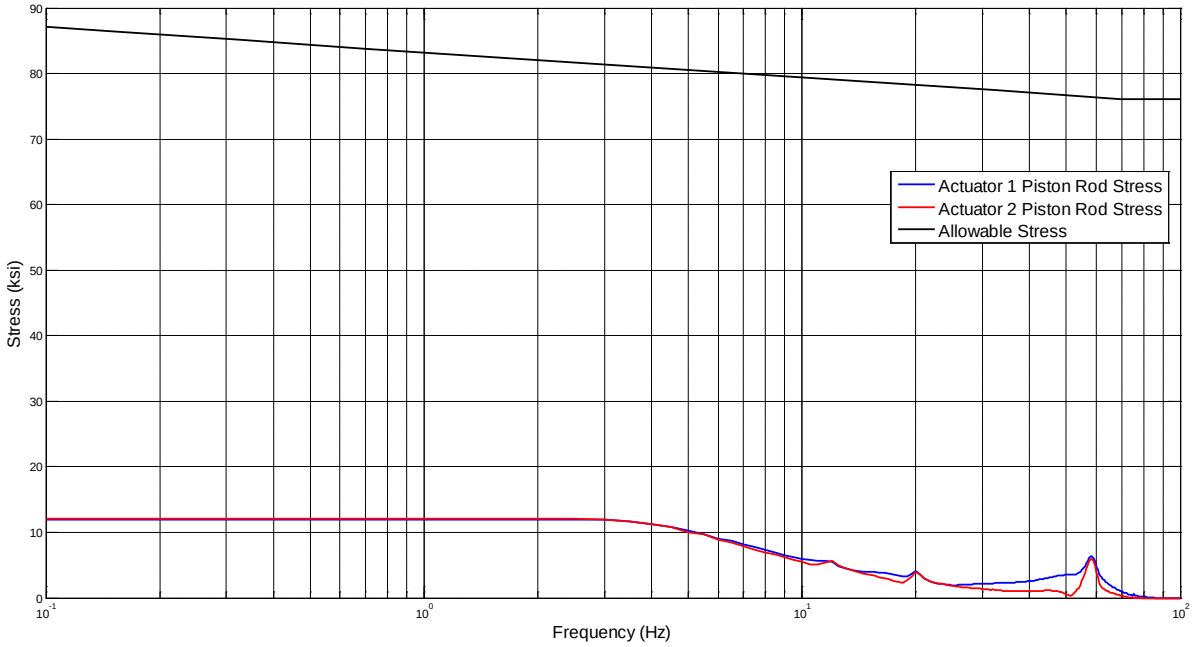

Figure 4-28 – Comparison between stress frequency response due to an square wave electrical failure and the allowable stress for the piston rod wall

Source: Developed by the author

The results shown on the Figure 4-28 clearly indicates that, for the whole analyzed range of frequencies, the fatigue life consumption will be much lower than the allowable 10% for that flight. Therefore, from the point of view of the actuator piston rod, it will not rupture in case this failure occurs.

Nevertheless the surface fixture is subjected to the same amount of load, and therefore, must be analyzes as well. The Figure 4-29 represents the surface fixture with the highlighted concern areas A1 and A2. It is considered that these areas will be subjected to the highest level of stress. Therefore, it has to be analyzed the fatigue life consumption of the fixture for the predicted cross sections A1 and A2.

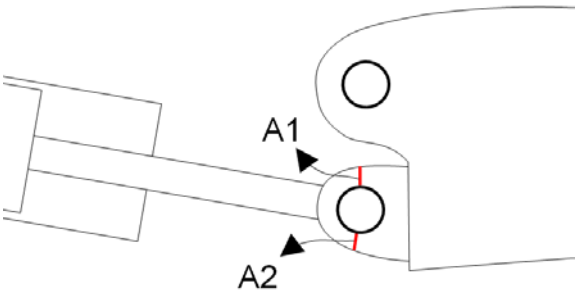

Figure 4-29 – Control Surface Fixture Cross Section Areas

Source: Developed by the author

The areas A1 and A2 are equal and its cross section is a rectangle of 0.25in of length and 0.2in of width, resulting in an area of 0.05in². Considering that the load is equally distributed between A1 and A2, and that the fixture is composed by two lugs with the actuator piston rod end assembled between them, thus the load is equally distributed between each lug. Therefore the load transmitted through the piston is divided by four areas of 0.05in².

The considered material of the fixture is aluminum alloy 7075-T74, which S-N curve can be found on the MIL-HDBK-5J [11], as shown on the Figure 4-30. It was considered that the lug will have a stress concentrator, thus it was considered the notched, Kt equal to 3, S-N curve.

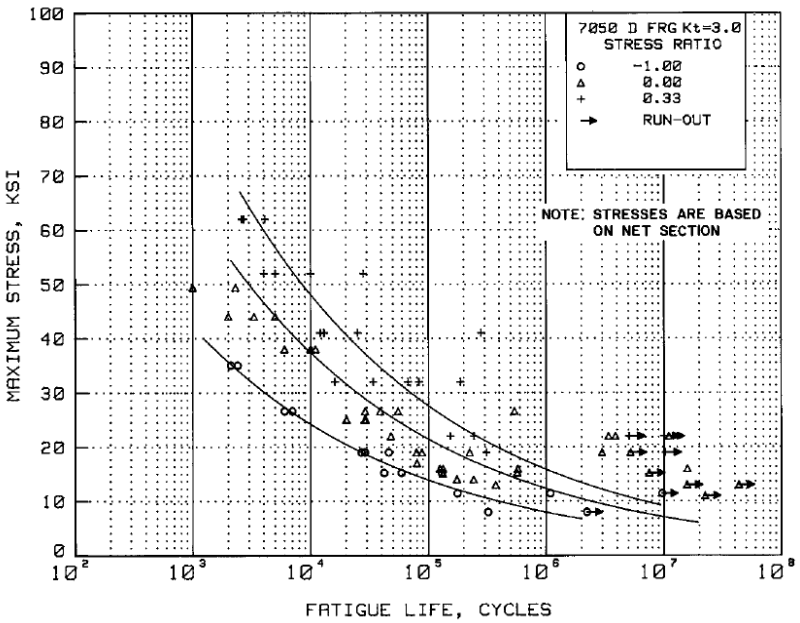

Figure 4-30 – S-N curve for notched 7075-T74 die forging aluminum alloy

Source: MIL-HDBK-5J “Metallic Materials and Elements for Aerospace Vehicle Structures”

Considering that the cross section of study will only be subjected to tension loads, thus the stress ratio to be considered is equal to zero. Therefore it can be compared the stress generated on the failure mode to the equivalent stress of the allowable fatigue life consumption. This comparison is shown on the Figure 4-31.

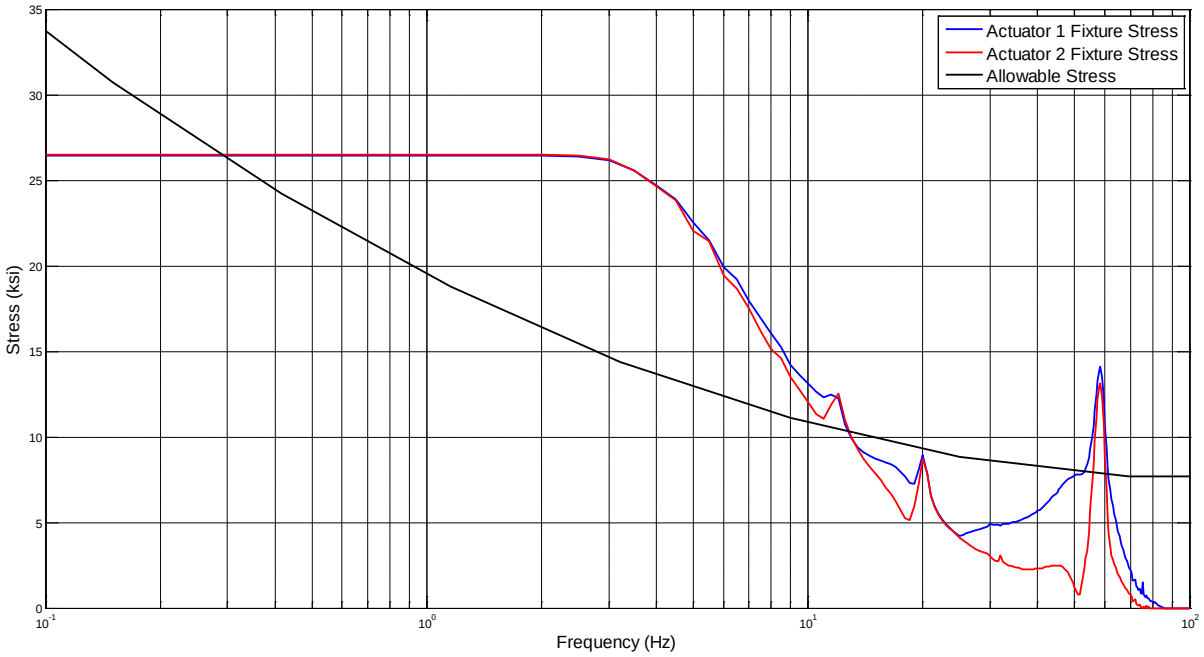

Figure 4-31 – Comparison between stress frequency response due to an square wave electrical failure and the allowable stress for the surface fixture

Source: Developed by the author

As shown on the Figure 4-31, for frequencies higher than 0.3Hz and lower than approximately 13Hz, the system might generate a stress on the fixture lug higher than the allowable considering 10% fatigue consumption for the whole flight. Also it can be noticed that between approximately 53Hz and 62Hz, the system generated a stress higher than the allowable stress as well. This it can be clearly noticed the importance of a modeling with a high level of confidence at high frequencies, once that without the high frequencies behaviors implemented herein, it would not be possible to identify high frequency band where a rupture might occur.

Thus, for these two bands of frequencies, the system is susceptible to a rupture on the surface fixture. Two alternatives might solve the issue, one is to redesign the fixture and add

some material, with the drawback to increase weight on the system, and the other is to monitor this failure in order to prevent the rupture. The design of the monitor for this failure can be very hard to develop. Nevertheless it can be suggested for future works the development of a monitoring logic to prevent this type of failure.

5. CONCLUSION

The purpose of this thesis was to design a model of a hydraulic actuation system with a high fidelity even at high frequencies and to analyze its response for failure scenarios where the high frequencies dynamics can have a major impact on the conclusions made.

As shown on the analyses results, the model herein developed can represent, with a high level of confidence, a hydraulic actuation system performance, as well as its high frequencies dynamics. In order to make this possible, it was indispensable the modeling of the high frequencies dynamics of the system components, in special the modeling of the servovalve and the surface dynamics.

With the model developed, it is possible to analyze failure modes that might occur up to high frequencies, such as the oscillatory mal-functions, which were analyzed as well on this thesis, showing the importance of a high frequency modeling, once that, without the high frequencies dynamics implemented, it would not be possible to detect that the failure might be a problem at a high frequency.

Also is important to highlight the crucial importance of the system non-linearities implemented, which without them, it would not be possible to detect the real behavior of the system at high frequencies.

Nonetheless some additional works must be done in order to improve even more the analyses at high frequencies. Some of them are the modeling off a flexible surface with more than one mode of vibration, which can change the results depending on the modes of the surface under analysis; also the modeling of the Aerodynamics to be joined to this model in

order to reach a higher level of confidence of a real hydraulic actuation system; furthermore it can be modeled the remaining parts that was disregarded on the development herein presented, such as the reservoir; at last, one of the most important recommendation for future works is the validation of the results obtained with the model designed herein with a real hydraulic actuation system.

From the Oscillatory Mal-Function perspective, since it was detected that the system can be subjected to the possibility of the fixture rupture, it can be suggested the development the design of the monitor for this particular failure, based on the allowable structural fatigue consumption and the stress that the system can generate. Also it can be recommended additional analyses of different failure modes that can cause an oscillatory mal-function, using the model designed herein

Finally it can be concluded that, when it is used a model in order to analyze a scenario where the high frequencies dynamics are relevant, it is indispensable the usage of a model similar to the one designed on this thesis, otherwise some important behaviors will not be detected and it might lead to an erroneous conclusion of the analysis.

6. BIBLIOGRAPHY

[1] ADADE FILHO, A., “Análise de Sistemas Dinâmicos”, ver 2.1, São José dos Campos: Instituto Tecnológico da Aeronáutica, 2000.

[2] ANDRIOLI JR., R. L., “Modelagem e Análise dos Efeitos da Rigidez Estrutural na Estabilidade de um Sistema Eletro-Hidráulico de Comando de Profundor”, São José dos Campos: Instituto Tecnológico da Aeronáutica, 2005.

[3] AIR4094, “Aircraft Flight Control System Descriptions”, Society of Automotive Engineers International, 1990.

[4] AIR4253, “Description of Actuation Systems for Aircraft With Fly-By-Wire Flight Control Systems”, rev. A, Society of Automotive Engineers International, 2001.

[5] AIR4922, “Primary Flight Control Hydraulic Actuation System – Interface Definition”, Society of Automotive Engineers International, 2008.

[6] ARP1281, “Actuators: Aircraft Flight Controls, Power Operated, Hydraulic, General Specification For”, rev. C, Society of Automotive Engineers International, 2002.

[7] ARP490, “Electrohydraulic Servovalves”, rev. E, Society of Automotive Engineers International, 1993.

[8] FOX, R. W., and MCDONALD, A. T., “Introduction to Fluid Dynamics”, New York: Wiley, 1998.

[9] MENDONÇA, C. H., “Modelagem e Análise de um Sistema de Comando de Aileron”, São José dos Campos: Instituto Tecnológico da Aeronáutica, 2005.

[10] MERRITT, H. E., “Hydraulic Control Systems”, New York: Wiley, 1967.

[11] MIL-HDBK-5J, “Metallic Materials and Elements for Aerospace Vehicle Structures”, Department Of Defense Handbook, 2003.

[12] OGATA, K, “Modern Control Engineering”, New Jersey: Pearson, 2002.

[13] Wikipedia, http://en.wikipedia.org/wiki/Flight_control_system, accessed at 20/01/2010.

[14] Wikipedia, http://en.wikipedia.org/wiki/Check_valve, accessed at 20/01/2010.

APPENDIX

Load_Parameters.m Script

```
% Load_Parameters
% Script created to run the model PFCS.mdl
% The model and script was made by Carlos A Constantino

% Hydraulic System
K_Supply1 = 75; % Pressure loss gain, psi.s/in³
K_Supply2 = 75; % Pressure loss gain, psi.s/in³

% LVDT
Tol_LVDT1 = 1; % LVDT error gain for Act1
Tol_LVDT2 = 1; % LVDT error gain for Act2
NB_LVDT1 = 0; % LVDT null bias error for Act1
NB_LVDT2 = 0; % LVDT null bias error for Act2

% Hardware_in
T_ES = 1/500; % Electronic System running at 500Hz

% Position Loop
Rate_Limit = 40; % Rate Limit, deg/s
Max_Cmd = 15; % Maximum command allowable, deg
Min_Cmd = -25; % Minimum command allowable, deg
Kp = 30; % Proportional gain in PID Controller
Ki = .5; % Integral gain in PID Controller
Kd = .4; % Derivative gain in PID Controller
Limit_Int = .5; % Integral Limit, mA
Imax = 8; % Maximum EHSV Current, mA

% Kinematics Nominal
L0 = 12; % Neutral length of the Act, in
C = 13;  % Hinges distances, in
R = 4; % Actuation Radius, in
Theta0 = acos((C^2+R^2-L0^2)/(2*C*R)); % Theta angle at neutral, rad

% Kinematics Act1
L01 = 12; % Neutral length of the Act, in
C1 = 13;  % Hinges distances, in
R1 = 4; % Actuation Radius, in
Theta01 = acos((C1^2+R1^2-L01^2)/(2*C1*R1)); % Theta angle at neutral, rad

% Kinematics Act2
L02 = 12; % Neutral length of the Act, in
C2 = 13;  % Hinges distances, in
R2 = 4; % Actuation Radius, in
Theta02 = acos((C2^2+R2^2-L02^2)/(2*C2*R2)); % Theta angle at neutral, rad

% Hardware_out
Tol_SA1 = 1; % Servo Amplifier error gain for ES1
Tol_SA2 = 1; % Servo Amplifier error gain for ES2
```

```
% Inlet Check Valve
Acv = 0.003; % Check Valve Area, in²
Pcvi = 5; % Inlet cracking pressure, psi
Vcv = 1; % Check valve volume, in³
Ps0 = 3000; % Initial inlet pressure, psi

% Return Check Valve
Pcvr = 100; % Return cracking pressure, psi
Pt0 = 200; % Initial return pressure, psi

% EHSV 1st Stage
a=0.15; % radius of armature from pivot to center of pole face, in
g=0.001; % length of each air gap at neutral, in
Nc = 1e4; % number of turns in each coil
fig = 300; % magnetic flux of permanent magnet, maxwells
Kt = 4.43e-8*4*(a/g)*Nc*fig; % torque constant of the torque motor,
in.lb/amp
Ja = 1e-3; % inertia of armature and any attached load, in.lb.s²
Kf = 4.7e4; %spring constant of the cantilevered feedback spring at the
free end, lb/in
r = 0.5; % distance between center of armature and flapper, in
b = 0.2; % distance between flapper and spool, in
Kqp = 5; % flow gain of flapper valve, in³/s/in
Av = pi*0.2^2/4; % area of spool, in²
Vp = Av*0.1; % Volume of fluid at spool end chambers, in³
Mv = .25; % Spool mass, lb
Be = 100000; % Bulk Modulus, psi
whp = sqrt(2*Be*Av^2/(Vp*Mv)); % hydraulic natural frequency of pilot
stage, rad/sec
Kcp = 4e-6; % flow pressure coeficient of pilot valve, in³/s/psi
sihp = whp*Kcp*Mv/(2*Av^2); % damping ratio of pilot stage
Kf1 = Kf;
Kf2 = Kf;

% EHSV 2nd Stage
Xlenght = .25; % EHSV slot lenght
Xwidth = .15; % EHSV slot width
Xov = 5e-4; % EHSV slot overlap
Aleak1 = pi*.001^2/4; % Equivalent orifice area for path 1 leakage, in²
Aleak2 = pi*.001^2/4; % Equivalent orifice area for path 2 leakage, in²
Aleak3 = pi*.001^2/4; % Equivalent orifice area for path 3 leakage, in²
Aleak4 = pi*.001^2/4; % Equivalent orifice area for path 4 leakage, in²
Aleak5 = pi*.01^2/4; % Equivalent orifice area for path 5 leakage, in²
Cd = 0.67; % Discharge Coefficient
Temp = 80; % Fuid Temperature, ºF
% According to SAE AIR1362 Rev. B
Rho = (1.08-0.95)/(-70-90)*(Temp-90)+0.95; % Fluid density, N.s²/m?
Rho = 0.00009357268*Rho; % Fluid density, lbf.s²/in?

% Cylinder Dynamics
Ap1 = 2; % Piston area Act1, in²
Ap2 = 2; % Piston area Act2, in²
Aleakext = pi*.001^2; % Equivalent orifice area for external leakage, in²
Aleakint = pi*.005^2; % Equivalent orifice area for internal leakage, in²
Pcvac = 5; % Anti-Cavitation Valve cracking pressure, psi
Xpmax = 2; % Maximum Xp value (extension), in
Xpmin = -1.5; % Minimum Xp value (retraction), in
V011 = 1.2*Ap1*abs(Xpmax);
```

```
V021 = 1.2*Ap1*abs(Xpmin);
V012 = 1.2*Ap2*abs(Xpmax);
V022 = 1.2*Ap2*abs(Xpmin);
Ffric1 = 150; % Piston Friction for Act1, lbf
Ffric2 = 150; % Piston Friction for Act2, lbf
Ka1 = 2e5; % Stiffness for Act1, lbf/in
Ka2 = 2e5; % Stiffness for Act2, lbf/in
Kst = 1e9; % Stiffness of the end stop for both Act, lbf/in
Mp1 = 2; % Piston mass for Act1, lb
Mp2 = 2; % Piston mass for Act2, lb
Bp1 = 1; % Damping coefficient for Act1, lbf.s/in
Bp2 = 1; % Damping coefficient for Act2, lbf.s/in
P10 = 1600; % Initial pressure on extension chamber, psi
P20 = 1600; % Initial pressure on retraction chamber, psi

% Surface
Backlash1 = .06*pi/180; % Backlash for Act1 (+-.06º), in
Backlash2 = .06*pi/180; % Backlash for Act2 (+-.06º), in
Kl1 = 1.5e6; % Lug Stiffness for Act1, lbf/rad
Kl2 = 1.5e6; % Lug Stiffness for Act2, lbf/rad
Kstr = 1.5e6; % Surface Stiffness, lbf/rad
Bstr = 3e3; % Structural damping, in.lbf/(rad/s)
I = 8; % Surface inertia, in.lbf/(rad/s²)
```

ff_gen.m Script

```
% Create Force-Fight
% Script created to differentiate the Act 1 and 2 dynamics in order to
% generate the Force-Fight between them
% The model and script was made by Carlos A Constantino

% Hydraulic System
D_Supply = 0.1;
K_Supply1 = K_Supply1*(1+D_Supply); % Pressure loss gain, psi.s/in³
K_Supply2 = K_Supply2*(1-D_Supply); % Pressure loss gain, psi.s/in³

% LVDT
D_LVDT = 0.01;
Tol_LVDT1 = 1*(1+D_LVDT); % LVDT error gain for Act1
Tol_LVDT2 = 1*(1-D_LVDT); % LVDT error gain for Act2

% Kinematics Act1
D_L0 = 0.1;
L01 = L01+D_L0; % Neutral length of the Act, in
L02 = L02-D_L0; % Neutral length of the Act, in

D_C = 0.1;
C1 = C1+D_C;  % Hinges distances, in
C2 = C2+D_C;  % Hinges distances, in

D_R = 0.1;
R1 = R1+D_R; % Actuation Radius, in
R2 = R2+D_R; % Actuation Radius, in
```

```
Theta01 = acos((C1^2+R1^2-L01^2)/(2*C1*R1)); % Theta angle at neutral, rad
Theta02 = acos((C2^2+R2^2-L02^2)/(2*C2*R2)); % Theta angle at neutral, rad

% Hardware_out
D_SA = 0.025;
Tol_SA1 = 1*(1+D_SA); % Servo Amplifier error gain for ES1
Tol_SA2 = 1*(1-D_SA); % Servo Amplifier error gain for ES2

% Cylinder Dynamics
D_Ap = 0.01;
Ap1 = Ap1*(1+D_Ap); % Piston area Act1, in²
Ap2 = Ap2*(1-D_Ap); % Piston area Act2, in²

V011 = 1.2*Ap1*abs(Xpmax);
V021 = 1.2*Ap1*abs(Xpmin);
V012 = 1.2*Ap2*abs(Xpmax);
V022 = 1.2*Ap2*abs(Xpmin);

D_fric = 0.1;
Ffric1 = Ffric1*(1+D_fric); % Piston Friction for Act1, lbf
Ffric2 = Ffric2*(1-D_fric); % Piston Friction for Act2, lbf

D_Ka = 0.05;
Ka1 = Ka1*(1+D_Ka); % Stiffness for Act1, lbf/in
Ka2 = Ka2*(1-D_Ka); % Stiffness for Act2, lbf/in

D_Mp = 0.01;
Mp1 = Mp1*(1+D_Mp); % Piston mass for Act1, lb
Mp2 = Mp2*(1-D_Mp); % Piston mass for Act2, lb

D_Bp = 0.01;
Bp1 = Bp1*(1+D_Bp); % Damping coefficient for Act1, lbf.s/in
Bp2 = Bp2*(1-D_Bp); % Damping coefficient for Act2, lbf.s/in

% Surface
D_Blsh = 0.05;
Backlash1 = Backlash1*(1+D_Blsh); % Backlash for Act1 (+-.06°), in
Backlash2 = Backlash2*(1-D_Blsh); % Backlash for Act2 (+-.06°), in

D_Kl = 0.05;
Kl1 = Kl1*(1+D_Kl); % Lug Stiffness for Act1, lbf/in
Kl2 = Kl2*(1-D_Kl); % Lug Stiffness for Act2, lbf/in
```

Run_StepInput.m Script

```
% Run_StepInput
% Script created to analyze the step input response of the model PFCS.mdl
% The model and script was made by Carlos A Constantino

clear all
```

```
Load_Parameters
ff_gen

Time = 1.5; % Simulation time (s)

Cmd = 15; % Command input (deg)

HM = -23200*0; % Aerodynamic load (lbf.in)


sim('NoFAIL');

Output = Theta.signals.values; % Output from the model

n=length(Output(:,1));

final = Output(n,2);

Td = 0;
Tr1 = 0;
Tr2 = 0;
Ts = 0;
Tp = 0;
Mp = 0;

dOutput = diff(Output(:,2));

for i=1:n
    if abs(Output(i,2))>=abs(0.5*final) && Td==0
        Td = Theta.time(i);
    end
    if abs(Output(i,2))>=abs(0.1*final) && Tr1==0
        Tr1 = Theta.time(i);
    end
    if abs(Output(i,2))>=abs(0.9*final) && Tr2==0
        Tr2 = Theta.time(i);
    end
    if abs(Output(i,2))>=abs(0.98*final) && ...
            abs(Output(i,2))<=abs(1.02*final) && Ts==0
        Ts = Theta.time(i);
    end
    if abs(Output(i,2))<abs(0.98*final) || abs(Output(i,2))>abs(1.02*final)
        Ts = 0;
    end
end
for i=1:n-2
    if final>0
        if dOutput(i)>0 && dOutput(i+1)<=0 && Output(i+1,2)>Mp*final
            Tp = Theta.time(i);
            Mp = Output(i+1,2)/final;
        end
    else
        if dOutput(i)<0 && dOutput(i+1)>=0 && Output(i+1,2)<Mp*final
            Tp = Theta.time(i);
            Mp = Output(i+1,2)/final;
        end
```

```
    end
end
```

Run_FreqRes.m Script

```
% Run_FreqRes
% Script created to analyze the frequency response of the model PFCS.mdl
% The model and script was made by Carlos A Constantino

clear all

Load_Parameters

% No aerodynamic load
HM = 0;

% Backlash is eliminated on this analysis
Backlash1 = 0;
Backlash2 = 0;

% Vector of frequencies to be analyzed
freqs =[.1:.2:.9 1:2:59 60:2:100]; % Hz
nfreqs = length(freqs);

% Commanded input sine wave signal of cmd of Amplitude
A = .5; % deg

Output = nan*zeros(nfreqs,3);

for n = 1: nfreqs

    Freq = freqs(n);

    Time = 1/Freq +1; % Simulation time

    sim('NoFAILFR');

    Output(n,:) = [ Freq Gain Phase ]; % Output from the model
end
```

Run_EF.m Script

```
% Run_EF
% Script created to analyze the electrical OMF using the model PFCS.mdl
% The model and script was made by Carlos A Constantino

clear all
```

```
Load_Parameters

HM = 0; % Aerodynamic load, lbf.in

freqs = [.1:.1:.9 1:.5:100]; % Vector of frequencies to be analyzed, Hz
nfreqs = length(freqs); % No of frequencies to be analyzed

A = 100;  % Amplitude of error, mA

Output1 = nan*zeros(nfreqs,3);
Output2 = nan*zeros(nfreqs,3);
Output3 = nan*zeros(nfreqs,2);

for i = 1: nfreqs

    Freq = freqs(i);

    if Freq>80
        Time = 1/Freq +3; % Simulation time
    else
        Time = 1/Freq +1; % Simulation time
    end

    Tn=1e5/Freq;

    sim('PFCS_EF');

    Loadp1 = max(Load.signals.values(1:Tn,1));
    Loadn1 = min(Load.signals.values(1:Tn,1));

    Loadp2 = max(Load.signals.values(1:Tn,2));
    Loadn2 = min(Load.signals.values(1:Tn,2));

    Theta_travel = max(Theta.signals.values(1:Tn,2))...
        -min(Theta.signals.values(1:Tn,2));

    Output1(i,:) = [Freq Loadp1 Loadn1]; % Output from the model
    Output2(i,:) = [Freq Loadp2 Loadn2]; % Output from the model
    Output3(i,:) = [Freq Theta_travel];
end
```